The Motor Thalamus: An Invigorating Hub of Neural Activity

By

Matthew Gaidica

A dissertation submitted in partial fulfillment
of the requirements for the degree of
Doctor of Philosophy
(Neuroscience)
in The University of Michigan
2019

Doctoral Committee:

Assistant Professor Daniel Leventhal, Chair
Professor Wayne Aldridge
Assistant Professor Sara Aton
Associate Professor Cynthia Chestek
Professor William Dauer

Matthew Gaidica

mgaidica@umich.edu

ORCID iD: 0000-0002-0191-1899

ACKNOWLEDGEMENTS

Many thanks are in order to an enormous amount of people and institutions who have ardently supported my work and progression through graduate school. Firstly, to my committee for your efforts in reviewing my work, supporting my progress, and holding me to high standards. Foremost, my principal investigator, Dr. Daniel Leventhal, for taking me under his wing, working closely with me to solve hard problems, and allowing me to explore and innovate.

The Neuroscience Graduate Program—Rachel Harbach, Carol Skala, Valerie Smith, Dr. Ed Stuenkel and Dr. Audrey Seasholtz—has been beyond accommodating, providing resources and opportunities to grow personally and academically. Dr. Richard Hume and Dr. Amy Oakley for their time spent mentoring me as a Graduate Student Instructor and entrusting me with course design and lectures. Dr. Roger Albin has provided wonderful insight, commentary and support to my work. Howard Oishi and Denice Heckel for being wonderful administrators.

The NIH National Institute of Neurological Disorders and Stroke (NINDS) Parkinson's Disease Research Centers of Excellence program has offered several opportunities to share and connect with my peers in a specialized manner. Similarly, the International Conference for Advanced Neurotechnology has offered meaningful opportunities domestically and abroad.

Finally, to my friends and family, including my lab mates. This endeavor has taken time and support from you all.

TABLE OF CONTENTS

LIST OF FIGURES

ABSTRACT

The motor thalamus (Mthal) is poised between subcortical and cortical motor structures and is, in the simplest terms, understood as a "relay" for neural activity. However, it is increasingly appreciated that Mthal plays a complex, integrative function. This view is emerging from clinical applications where modifying Mthal activity ameliorates the motor symptoms of several movement disorders, including Parkinson's disease (PD). Little is understood, however, about how neural signals are integrated by Mthal and how this integration shapes ongoing behavior. Answers to these questions hold important implications for basic science and future therapies of brain disease.

My studies address major questions about Mthal physiology by recording chronic, *in vivo* electrophysiology in behaving rats. Given the parallels between rodent and human motor circuits, rats are a useful translational model. I leveraged a two-alternative forced choice task where movement is both ballistic and lateralized. I found that Mthal single unit activity (or "spiking") is greatly enhanced around movement initiation. Importantly I identified units that fired in a manner that was either "directionally selective" or "non-directionally selective". Using two performance measures, reaction time (RT) and movement time (MT), I also show that Mthal activity is proportional to the speed of movement. Directionally selective units correlate with RT and MT, non-directionally selective units correlate exclusively with RT.

Mthal spiking is known to be correlated with rhythmic oscillations in the extracellular local field potential (LFP). I therefore determined relationships between Mthal unit spiking, behavior and LFP. I discovered that the phase of low frequency oscillations in the delta band (1-

4 Hz) predicts spike timing, especially for directionally selective units. Delta phase also predicts RT and aligns to each event, suggesting a role in task timing. The power of higher frequency oscillations, namely beta (13-30 Hz) and low-gamma (30-70 Hz), are nested within the delta phase. Taken together, these results support a model whereby delta phase regulates high-frequency interactions and neuronal excitability in Mthal, which reflects motor performance.

To begin parsing behavioral causality with spatiotemporal precision, I implemented a suite of optogenetic tools to anatomically isolate Mthal circuitry. I show that an adeno-associated virus injected in upstream structures can be reliably trafficked to and expressed in Mthal. These techniques establish methods to test hypotheses concerning complex spike-LFP and LFP-LFP interactions ultimately leading to a better understanding of how movement signals are mediated by Mthal.

CHAPTER 1: Introduction

Background

The motor thalamus (Mthal) is the largest subcortical motor input to the cortex and physiologically represents a consolidation of motor signals, most notably from the basal ganglia (BG) and cerebellum (Figure 1-1) (Bosch-Bouju, Hyland, & Parr-Brownlie, 2013; Kuramoto et al., 2011). However, the functional integration occurring in Mthal, shaped in part by reentrant cortical input (Bédard, Kröger, & Destexhe, 2004; Galvan et al., 2016), has remained understudied leaving many questions unanswered concerning how normal behaviors are expressed (Garcia-Munoz & Arbuthnott, 2015) and disease might be manifested (Devetiarov et al., 2017) through this pathway. Two viewpoints have been vital in making sense out of circuit-level, electrical phenomena associated with the BG-thalamocortical system. *The Standard Rate Model* outlines how single unit firing influences movement through a series of neurochemical gates (Figure 1-2). *The Brain Rhythm Model* posits that electrical rhythms are responsible for enabling motor coordination between distributed nuclei. While these models are not necessarily mutually exclusive, they have largely been considered separately. This is partly to blame on the fact that research methods are non-overlapping, but it also concerns a perennial question, *what is the currency of the brain?* In the following chapter, these models are explained in detail and put into a framework by which they can be understood together and in the context of my research.

The Standard Rate Model. In the 1980's there was a growing need to make sense of a number of movement disorders associated with BG dysfunction. Seminal work established a functional anatomy that explained how firing rates influenced neurotransmitter release through

the BG-thalamocortical circuit (Albin, Young, & Penney, 1989; DeLong, 1990). Their model describes how dopamine modulation in the BG promotes and inhibits movement by regulating the activity of the striatal "direct" and "indirect" pathways, respectively. The complexity of the BG circuit converges at the output node where the substantia nigra pars reticulata (SNr) and globus pallidus internus (GPi) project to Mthal. The SNr/Gpi output pathway inhibits Mthal by way of GABAergic synapses. Therefore, an increase in BG-output activity reduces Mthal firing (Edgerton & Jaeger, 2014). Mthal projects to the cortex via glutamatergic synapses which goes directly regulates corticospinal activity (Herkenham, 1980; Kuramoto et al., 2015). Given that Mthal preserves the "sign" of neuronal firing, and that a single line can be drawn from the BG to cortex through the thalamus, its status as a "relay" is only emboldened by this schematization.

The standard rate model elegantly links the neuropathology of Parkinson's disease (PD) to the motor symptoms, namely bradykinesia (slowness of movement) and rigidity (Ellens & Leventhal, 2013). Dopaminergic denervation leads to an increase in BG output, and in turn, impedes movement by decreasing Mthal activity. Alternative interpretations of BG function rely on similar arguments: that the BG are broadly responsible for inhibiting competing motor programs and enabling the 'right' movement through disinhibition of Mthal (Mink, 1996). However, the standard rate model is challenged by paradoxical observations from stereotactic surgeries where lesions or deep brain stimulation (DBS) of the BG-output improves parkinsonism and relieves hyperkinetic disorders (Cif & Hariz, 2017; Marsden & Obeso, 1994). In a primate model of PD, DBS effectively treats motor symptoms but reduces firing rates in Mthal when applied to the subthalamic nucleus (STN) (Xu, Russo, Hashimoto, Zhang, & Vitek, 2008) and GPi (Muralidharan et al., 2017). Additionally, lesioning the BG-output in healthy

primates, thereby disinhibiting Mthal, slows (Horak & Anderson, 1984) or has little effect at all (Desmurget & Turner, 2008) on movement.

Other modes of operation for Mthal have been proposed that are not entirely inconsistent with the standard rate model, but instead rely on cortically-based fine tuning of glutamate in Mthal (Figure 1-3A, also see Goldberg, Farries, & Fee, 2013). When glutamate input is absent, Mthal neurons undergo hyperpolarization that deinactivates a T-type calcium channels responsible for "rebound bursting" (Kim et al., 2017b; Bosch-Bouju et al., 2013). When present at moderate to high levels, glutamate enhances neuronal excitability, thereby upscaling Mthal firing during pauses of the BG-output, similar to the standard rate model (Figure 1-3B). In this manner, the cortical mechanism is transitions Mthal between "burst" and "tonic" firing (Sherman, 2001).

While the average firing rate can remain matched between tonic and burst modes, the activity patterns have profound physiological implications, supporting the hypothesis that firing patterns rather than firing rates are more salient to the study of movement and behavior (Galvan, Devergnas, & Wichmann, 2015). Mthal in healthy rats is rapidly modulating during a skilled reaching behavior (Bosch-Bouju, Smither, Hyland, & Parr-Brownlie, 2014). The authors extended their study to show that after rats were rendered parkinsonian, motor function improved as the optogenetic stimulation pattern of Mthal was made more irregular (while maintaining a consistent mean firing rate) (Seeger-Armbruster et al., 2015).

However, when dysregulated, neuronal bursting can be pathological (Cain & Snutch, 2012). Persistent bursting itself may limit the flexibility of motor circuits to establish motor plans or neuromodulatory control over movement (Guo, Rubin, McIntyre, Vitek, & Terman, 2008) specifically by reducing the fidelity of the thalamocortical relay (Guo, Park, Worth, &

Rubchinsky, 2013). Mthal bursting coincides with a higher proportion of correlated units in parkinsonian primates, and in theory, may promote antagonist motor programs that lead to bradykinesia (Pessiglione et al., 2005). The ratio of burst to tonic firing in BG-recipient zones of Mthal is enhanced in human PD (Molnar, Pilliar, Lozano, & Dostrovsky, 2005 Devetiarov et al., 2017) and parkinsonian animal models (Wichmann & Soares, 2006). Finally, BG-targeted DBS that attenuates PD motor symptoms reduces neuronal bursting in Mthal (Xu et al., 2008), suggesting a causal mechanism.

Anatomical updates to the standard rate model schematic have become an increasingly important consideration. Highlighting this matter is the observation that cerebellar inputs to Mthal are associated with essential tremor (ET), but that ET is only sometimes associated with BG disorders, such as PD (Ellens & Leventhal, 2013). Cerebellar and BG projections remain relatively well-delineated through Mthal into cortical motor nuclei (Hintzen, Pelzer, & Tittgemeyer, 2017; Kuramoto et al., 2011; Nakamura, Sharott, & Magill, 2014). Although both structures are involved in movement, experimental data point to subtle differences. The BG has been more strongly associated with motor learning (Turner & Desmurget, 2010), action selection (Graybiel & Grafton, 2015), and invigorating movement (Panigrahi et al., 2015). On the other hand, the cerebellum is associated with precise timing of events (Bareš et al., 2018) and initiating movements (Heiney, Kim, Augustine, & Medina, 2014; Lee et al., 2015). This functional arrangement may be explained by the fact that through Mthal, BG projections preferentially innervate premotor and associative areas of the cortex (Bosch-Bouju et al., 2013) while cerebellar efferents innervate layer 5 pyramidal tract neurons of primary motor cortex, enabling direct control over movement (see Figure 5E Yamawaki & Shepherd, 2015). The knowledge of this arrangement makes the question regarding the anatomical origins of ET perhaps more

mysterious. However, recent work has shown that there are subcortical connections between the BG and cerebellum (Bostan & Strick, 2010). Therefore, instead of the canonical notion that BG-cerebellar coordination is mediated through recurrent thalamocortical loops (Hintzen et al., 2017), there appear to be more direct routes of communication (Chen, Fremont, Arteaga-Bracho, & Khodakhah, 2014). Broken BG function may result in aberrant signaling directly to the cerebellum, hijacking the same circuits that are, in some cases, independently responsible for ET (Lewis et al., 2013).

In summary, the standard rate model has advanced our understanding of how the BG operate under normal and adverse physiologic conditions. It continues to serve as a useful, if not falsifiable starting point to compare and contrast single unit data and describe how neuronal firing gates movement (Bar-Gad & Bergman, 2001). However, its treatment of the function, neuronal dynamics, and anatomical connections associated with the thalamus is lacking, which in light of emerging research, deserves more attention. A more informed understanding of how neuronal signals arrive and are integrated in Mthal, which sits central to the BG-thalamocortical network, holds the potential for new therapeutic approaches to several movement disorders, perhaps most of all, PD.

The Brain Rhythm Model.

Rhythmicity is a fundamental component of many behaviors. You only have to look as far as music to recognize that humans enjoy rhythm, can entrain to it, and have a striking ability to store and recall properties like frequency and duration. Specific to neuroscience are questions regarding how rhythms are involved in executing motor tasks and what their neural basis might be (Buzsaki, 2006). Indeed, specific features of electrical rhythms (also called “oscillations”) are

correlated with associative, sensory and motor functions (Arce-McShane, Ross, Takahashi, Sessle, & Hatsopoulos, 2016).

Measuring electrical oscillations in the brain can be accomplished through many modalities. A common technique is through wire or silicon electrodes placed extracellularly and recording the local field potential (LFP). This method affords high resolution and spatial specificity, but is also invasive. Non-invasive methods include electroencephalography (EEG) and magnetoencephalography (MEG). Signals gathered from the LFP, EEG, and MEG are assumed to measure neuronal activity on a circuit, rather than cellular level (see below). Most studies focus on neural oscillations that cycle anywhere between once a second to several hundred times (~1–200 Hz), thus creating a scale from slow to fast. Greek letters have been attributed to frequency ranges that are common among experimental models, which include but are not limited to: delta (δ, 1–4 Hz), theta (θ, 4–7 Hz), alpha/mu (α/μ,7–12 Hz), beta (β, 13–30 Hz), low-gamma (γ_L,30-70 Hz) and high-gamma (γ_H,70–200 Hz). Within each frequency band, the two signal properties that have emerged as being centrally important are power (squared magnitude) and phase (instantaneous angle).

Several authors have treated the breadth of function that these bands are associated with (Buzsaki, 2006 Basar, 2004). Broadly speaking, neural oscillations potentially solve the long-standing "binding problem" that asks how distant brain regions coordinate activity with precision (Singer, 1999). The answer may be that electrical oscillations modulate cellular excitability and activity across brain structures becomes coherent when entrained to the same oscillation (Womelsdorf et al., 2007; Fries, 2005).

Understanding the origin of brain oscillations is one step towards appreciating their significance. However, there is not one clear answer. At the smallest scale, some neuron types

have intrinsic properties that elicit rhythmic firing (Marder & Calabrese, 1996). These "pacemaker" neurons often contribute to a subclass of neural circuits known as central pattern generators associated with controlling rhythmic functions like respiration, heart rate, and even locomotion (Grillner, 2006). Alternatively, some models suggest that "line delays" (i.e., the brain wiring itself) can mediate reverberations between local and distant structures to produce oscillations through feedforward and feedback networks (Singer, 2017). However, delay-based models fail to explain why neuronal oscillations are consistent across mammalian species, large and small (Buzsáki, Logothetis, & Singer, 2013). Of course, external stimuli are also responsible for modulating neurons and neural networks that results in oscillations that encode the stimulus properties (Haegens & Zion Golumbic, 2018).

The question of oscillatory origin is distinct from what the recorded LFP represents in an organism. A well-accepted answer is that the LFP represents the amalgamation of synaptic activity and transmembrane potentials (Buzsáki, Anastassiou, & Koch, 2012). One alternative explanation focuses on the influence of electromagnetic "crosstalk," called ephaptic coupling, that occurs independent of synaptic activity between nearby neurons (Martinez-Banaclocha, 2018). Along the same lines, it is important to recognize that the electric field potential is not necessarily governed entirely by neurons, as other cell types contribute to ionic fluctuations and have oscillatory properties themselves (Charles, Merrill, Dirksen, & Sanderson, 1991). In fact, neural glia may be a key mediator of neural oscillations (Kühn et al., 2008; Fields, Woo, & Basser, 2015; Lee et al., 2014). The most unsatisfying claim is that neural oscillations are complex epiphenomena with no central mechanism (Steriade, 2006). However, even that possibility does not limit their ability to act as a "fingerprint" of neuronal computations (Ames, Ryu, & Shenoy, 2014; Tzagarakis, Ince, Leuthold, & Pellizzer, 2010; Siegel, Donner, & Engel,

2012) or address clinical conditions (Gantner, Bodart, Laureys, & Demertzi, 2013) and applications (Little et al., 2013). Recent technologies, such as transcranial alternating current stimulation (tACS), are being leveraged to test these questions by inducing frequency-specific oscillations in the motor system (Joundi, Jenkinson, Brittain, Aziz, & Brown, 2012 Pogosyan, Gaynor, Eusebio, & Brown, 2009).

Particular importance has been paid to the beta oscillations for their role in motor control (Rubino, Robbins, & Hatsopoulos, 2006). Across a variety of brain structures, beta power is enhanced during hold periods and states of steady contraction (Baker, Kilner, Pinches, & Lemon, 1999; Murthy & Fetz, 1996; Pfurtscheller, Zalaudek, & Neuper, 1998; Sanes & Donoghue, 1993) suggesting that beta oscillations are "antikinetic" or signal maintenance of the "status quo" (Engel & Fries, 2010). In agreement with this hypothesis, beta power is enhanced in PD and decreased following therapeutic doses of levodopa or high frequency DBS (Brown, 2006).

A more nuanced interpretation concerning the role of beta oscillations is realized when an instruction concerning choice is given prior to an imperative "go" cue prompting movement. This important distinction disassociates the movement from decision signal. When the instruction is properly utilized (e.g., move left), beta oscillations are enhanced around the instruction cue, and therefore, not actually linked to movement (Leventhal et al., 2012). The interpretation of such findings is that beta oscillations reflect a "post-decision" state, where the motor system is stabilized and resistant to alternative actions. Any pathological dysregulation specifically affecting beta state transitions may therefore limit the flexibility of the motor system and inhibit normal behavior (Feingold, Gibson, DePasquale, & Graybiel, 2015).

The delta band is particularly well suited to sync distant brain structures (Kayser, Montemurro, Logothetis, & Panzeri, 2009; Kösem, Gramfort, & van Wassenhove, 2014;

Buzsáki, 2010) and may establish a 'sense of time' (Scharnowski, Rees, & Walsh, 2013). Delta oscillations correlate with the excitability of neural ensembles, sometimes referred to as "up" and "down" states, which may casually influence neuronal firing (Kelly, Smith, Kass, & Lee, 2010) and plasticity (Steriade, 2006; Crunelli, David, Lőrincz, & Hughes, 2015). Delta oscillations are enhanced in rhythmic tasks and aid performance by entraining to external stimuli (Stefanics et al., 2010), thereby offering "windows of opportunity" where the state of neuronal excitability benefits the objective (Wyart, de Gardelle, Scholl, & Summerfield, 2012). Phase-locking (or "resetting") may underlie effective coding and communication schemes established around specific events (Canavier, 2015). Interestingly, delta oscillations are sensitive to dopamine (Cheng, Tipples, Narayanan, & Meck, 2016) and attenuated in PD (Güntekin et al., 2018; Serizawa et al., 2008; Parker, Chen, Kingyon, Cavanagh, & Narayanan, 2015) supporting the notion that motor function is not only slowed, but ill-timed in parkinsonism (Jones, Malone, Dirnberger, Edwards, & Jahanshahi, 2008). When rats are rendered parkinsonian, delta-band optogenetic stimulation of dopamine neurons reverses timing deficits (Kim et al., 2017b).

The fact that oscillatory activity in multiple frequency bands correlates with the same motor behaviors (or symptoms), although interesting, lacks a unifying theory (Lakatos et al., 2005). Cross-frequency coupling is one way by which oscillations may coordinate and give rise to complex behavior (Fiebelkorn et al., 2013; Lisman & Jensen, 2013). This suggestion is supported by models that show neural oscillations arise hierarchically (Aru et al., 2015; Canolty & Knight, 2010). One commonly observed arrangement is low-frequency phase comodulating with higher frequency power, called phase-amplitude coupling (PAC) (Penny, Duzel, Miller, & Ojemann, 2008; Combrisson et al., 2017). For example, delta-beta PAC predicts reaction time (RT) (Hamel-Thibault, Thénault, Whittingstall, & Bernier, 2018; Schroeder & Lakatos, 2009)

and the timing of task-relevant cues (Saleh, Reimer, Penn, Ojakangas, & Hatsopoulos, 2010). These effects may be the result of the delta oscillation providing a time-structured signal that modulates the precision of higher frequency sensorimotor streams (Arnal, Doelling, & Poeppel, 2015).

In summary, neural oscillations offer a solution to the problem of widescale coordination of brain circuits over a considerable spatiotemporal scale. Specific frequency bands appear to subserve physiologic roles by encoding information in their power and phase. The possibility that specific frequency bands are intrinsically coupled or "nested" expand the utility of this model by offering a cohesive cross-frequency interpretation of the physiology underlying behavior. The possibility that oscillations modulate neuronal excitability or can be used as a timing substrate for phase encoding (Jacobs, Kahana, Ekstrom, & Fried, 2007) make them an adjunct to models that rely on the coordinated firing between separate brain regions.

Research Focus

My primary objective was to characterize the electrophysiological correlates of behavior in Mthal and develop tools to address the anatomical origin of these signals. In following, I briefly review what is known about the activity of the major Mthal inputs, the BG and cerebellum, to give context to the hypotheses presented my specific aims.

BG Influences on Mthal. Previous work from my collaborators recorded from the BG-output support the standard rate model, where single unit activity is inversely related to movement (Schmidt, Leventhal, Mallet, Chen, & Berke, 2013). In this regard, Mthal may respond in the canonical fashion, increasing activity during and throughout movement. Other work has found that BG efferents can elicit high-frequency, rebound-like firing in Mthal given prolonged periods of hyperpolarization, which is an alternative way by which Mthal may drive

and scale ballistic movements (Kim et al., 2017a). However, here is still debate as to whether this type of high frequency firing is present in Mthal under normal physiological conditions and if (or how) it correlates with movement (Edgerton & Jaeger, 2014).

The BG LFP suggest a unique role for beta oscillations in utilizing directional cues and speeding RT (Leventhal et al., 2012). Beta oscillation patterns are mirrored in cortex, suggesting that they resonate throughout the entire BG-thalamocortical circuit, however, Mthal has not been specifically studied.

Cerebellar Modulation of Mthal. Although less studied, the cerebellum has gained considerable appreciation for its role in motor function, specifically, tasks involving sequences and rigid timing criteria (Koekkoek et al., 2003; Manto et al., 2012). Therapies for PD that are anatomically focused on cerebellar circuitry (Lewis et al., 2013), along with other movement disorders that are of distinct cerebellar origin (Bares et al., 2007; Ivry, 1997), highlight an undeniable role for the cerebellum in mediating normal motor function. BG-cerebellar interactions have been characterized in the past as occurring purely through overlapping circuit loops, implicating Mthal and cortex as key regions of interplay (Middleton & Strick, 2000). However, more direct subcortical pathways are challenging how we think about these circuits from a behavioral and pathological perspective (Bostan, Dum, & Strick, 2010). Included in this conversation is the notion that cerebellar circuitry is well suited for low-latency movement initiation either through Mthal or brainstem circuits (Thach, 2014; Bareš et al., 2018), which has long been considered a function computed and implemented solely by the BG (Donahue & Kreitzer, 2015). Therefore, while it is likely that the cerebellum influences Mthal during movement initiation, it has since not been a topic of prior investigation.

Research Value. Despite being central to the convergence of several important motor structures, the neural correlates of behavior are not well understood in Mthal. Competing models have yet to build sufficient bridges from single unit activity to neural oscillations, potentially limiting progress towards better theories of how motor behaviors are executed. Addressing these basic circuit questions in healthy animals establishes an important point of contrast to pathological states, and aids in addressing optimal routes of therapy for several movement disorders.

Specific Aims

Specific Aim 1: Determine the behavioral correlates of single unit activity in Mthal.

Hypothesis: Mthal encodes direction and vigor at movement onset and is continually active through movement execution.

Specific Aim 2-A: Determine the behavioral correlates of LFP activity in Mthal.

Hypothesis: Consistent with recordings from the BG, Mthal beta oscillations occur after movement onset and correlate with RT.

Specific Aim 2-B: Determine the Spike-LFP and LFP-LFP interactions in Mthal.

Hypothesis: Low-frequency oscillations phase-lock to the task timing structure, modulate single unit spiking, and comodulate higher frequency oscillations through PAC.

Specific Aim 3: Independently isolate BG and cerebellar afferents in Mthal using optogenetic tools.

Hypothesis: BG and cerebellar regions of Mthal can be targeted using a synapsin-promoted viral construct injected into the respective upstream structures.

To achieve these aims, I used a previously established two-alternative forced choice task where a rat is rewarded after successfully poking its nose from a center port to a side port with

the direction being based on the pitch of an instructional tone (Leventhal et al., 2012). The behavior is cued, ballistic, and lateralized, offering a rich data set to investigate behavioral correlates of the accompanying physiology. I also developed a high-density recording array comprised either of tetrodes or single electrodes that were implanted on a drivable platform capable of recording single unit and LFP activity in Mthal over multiple days (Figure 1-4).

Figures

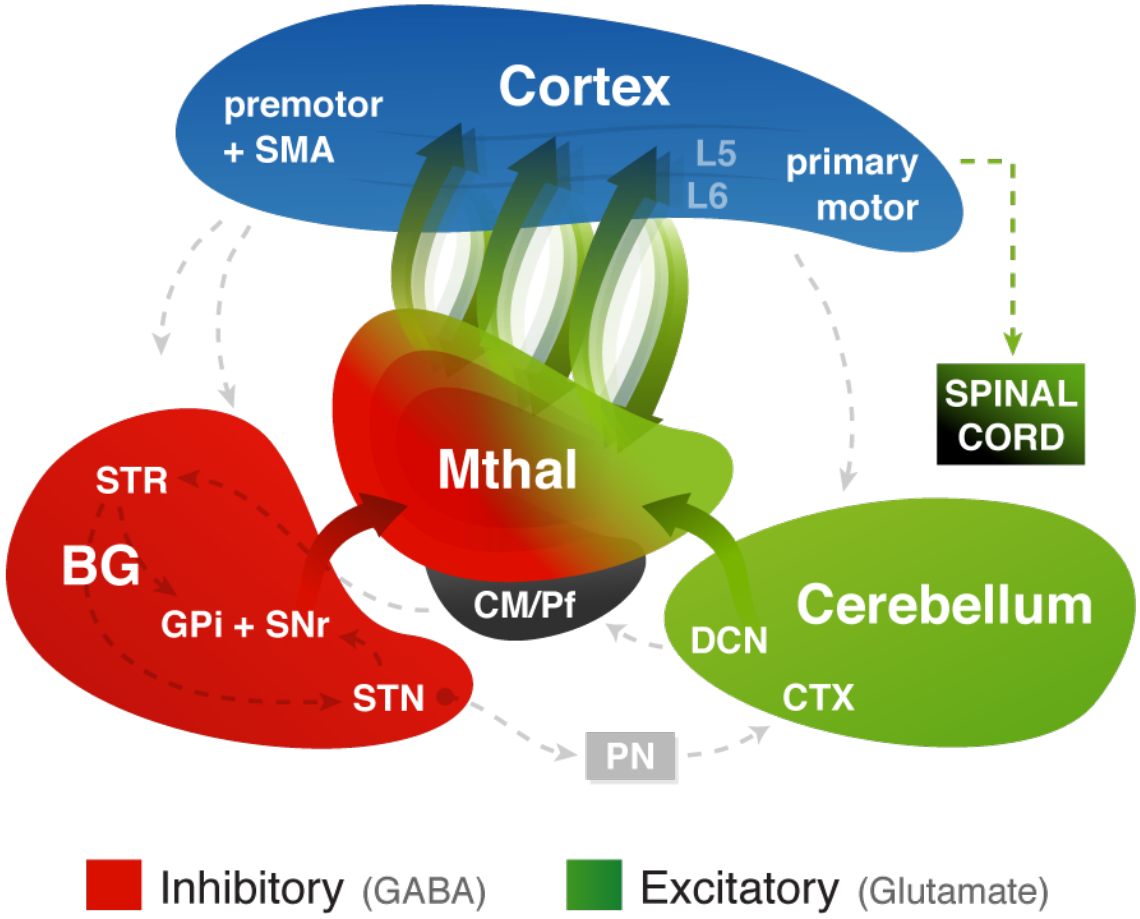

Figure 1-1: Motor thalamic functional anatomy schematic

A simplified functional-anatomical schematic of motor thalamic (Mthal) pathways between the cortex, basal ganglia (BG), and cerebellum. The primary subcortical inputs are the BG and cerebellum, which are themselves connected via two disynaptic pathways: the subthalamic nucleus (STN) to the pontine nuclei (PN) to the cerebellar cortex (CTX), and the deep cerebellar nuclei (DCN) to the central median/parafascicular nuclei of the thalamus (CM/Pf) to the striatum (STR). The BG project to ventromedial Mthal via the globus pallidus internus (GPi) and substantia nigra pars reticulata (SNr). The cerebellum projects to ventral anterior/ventral lateral Mthal from via the DCN. In general, reciprocal connections between Mthal and premotor, supplementary motor area (SMA), and primary motor areas of the cortex terminate in layer 5 (L5) and are projected back to Mthal by layer 6 (L6). The primary motor cortex (L5) influences movement via the spinal cord pathway.

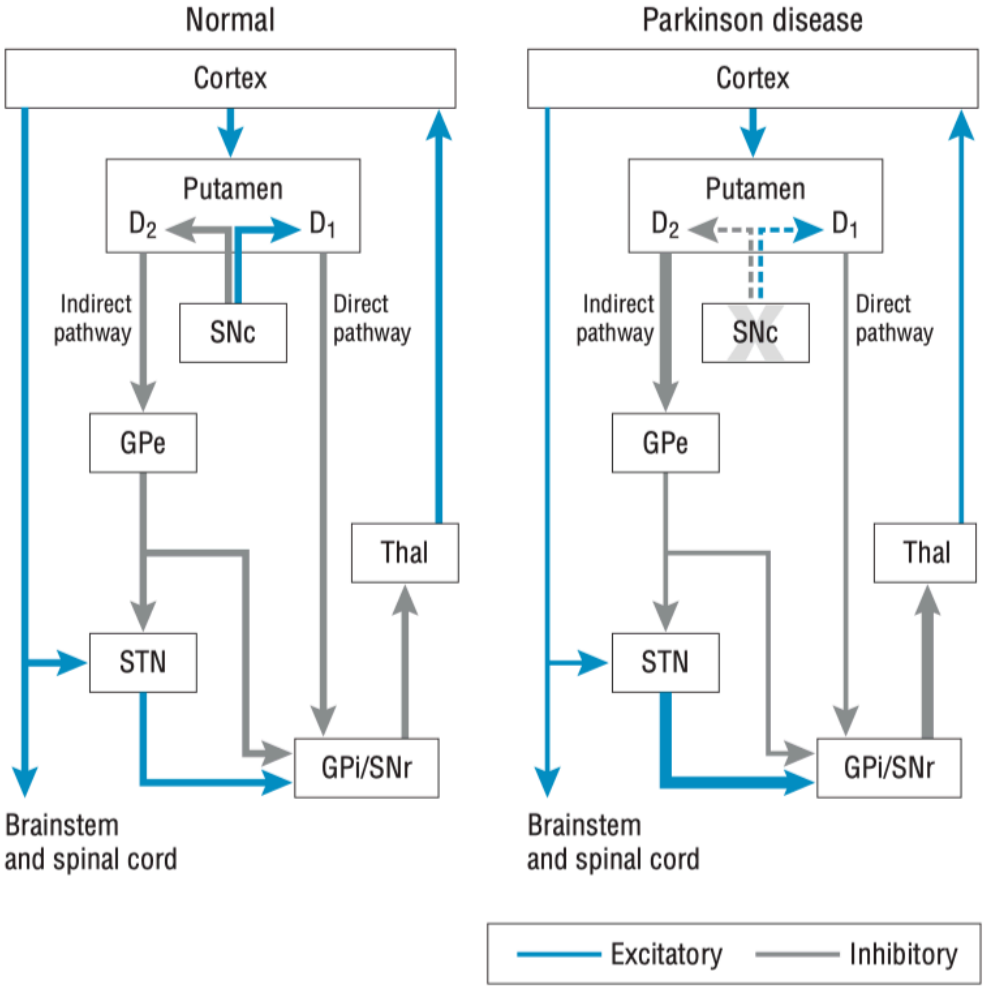

Figure 1-2: Basal ganglia-thalamo-cortical circuit schematic in the normal and parkinsonian states

Thickness of the arrows indicates strength of the connections. Loss of substantia nigra neurons leads to increased thalamic inhibition. The diagram does not account for firing pattern and oscillatory activity, both of which are important factors in understanding the effects of deep brain stimulation on the network. D_1 and D_2 indicate postsynaptic dopamine receptor type; GPe, globus pallidus externus; GPi, globus pallidus internus; SNc, substantia nigra pars compacta; SNr, substantia nigra pars reticulata; STN, subthalamic nucleus; and Thal, thalamus. Figure source: Miocinovic, Somayajula, Chitnis, & Vitek, 2013

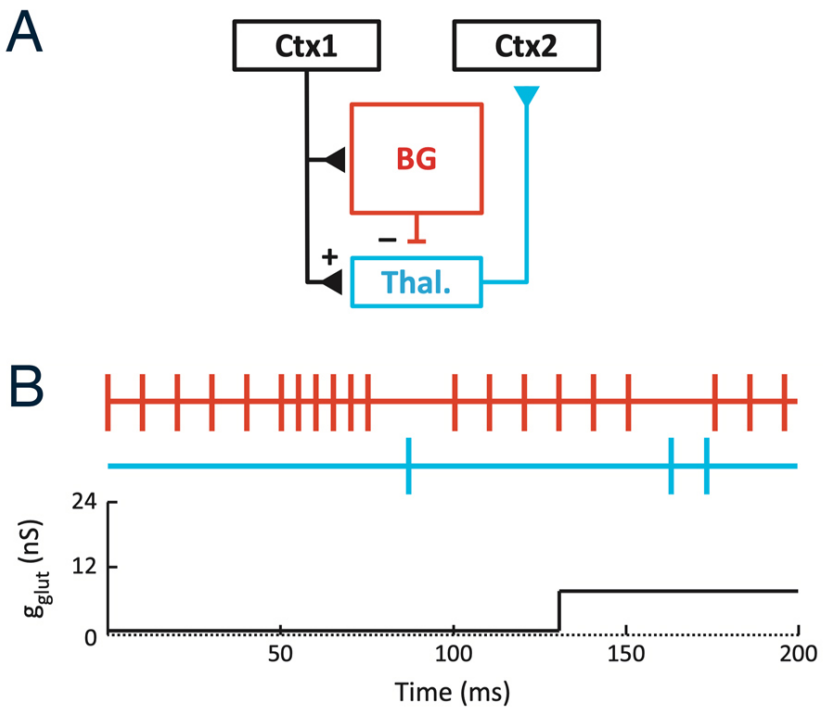

Figure 1-3: Model of connections that regulate thalamic firing

(A) The basal ganglia (BG) inhibit the thalamus (Thal) while descending cortical structures (Ctx1) modulate glutamate to influence efferent Thal spiking to cortex (Ctx2). **(B)** Simulation postsynaptic thalamic spike train (blue trace) during rebound (middle) and gating/entrainment (right) modes of BG–thalamic transmission as a function of excitatory glutamatergic conductance (g_{glut}). Red trace indicates pallidal spike train from the BG. Modified from: Goldberg, Farries, & Fee, 2013

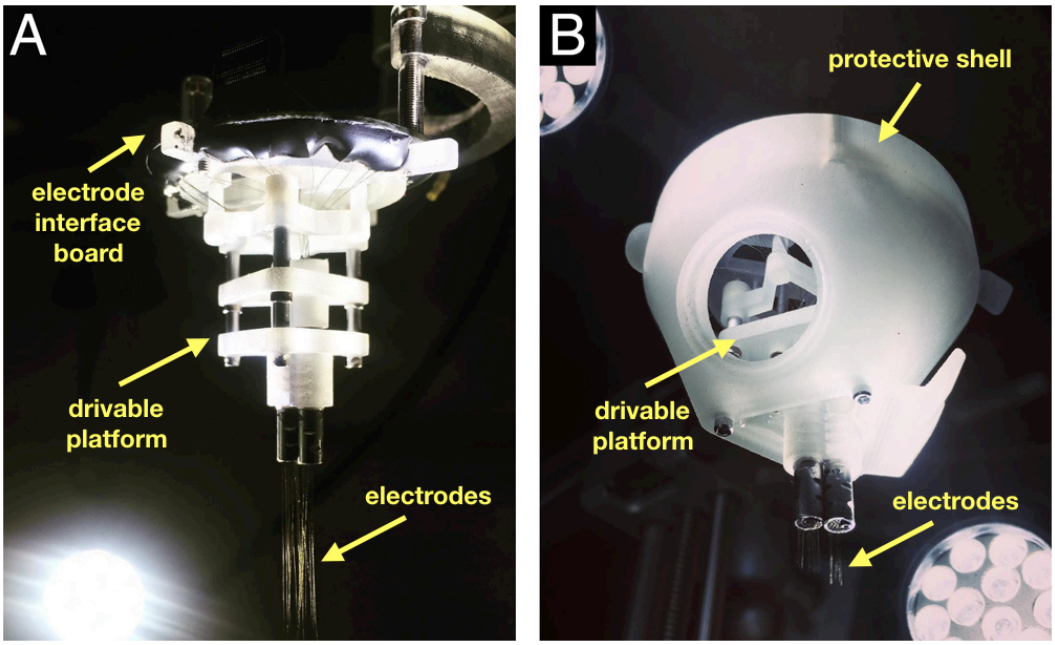

Figure 1-4: 3D printed neural implant

(A) The internal driving mechanism responsible for shuttling electrodes into the brain. The electrode interface board sends signals to a computer through an amplifier. **(B)** The same mechanism in (A), visible through a circular window, encased in a protective shell.

References

Albin, R. L., Young, A. B., & Penney, J. B. (1989). The functional anatomy of basal ganglia disorders. *Trends Neurosci*, *12*, 366-375.

Ames, K. C., Ryu, S. I., & Shenoy, K. V. (2014). Neural dynamics of reaching following incorrect or absent motor preparation. *Neuron*, *81*, 438-451.

Arce-McShane, F. I., Ross, C. F., Takahashi, K., Sessle, B. J., & Hatsopoulos, N. G. (2016). Primary motor and sensory cortical areas communicate via spatiotemporally coordinated networks at multiple frequencies. *Proceedings of the National Academy of Sciences*, *113*(18), 5083-5088.

Arnal, L. H., Doelling, K. B., & Poeppel, D. (2015). Delta-Beta Coupled Oscillations Underlie Temporal Prediction Accuracy. *Cereb Cortex*, *25*(9), 3077-3085.

Aru, J., Aru, J., Priesemann, V., Wibral, M., Lana, L., Pipa, G. et al. (2015). Untangling cross-frequency coupling in neuroscience. *Curr Opin Neurobiol*, *31*, 51-61.

Baker, S. N., Kilner, J. M., Pinches, E. M., & Lemon, R. N. (1999). The role of synchrony and oscillations in the motor output. *Exp Brain Res*, *128*, 109-117.

Bar-Gad, I., & Bergman, H. (2001). Stepping out of the box: information processing in the neural networks of the basal ganglia. *Curr Opin Neurobiol*, *11*, 689-695.

Bareš, M., Apps, R., Avanzino, L., Breska, A., D'Angelo, E., Filip, P. et al. (2018). Consensus paper: Decoding the Contributions of the Cerebellum as a Time Machine. From Neurons to Clinical Applications. *Cerebellum*.

Bares, M., Lungu, O., Liu, T., Waechter, T., Gomez, C. M., & Ashe, J. (2007). Impaired predictive motor timing in patients with cerebellar disorders. *Exp Brain Res*, *180*, 355-365.

Basar, E. (2004). *Memory and brain dynamics: Oscillations integrating attention, perception, learning, and memory*. CRC press.

Bédard, C., Kröger, H., & Destexhe, A. (2004). Modeling extracellular field potentials and the frequency-filtering properties of extracellular space. *Biophys J*, *86*, 1829-1842.

Bosch-Bouju, C., Hyland, B. I., & Parr-Brownlie, L. C. (2013). Motor thalamus integration of cortical, cerebellar and basal ganglia information: implications for normal and parkinsonian conditions. *Front Comput Neurosci*, *7*, 163.

Bosch-Bouju, C., Smither, R. A., Hyland, B. I., & Parr-Brownlie, L. C. (2014). Reduced reach-related modulation of motor thalamus neural activity in a rat model of Parkinson's disease. *Journal of Neuroscience*, *34*(48), 15836-15850.

Bostan, A. C., Dum, R. P., & Strick, P. L. (2010). The basal ganglia communicate with the cerebellum. *Proc Natl Acad Sci U S A*, *107*, 8452-8456.

Bostan, A. C., & Strick, P. L. (2010). The cerebellum and basal ganglia are interconnected. *Neuropsychol Rev*, *20*, 261-270.

Brown, P. (2006). Bad oscillations in Parkinson's disease. *J Neural Transm Suppl*, 27-30.

Buzsáki, G. (2010). Neural syntax: cell assemblies, synapsembles, and readers. *Neuron*, *68*(3), 362-385.

Buzsáki, G., Logothetis, N., & Singer, W. (2013). Scaling brain size, keeping timing: evolutionary preservation of brain rhythms. *Neuron*, *80*(3), 751-764.

Buzsaki, G. (2006). *Rhythms of the Brain*. Oxford University Press.

Buzsáki, G., Anastassiou, C. A., & Koch, C. (2012). The origin of extracellular fields and currents--EEG, ECoG, LFP and spikes. *Nat Rev Neurosci*, *13*, 407-420.

Cain, S. M., & Snutch, T. P. (2012). T-type calcium channels in burst-firing, network synchrony, and epilepsy. *Biochim Biophys Acta*.

Canavier, C. C. (2015). Phase-resetting as a tool of information transmission. *Curr Opin Neurobiol*, *31*, 206-213.

Canolty, R. T., & Knight, R. T. (2010). The functional role of cross-frequency coupling. *Trends Cogn Sci*, *14*(11), 506-515.

Charles, A. C., Merrill, J. E., Dirksen, E. R., & Sanderson, M. J. (1991). Intercellular signaling in glial cells: calcium waves and oscillations in response to mechanical stimulation and glutamate. *Neuron*, *6*, 983-992.

Chen, C. H., Fremont, R., Arteaga-Bracho, E. E., & Khodakhah, K. (2014). Short latency cerebellar modulation of the basal ganglia. *Nat Neurosci*, *17*, 1767-1775.

Cheng, R.-K., Tipples, J., Narayanan, N. S., & Meck, W. H. (2016). Clock Speed as a Window into Dopaminergic Control of Emotion and Time Perception. *Timing & Time Perception*, *4*(1), 99-122.

Cif, L., & Hariz, M. (2017). Seventy years of pallidotomy for movement disorders. *Mov Disord*, *32*, 972-982.

Combrisson, E., Perrone-Bertolotti, M., Soto, J. L., Alamian, G., Kahane, P., Lachaux, J. P. et al. (2017). From intentions to actions: Neural oscillations encode motor processes through phase, amplitude and phase-amplitude coupling. *Neuroimage*, *147*, 473-487.

Crunelli, V., David, F., Lőrincz, M. L., & Hughes, S. W. (2015). The thalamocortical network as a single slow wave-generating unit. *Curr Opin Neurobiol*, *31*, 72-80.

DeLong, M. R. (1990). Primate models of movement disorders of basal ganglia origin. *Trends Neurosci*, *13*, 281-285.

Desmurget, M., & Turner, R. S. (2008). Testing basal ganglia motor functions through reversible inactivations in the posterior internal globus pallidus. *J Neurophysiol*, *99*, 1057-1076.

Devetiarov, D., Semenova, U., Usova, S., Tomskiy, A., Tyurnikov, V., Nizametdinova, D. et al. (2017). Neuronal activity patterns in the ventral thalamus: Comparison between Parkinson's disease and cervical dystonia. *Clin Neurophysiol*, *128*, 2482-2490.

Donahue, C. H., & Kreitzer, A. C. (2015). A Direct Path to Action Initiation. *Neuron*, *88*, 240-241.

Edgerton, J. R., & Jaeger, D. (2014). Optogenetic activation of nigral inhibitory inputs to motor thalamus in the mouse reveals classic inhibition with little potential for rebound activation. *Front Cell Neurosci*, *8*, 36.

Ellens, D. J., & Leventhal, D. K. (2013). Review: electrophysiology of basal ganglia and cortex in models of Parkinson disease. *J Parkinsons Dis*, *3*, 241-254.

Engel, A. K., & Fries, P. (2010). Beta-band oscillations--signalling the status quo? *Curr Opin Neurobiol*, *20*, 156-165.

Feingold, J., Gibson, D. J., DePasquale, B., & Graybiel, A. M. (2015). Bursts of beta oscillation differentiate postperformance activity in the striatum and motor cortex of monkeys performing movement tasks. *Proc Natl Acad Sci U S A*, *112*, 13687-13692.

Fiebelkorn, I. C., Snyder, A. C., Mercier, M. R., Butler, J. S., Molholm, S., & Foxe, J. J. (2013). Cortical cross-frequency coupling predicts perceptual outcomes. *Neuroimage*, *69*, 126-137.

Fields, R. D., Woo, D. H., & Basser, P. J. (2015). Glial Regulation of the Neuronal Connectome through Local and Long-Distant Communication. *Neuron*, *86*(2), 374-386.

Fries, P. (2005). A mechanism for cognitive dynamics: neuronal communication through neuronal coherence. *Trends Cogn Sci*, *9*, 474-480.

Galvan, A., Devergnas, A., Pittard, D., Masilamoni, G., Vuong, J., Daniels, J. S. et al. (2016). Lack of Antiparkinsonian Effects of Systemic Injections of the Specific T-Type Calcium Channel Blocker ML218 in MPTP-Treated Monkeys. *ACS Chem Neurosci*.

Galvan, A., Devergnas, A., & Wichmann, T. (2015). Alterations in neuronal activity in basal ganglia-thalamocortical circuits in the parkinsonian state. *Front Neuroanat*, *9*, 5.

Gantner, I. S., Bodart, O., Laureys, S., & Demertzi, A. (2013). Our rapidly changing understanding of acute and chronic disorders of consciousness: challenges for neurologists. *Future Neurology*, *8*(1), 43-54.

Garcia-Munoz, M., & Arbuthnott, G. W. (2015). Basal ganglia-thalamus and the "crowning enigma". *Front Neural Circuits*, *9*, 71.

Goldberg, J. H., Farries, M. A., & Fee, M. S. (2013). Basal ganglia output to the thalamus: still a paradox. *Trends Neurosci*.

Graybiel, A. M., & Grafton, S. T. (2015). The striatum: where skills and habits meet. *Cold Spring Harb Perspect Biol*, *7*, a021691.

Grillner, S. (2006). Biological pattern generation: the cellular and computational logic of networks in motion. *Neuron*, *52*(5), 751-766.

Güntekin, B., Hanoğlu, L., Güner, D., Yılmaz, N. H., Çadırcı, F., Mantar, N. et al. (2018). Cognitive Impairment in Parkinson's Disease Is Reflected with Gradual Decrease of EEG Delta Responses during Auditory Discrimination. *Front Psychol*, *9*, 170.

Guo, Y., Park, C., Worth, R. M., & Rubchinsky, L. L. (2013). Basal ganglia modulation of thalamocortical relay in Parkinson's disease and dystonia. *Front Comput Neurosci*, *7*, 124.

Guo, Y., Rubin, J. E., McIntyre, C. C., Vitek, J. L., & Terman, D. (2008). Thalamocortical relay fidelity varies across subthalamic nucleus deep brain stimulation protocols in a data-driven computational model. *J Neurophysiol*, *99*, 1477-1492.

Haegens, S., & Zion Golumbic, E. (2018). Rhythmic facilitation of sensory processing: A critical review. *Neurosci Biobehav Rev*, *86*, 150-165.

Hamel-Thibault, A., Thénault, F., Whittingstall, K., & Bernier, P. M. (2018). Delta-Band Oscillations in Motor Regions Predict Hand Selection for Reaching. *Cereb Cortex*, *28*(2), 574-584.

Heiney, S. A., Kim, J., Augustine, G. J., & Medina, J. F. (2014). Precise control of movement kinematics by optogenetic inhibition of Purkinje cell activity. *J Neurosci*, *34*, 2321-2330.

Herkenham, M. (1980). Laminar organization of thalamic projections to the rat neocortex. *Science*, *207*, 532-535.

Hintzen, A., Pelzer, E. A., & Tittgemeyer, M. (2017). Thalamic interactions of cerebellum and basal ganglia. *Brain Struct Funct*.

Horak, F. B., & Anderson, M. E. (1984). Influence of globus pallidus on arm movements in monkeys. I. Effects of kainic acid-induced lesions. *J Neurophysiol*, *52*, 290-304.

Ivry, R. (1997). Cerebellar timing systems. *International review of neurobiology*, 555-573.

Jacobs, J., Kahana, M. J., Ekstrom, A. D., & Fried, I. (2007). Brain oscillations control timing of single-neuron activity in humans. *J Neurosci*, *27*, 3839-3844.

Jones, C. R., Malone, T. J., Dirnberger, G., Edwards, M., & Jahanshahi, M. (2008). Basal ganglia, dopamine and temporal processing: performance on three timing tasks on and off medication in Parkinson's disease. *Brain Cogn*, *68*(1), 30-41.

Joundi, R. A., Jenkinson, N., Brittain, J. S., Aziz, T. Z., & Brown, P. (2012). Driving oscillatory activity in the human cortex enhances motor performance. *Curr Biol*, *22*(5), 403-407.

Kayser, C., Montemurro, M. A., Logothetis, N. K., & Panzeri, S. (2009). Spike-phase coding boosts and stabilizes information carried by spatial and temporal spike patterns. *Neuron*, *61*, 597-608.

Kelly, R. C., Smith, M. A., Kass, R. E., & Lee, T. S. (2010). Local field potentials indicate network state and account for neuronal response variability. *J Comput Neurosci*, *29*(3), 567-579.

Kim, J., Kim, Y., Nakajima, R., Shin, A., Jeong, M., Park, A. H. et al. (2017a). Inhibitory Basal Ganglia Inputs Induce Excitatory Motor Signals in the Thalamus. *Neuron*, *95*, 1181-1196.e8.

Kim, Y. C., Han, S. W., Alberico, S. L., Ruggiero, R. N., De Corte, B., Chen, K. H. et al. (2017b). Optogenetic Stimulation of Frontal D1 Neurons Compensates for Impaired Temporal Control of Action in Dopamine-Depleted Mice. *Curr Biol*, *27*(1), 39-47.

Koekkoek, S. K., Hulscher, H. C., Dortland, B. R., Hensbroek, R. A., Elgersma, Y., Ruigrok, T. J. et al. (2003). Cerebellar LTD and learning-dependent timing of conditioned eyelid responses. *Science*, *301*(5640), 1736-1739.

Kösem, A., Gramfort, A., & van Wassenhove, V. (2014). Encoding of event timing in the phase of neural oscillations. *Neuroimage*, *92*, 274-284.

Kühn, A. A., Brücke, C., Hübl, J., Schneider, G.-H., Kupsch, A., Eusebio, A. et al. (2008). Motivation modulates motor-related feedback activity in the human basal ganglia. *Current Biology*, *18*(15), R648-R650.

Kuramoto, E., Fujiyama, F., Nakamura, K. C., Tanaka, Y., Hioki, H., & Kaneko, T. (2011). Complementary distribution of glutamatergic cerebellar and GABAergic basal ganglia afferents to the rat motor thalamic nuclei. *Eur J Neurosci*, *33*, 95-109.

Kuramoto, E., Ohno, S., Furuta, T., Unzai, T., Tanaka, Y. R., Hioki, H. et al. (2015). Ventral medial nucleus neurons send thalamocortical afferents more widely and more preferentially to layer 1 than neurons of the ventral anterior-ventral lateral nuclear complex in the rat. *Cereb Cortex*, *25*, 221-235.

Lakatos, P., Shah, A. S., Knuth, K. H., Ulbert, I., Karmos, G., & Schroeder, C. E. (2005). An oscillatory hierarchy controlling neuronal excitability and stimulus processing in the auditory cortex. *J Neurophysiol*, *94*, 1904-1911.

Lee, H. S., Ghetti, A., Pinto-Duarte, A., Wang, X., Dziewczapolski, G., Galimi, F. et al. (2014). Astrocytes contribute to gamma oscillations and recognition memory. *Proc Natl Acad Sci U S A*, *111*(32), E3343-52.

Lee, K. H., Mathews, P. J., Reeves, A. M. B., Choe, K. Y., Jami, S. A., Serrano, R. E. et al. (2015). Circuit mechanisms underlying motor memory formation in the cerebellum. *Neuron*, *86*, 529-540.

Leventhal, D. K., Gage, G. J., Schmidt, R., Pettibone, J. R., Case, A. C., & Berke, J. D. (2012). Basal Ganglia Beta oscillations accompany cue utilization. *Neuron*, *73*, 523-536.

Lewis, M. M., Galley, S., Johnson, S., Stevenson, J., Huang, X., & McKeown, M. J. (2013). The Role of the Cerebellum in the Pathophysiology of Parkinson's Disease. *The Canadian Journal of Neurological Sciences*, *40*(03), 299-306.

Lisman, J. E., & Jensen, O. (2013). The θ-γ neural code. *Neuron*, *77*(6), 1002-1016.

Little, S., Pogosyan, A., Neal, S., Zavala, B., Zrinzo, L., Hariz, M. et al. (2013). Adaptive deep brain stimulation in advanced Parkinson disease. *Ann Neurol*, *74*, 449-457.

Manto, M., Bower, J. M., Conforto, A. B., Delgado-García, J. M., da Guarda, S. N., Gerwig, M. et al. (2012). Consensus paper: roles of the cerebellum in motor control--the diversity of ideas on cerebellar involvement in movement. *Cerebellum*, *11*(2), 457-487.

Marder, E., & Calabrese, R. L. (1996). Principles of rhythmic motor pattern generation. *Physiol Rev*, *76*(3), 687-717.

Marsden, C. D., & Obeso, J. A. (1994). The functions of the basal ganglia and the paradox of stereotaxic surgery in Parkinson ' s disease. *Brain*, *117*, 877-897.

Martinez-Banaclocha, M. (2018). Ephaptic Coupling of Cortical Neurons: Possible Contribution of Astroglial Magnetic Fields. *Neuroscience*, *370*, 37-45.

Middleton, F. A., & Strick, P. L. (2000). Basal ganglia and cerebellar loops: motor and cognitive circuits. *Brain Res Brain Res Rev*, *31*, 236-250.

Mink, J. W. (1996). The basal ganglia: focused selection and inhibition of competing motor programs. *Prog Neurobiol*, *50*, 381-425.

Miocinovic, S., Somayajula, S., Chitnis, S., & Vitek, J. L. (2013). History, applications, and mechanisms of deep brain stimulation. *JAMA Neurol*, *70*, 163-171.

Molnar, G. F., Pilliar, A., Lozano, A. M., & Dostrovsky, J. O. (2005). Differences in neuronal firing rates in pallidal and cerebellar receiving areas of thalamus in patients with Parkinson's disease, essential tremor, and pain. *J Neurophysiol*, *93*, 3094-3101.

Muralidharan, A., Zhang, J., Ghosh, D., Johnson, M. D., Baker, K. B., & Vitek, J. L. (2017). Modulation of Neuronal Activity in the Motor Thalamus during GPi-DBS in the MPTP Nonhuman Primate Model of Parkinson's Disease. *Brain Stimul*, *10*, 126-138.

Murthy, V. N., & Fetz, E. E. (1996). Oscillatory activity in sensorimotor cortex of awake monkeys: synchronization of local field potentials and relation to behavior. *J Neurophysiol*, *76*, 3949-3967.

Nakamura, K. C., Sharott, A., & Magill, P. J. (2014). Temporal coupling with cortex distinguishes spontaneous neuronal activities in identified basal ganglia-recipient and cerebellar-recipient zones of the motor thalamus. *Cereb Cortex*, *24*(1), 81-97.

Panigrahi, B., Martin, K. A., Li, Y., Graves, A. R., Vollmer, A., Olson, L. et al. (2015). Dopamine Is Required for the Neural Representation and Control of Movement Vigor. *Cell*, *162*, 1418-1430.

Parker, K. L., Chen, K. H., Kingyon, J. R., Cavanagh, J. F., & Narayanan, N. S. (2015). Medial frontal ~4-Hz activity in humans and rodents is attenuated in PD patients and in rodents with cortical dopamine depletion. *J Neurophysiol*, *114*(2), 1310-1320.

Penny, W. D., Duzel, E., Miller, K. J., & Ojemann, J. G. (2008). Testing for nested oscillation. *J Neurosci Methods*, *174*(1), 50-61.

Pessiglione, M., Guehl, D., Rolland, A.-S. S., François, C., Hirsch, E. C., Féger, J. et al. (2005). Thalamic neuronal activity in dopamine-depleted primates: evidence for a loss of functional segregation within basal ganglia circuits. *J Neurosci*, *25*, 1523-1531.

Pfurtscheller, G., Zalaudek, K., & Neuper, C. (1998). Event-related beta synchronization after wrist, finger and thumb movement. *Electroencephalogr Clin Neurophysiol*, *109*, 154-160.

Pogosyan, A., Gaynor, L. D., Eusebio, A., & Brown, P. (2009). Boosting cortical activity at Beta-band frequencies slows movement in humans. *Curr Biol*, *19*, 1637-1641.

Rubino, D., Robbins, K. A., & Hatsopoulos, N. G. (2006). Propagating waves mediate information transfer in the motor cortex. *Nat Neurosci*, *9*, 1549-1557.

Saleh, M., Reimer, J., Penn, R., Ojakangas, C. L., & Hatsopoulos, N. G. (2010). Fast and slow oscillations in human primary motor cortex predict oncoming behaviorally relevant cues. *Neuron*, *65*, 461-471.

Sanes, J. N., & Donoghue, J. P. (1993). Oscillations in local field potentials of the primate motor cortex during voluntary movement. *Proc Natl Acad Sci U S A*, *90*, 4470-4474.

Scharnowski, F., Rees, G., & Walsh, V. (2013). Time and the brain: neurorelativity. *Trends in Cognitive Sciences*, *17*(2), 51-52.

Schmidt, R., Leventhal, D. K., Mallet, N., Chen, F., & Berke, J. D. (2013). Canceling actions involves a race between basal ganglia pathways. *Nat Neurosci*, *16*, 1118-1124.

Schroeder, C. E., & Lakatos, P. (2009). Low-frequency neuronal oscillations as instruments of sensory selection. *Trends Neurosci*, *32*(1), 9-18.

Seeger-Armbruster, S., Bosch-Bouju, C., Little, S. T. C., Smither, R. A., Hughes, S. M., Hyland, B. I. et al. (2015). Patterned, but not tonic, optogenetic stimulation in motor thalamus improves reaching in acute drug-induced parkinsonian rats. *J Neurosci*, *35*, 1211-1216.

Serizawa, K., Kamei, S., Morita, A., Hara, M., Mizutani, T., Yoshihashi, H. et al. (2008). Comparison of quantitative EEGs between Parkinson disease and age-adjusted normal controls. *J Clin Neurophysiol*, *25*(6), 361-366.

Sherman, S. M. (2001). Tonic and burst firing: dual modes of thalamocortical relay. *Trends Neurosci*, *24*, 122-126.

Siegel, M., Donner, T. H., & Engel, A. K. (2012). Spectral fingerprints of large-scale neuronal interactions. *Nat Rev Neurosci*, *13*(2), 121-134.

Singer, W. (1999). Neuronal synchrony: a versatile code for the definition of relations? *Neuron*, *24*, 49-65,111.

Singer, W. (2017). Neuronal oscillations: unavoidable and useful. *Eur J Neurosci*.

Stefanics, G., Hangya, B., Hernádi, I., Winkler, I., Lakatos, P., & Ulbert, I. (2010). Phase entrainment of human delta oscillations can mediate the effects of expectation on reaction speed. *J Neurosci*, *30*, 13578-13585.

Steriade, M. (2006). Grouping of brain rhythms in corticothalamic systems. *Neuroscience*, *137*(4), 1087-1106.

Thach, W. T. (2014). Does the cerebellum initiate movement. *The Cerebellum*, *13*(1), 139-150.

Turner, R. S., & Desmurget, M. (2010). Basal ganglia contributions to motor control: a vigorous tutor. *Curr Opin Neurobiol*, *20*, 704-716.

Tzagarakis, C., Ince, N. F., Leuthold, A. C., & Pellizzer, G. (2010). Beta-band activity during motor planning reflects response uncertainty. *J Neurosci*, *30*, 11270-11277.

Wichmann, T., & Soares, J. (2006). Neuronal firing before and after burst discharges in the monkey basal ganglia is predictably patterned in the normal state and altered in parkinsonism. *J NEUROPHYSIOL*, *95*, 2120-2133.

Womelsdorf, T., Schoffelen, J.-M. M., Oostenveld, R., Singer, W., Desimone, R., Engel, A. K. et al. (2007). Modulation of neuronal interactions through neuronal synchronization. *Science*, *316*, 1609-1612.

Wyart, V., de Gardelle, V., Scholl, J., & Summerfield, C. (2012). Rhythmic fluctuations in evidence accumulation during decision making in the human brain. *Neuron*, *76*(4), 847-858.

Xu, W., Russo, G. S., Hashimoto, T., Zhang, J., & Vitek, J. L. (2008). Subthalamic nucleus stimulation modulates thalamic neuronal activity. *J Neurosci*, *28*, 11916-11924.

Yamawaki, N., & Shepherd, G. M. G. (2015). Synaptic circuit organization of motor corticothalamic neurons. *J Neurosci*, *35*, 2293-2307.

CHAPTER 2: Distinct Populations of Motor Thalamic Neurons Encode Action Initiation, Action Selection, And Movement Vigor

Co-authored by Amy Hurst, Christopher Cyr, and Daniel K. Leventhal — Published in Journal of Neuroscience 2018

Abstract

Motor thalamus (Mthal) comprises the ventral anterior, ventral lateral, and ventral medial thalamic nuclei in rodents. This subcortical hub receives input from the basal ganglia (BG), cerebellum, and reticular thalamus in addition to connecting reciprocally with motor cortical regions. Despite the central location of Mthal, the mechanisms by which it influences movement remain unclear. To determine its role in generating ballistic, goal-directed movement, we recorded single unit Mthal activity as male rats performed a two-alternative forced choice task. A large population of Mthal neurons increased their firing briefly near movement initiation and could be segregated into functional groups based on their behavioral correlates. The activity of "initiation" units was more tightly locked to instructional cues than movement onset, did not predict which direction the rat would move, and was anti-correlated with reaction time (RT). Conversely, the activity of "execution" units was more tightly locked to movement onset than instructional cues, predicted which direction the rat would move, and was anti-correlated with both RT and movement time (MT). These results suggest that Mthal influences choice RT performance in two stages: short latency, nonspecific action initiation followed by action selection/invigoration. We discuss the implications of these results for models of motor control incorporating BG and cerebellar circuits.

Introduction

The basal ganglia (BG) are implicated in action initiation, action selection, and movement vigor. BG neurons exhibit sharp responses as movements are initiated (Thorn et al., 2010) or suppressed (Schmidt et al., 2013), and selectively manipulating BG activity can provoke or suppress movement (Kravitz et al., 2010). Single unit BG activity reflects the selection of lateralized alternatives (i.e., left or right head movements or saccades) (Lauwereyns et al., 2002; Gage et al., 2010; Schmidt et al., 2013), BG manipulations bias action selection (Yamamoto et al., 2012; Leventhal et al., 2014; Hamid et al., 2016), and modeling studies suggest circuit-level mechanisms by which the BG could implement action selection (Maia and Frank, 2011). A BG role in regulating vigor, which can be conceptualized as the effort one is willing to exert in pursuit of a goal (Summerside et al., 2018), is suggested by the bradykinesia of Parkinson Disease and many basic investigations (Horak and Anderson, 1984b; Mink and Thach, 1991; Bastian et al., 2003; Desmurget and Turner, 2010; Panigrahi et al., 2015; Albin and Leventhal, 2017; Thura and Cisek, 2017). For example, BG activity is correlated with decision urgency (Thura and Cisek, 2017) and movement velocity (Panigrahi et al., 2015).

The BG project to motor thalamus (Mthal), which presumably transmits action initiation, selection, and/or vigor signals to corticospinal tracts. Standard "rate" models of BG-thalamocortical interactions suggest that GABAergic BG output tonically suppresses Mthal, which is released to generate movement when BG output pauses (Albin et al., 1989; DeLong, 1990). While this model makes many accurate predictions, it is incomplete (Ellens and Leventhal, 2013). Consistent with rate models, BG output lesions improve parkinsonism. However, they also treat hyperkinetic movement disorders (Cif and Hariz, 2017). High frequency stimulation of basal ganglia output nuclei, which likely activates efferent axons

(Hashimoto et al., 2003; McIntyre et al., 2004; Boulet et al., 2006; Chiken and Nambu, 2016; Xiao et al., 2018), has clinical effects similar to lesions. Furthermore, suppressing BG output consistently slows movement, in direct opposition to rate model predictions (Horak and Anderson, 1984b; Mink and Thach, 1991; Bastian et al., 2003; Desmurget and Turner, 2010).

Corticothalamic (Yamawaki and Shepherd, 2015; Galvan et al., 2016) and cerebellothalamic (Kuramoto et al., 2011) connections also strongly influence Mthal activity (Bosch-Bouju et al., 2013; Guo et al., 2017). Cortical layer V projection neurons send collaterals to Mthal, and layer VI neurons project both directly and indirectly via reticular thalamus to Mthal (Bosch-Bouju et al., 2013). Deep cerebellar nuclear (DCN) projections form strong perisomatic "driver-like" synapses on thalamocortical neurons that are largely distinct from BG-recipient neurons (Kuramoto et al., 2011; Rovó et al., 2012). These cortical, reticular thalamic, and cerebellar inputs are potential sources of divergence between BG output and Mthal activity. The precise behavioral function(s) of Mthal, as well as the mechanisms by which they are implemented, therefore remain unclear.

To study Mthal contributions to ballistic movement, we recorded single unit Mthal activity as rats performed a BG-dependent two-alternative forced choice task in which the pitch of an auditory cue instructs rats to move left or right (Carli et al., 1985; Dowd and Dunnett, 2005; Leventhal et al., 2012, 2014). In a stop-signal task with an identical forced-choice component, BG output decreases at movement onset, and remains low throughout movement (Schmidt et al., 2013). We therefore hypothesized that Mthal activity would be elevated throughout movement, predict which action is selected, and predict how quickly the rat completes the task. While our results partially agreed with our predictions, we found a complex

pattern of neuronal modulation suggesting that action initiation and invigoration are mediated by distinct populations of Mthal neurons.

Results

Motor thalamic modulation at movement onset. We trained rats on a two-alternative forced-choice task that strongly modulates BG activity (Schmidt et al., 2013) and depends on intact BG function (Leventhal et al., 2014). Rats were cued to poke and hold in one of the three center ports in a five-port behavior chamber for a variable interval, then directed one port to the left or right by the pitch of an instructional cue (Figure 2-1A, B). Choice accuracy (77 ± 17% during recording sessions), reaction time (RT) distributions, and movement time (MT) distributions were consistent with previous results (Schmidt et al., 2013; Leventhal et al., 2014) (Fig 1C). Once well-trained, rats were implanted with microelectrodes targeting Mthal.

To determine the behavioral correlates of Mthal activity, peri-event time histograms (PETHs) of single unit Z-scored firing rates were constructed and collapsed into a peri-event heatmap (Figure 2-2-2). The two non-adjacent events to which each unit responded most strongly were designated the "primary" (strongest response) and "secondary" (second strongest response) events for that unit. Units that failed to achieve an absolute Z-score of at least 1 were classified as non-responsive (N.R., 64/313, Figures 2B, 3A). Most task-responsive units (96%) were classified based on a positive Z-score (i.e., a peri-event increase in firing rate). Notably, 57% of all units were either primary or secondary Tone or Nose Out units, meaning that they were highly modulated when the rat decided which direction to move and quickly initiated that movement. These firing rate modulations were brief, returning to baseline or lower before the lateral movement completed ("Side In"). This result is inconsistent with a strict rate model, and suggests that Mthal may be required to initiate, but not sustain, movement.

While Tone and Nose Out units were modulated closely in time, they were preferentially time-locked to qualitatively different events. We further evaluated whether Tone and Nose Out units might represent functionally distinct populations by examining the distribution of their secondary classes (Figures 2B and 3B). The secondary events of primary Tone units were fairly evenly distributed among other task events. However, primary Nose Out units were more likely than primary Tone units to be secondary Side Out units, when the rat is changing direction and moving quickly ($p = 1.9 \times 10^{-4}$, chi-square goodness of fit test comparing proportions of secondary Side Out units). This suggests that "Nose Out" units may have a general role in generating movement, while Tone unit activity is specifically linked to external cues.

Action selection in the motor thalamus. Activity in multiple BG nuclei is correlated with action selection (i.e., the choice to move left or right) in similar nose-poke tasks (Gage et al., 2010; Schmidt et al., 2013), and unilateral inactivation of BG nuclei or striatal dopaminergic manipulations bias action selection (Carli et al., 1985; Baunez et al., 2001; Dowd and Dunnett, 2005; Leventhal et al., 2014). We therefore examined if action selection signals were transmitted through Mthal.

To determine if Mthal encodes movement direction, we subtracted mean peri-event z-scores for ipsilateral movements from those for contralateral movements (Figure 2-4), and determined the fraction of units at each moment whose firing rates correlated with movement direction (Figure 2-4B) (Schmidt et al., 2013). Directional coding increased earlier for contraversive than ipsiversive movements - contraversive selectivity peaked 140 ms after Nose Out while ipsiversive selectivity peaked 200 ms after Nose Out. The maximum fraction of units coding movement direction within any time bin was 24%, also occurring 200 ms after Nose Out.

Thus, Mthal strongly encodes movement direction, but not until just before movement initiation, suggesting that Mthal drives lateralized movement.

We next examined the functional characteristics of individual "directionally selective" units, defined by direction-specific activity for at least 2 consecutive time bins (40 ms) around the Nose Out event (Figure 2-4C). Mthal activity tended to correlate with the direction moved rather than the direction cued on the infrequent occasions that rats moved the wrong direction (14/21 directionally selective units with greater than 5 incorrect trials exhibited movement-correlated rather than instruction-correlated activity), suggesting that directionally-selective Mthal activity is linked to movement and not auditory perception. This is further supported by the observation that Nose Out units were more likely to be directionally selective than Tone units (39% of Nose Out units vs. 18% of Tone units were directionally selective, Figure 2-4D, $p = 1.6 \times 10^{-8}$). However, individual units frequently encoded opposite directions at the Nose- and Side-Out events (57% of units with concordant directional selectivity, $p = 0.17$ against the null hypothesis of 50% concordance). The median duration of single unit directional selectivity was 140 ms compared to the median MT of 258 ms. Therefore, Tone units may contribute to nonspecific aspects of movement initiation, after which Nose Out units provide a brief signal to drive movement to the left or right.

Motor thalamus encodes movement vigor. The BG are believed to play a critical role in appropriately invigorating or scaling movement (Desmurget and Turner, 2010; Dudman and Krakauer, 2016; Yttri and Dudman, 2016; Thura and Cisek, 2017). Movement vigor can be conceptualized as the metabolic cost of performing an action (Niv et al., 2007; Summerside et al., 2018). In the context of this forced-choice task, this metabolic cost should be related to how quickly rats initiate (RT) and execute (MT) their chosen action (Niv et al., 2007).

If the directional selectivity we observed in Mthal results from selective movement invigoration in one direction, then the activity of directionally selective, but not non-directionally selective, units should predict RT and MT. To investigate this possibility, we superimposed RT and MT on single trial rasters separately for directionally and non-directionally selective units around the Nose Out event (Figure 2-5). We then asked whether there was a relationship between trial-by-trial activity and RT/MT.

The RT distribution was divided into three regions (Noorani and Carpenter, 2011). The first is a set of very short RTs (< 50 ms, gray overlays at the top of the rasters in Figure 2-5A, B) that likely represents "express" movements in which the rat anticipated, rather than responded to, the instructional cue (Carpenter and Williams, 1995). At very long RTs (> 350 ms, gray overlays at the bottom of the rasters in Figure 2-5A, B), motor thalamic activity no longer was modulated by the task. We therefore focused on the intermediate "main" RT distribution (89% of all trials, cyan-violet overlay in Figure 2-5A, B). Non-directionally selective Tone and Nose Out units showed a single firing peak just prior to the Nose Out event, consistent with the fact that most Tone units were not directionally selective. To our surprise, however, the activity of these units was strongly related to RT (Figure 2-5A). Their firing rates at Nose Out were anti-correlated with RT ($R^2 = 0.75$, $p = 1.1 \times 10^{-3}$). Furthermore, there was a decrease in firing several hundred ms prior to Nose Out whose depth was also related to RT ($R^2 = 0.78$, $p = 6.8 \times 10^{-4}$). Finally, for very short and long RT, the approximately linear relationship between RT and neural activity disappeared.

We performed a similar analysis on the relationship between non-directionally selective unit activity and MT (Figure 2-5C). As was the case for RT, units were not strongly modulated around the Nose Out event for very long MT (greater than ~400 ms). Because there is no express

component of MT distributions, we analyzed correlations between motor thalamic activity and MTs between 0 and 400 ms (88% of all trials). Unlike for RT, there was no relationship between the firing rate of non-directionally selective units and MT in the pre- or peri-Nose Out periods ($R^2 = 0.0048$, $p = 0.85$ and $R^2 = 0.12$, $p = 0.33$, respectively).

The activity of directionally selective units included an early peak before the Nose Out event similar to non-directionally selective units, and also a slightly later peak (Figure 2-5B). As for non-directionally selective units, activity around the Nose Out event was anti-correlated with RT ($R^2 = 0.85$, $p = 1.5 \times 10^{-4}$), and there was an early depression in their activity that predicted RT ($R^2 = 0.54$, $p = 0.016$). Critically, and in contrast to non-directionally selective units, the activity of directionally selective units strongly predicted MT in the peri-Nose Out period ($R^2 = 0.94$, $p = 4.4 \times 10^{-6}$) (Figure 2-5D). There was no relationship between firing rates prior to Nose Out and MT for directionally selective units ($R^2 = 0.0074$, $p = 0.81$).

In summary, we identified two groups of Mthal neurons whose firing patterns were strongly related to movement initiation and action selection/execution. The activity of one group tended to be more tightly locked to the instruction cue, did not predict movement direction, and predicted RT. The activity of the second group was more tightly locked to movement initiation, predicted movement direction, and predicted both RT and MT. These results suggest that the apparent directional selectivity of Mthal neurons reflects a "vigor" signal transmitted through this central motor hub. Furthermore, subpopulations of motor thalamic neurons subserve related but distinct roles in initiating and executing motor plans.

Single Unit Anatomy and Physiology. The BG and cerebellar-recipient thalamus are largely segregated in the rat, with ventral-anterior regions of Mthal more likely to receive BG afferents and dorsal-posterior regions more likely to receive cerebellar afferents (Deniau et al.,

1992; Kuramoto et al., 2011). We therefore asked if units with different behavioral correlates (i.e., event-responsiveness or directional selectivity) tended to aggregate in Mthal subregions. There was no apparent anatomic clustering of units based on their directional selectivity (Figure 2-6A) or primary event class (Figure 2-6B), though it is difficult to determine recording sites precisely since electrodes were moved between recording sessions. Furthermore, directionally and non-directionally selective units were indistinguishable by conventional physiologic measures (Figure 2-6C). This is consistent with previous reports that extracellular recordings are homogeneous across Mthal subregions, at least when animals are not engaged in a specific task. (Anderson and Turner, 1991; Nakamura et al., 2014).

Discussion

We found functionally distinct neuronal populations in Mthal whose activity changes briefly around movement onset. Units that did not encode movement direction were more likely to respond to the instruction/imperative cue, and predicted RT ("initiation" units). Conversely, units whose activity correlated with movement direction predicted RT and MT, and were more likely to respond at movement onset ("execution" units). These results suggest that RT and MT may not be interchangeable measures of "vigor," and are regulated via distinct subcortical mechanisms. Furthermore, Mthal influences choice RT performance in two stages: short latency, nonspecific action initiation followed by action selection/invigoration.

Similar to our data (Figure 2-2), in simple RT tasks with one response option, Mthal activity changes are distributed from just before to just after movement onset (Macpherson et al., 1980; Anderson and Turner, 1991; Nambu et al., 1991; van Donkelaar et al., 1999; Tanaka, 2007). While the duration of firing rate changes was not systematically examined in these studies, several units exhibited brief increases that returned to baseline before movement

completion (compare Figure 2 to Anderson and Turner, 1991, Figure 2-7B). In a choice RT task, Mthal units were modulated around movement onset, and elevated firing did not persist through movement completion (Butler et al., 1992; Forlano et al., 1993). In contrast, rat Mthal activity was briefly modulated near the grasping phase of a skilled reaching task (Bosch-Bouju et al., 2014). However, because reaches were spontaneous, it is difficult to determine precisely how Mthal activity was modulated at reach initiation. Collectively, these data suggest that phasic changes in Mthal activity occur at movement transitions, whether from rest to reaching or reaching to grasping.

A pulse of Mthal activity could propel motor cortex from a preparatory state into movement execution. Upon imperative cue presentation, population-level motor cortical activity evolves dynamically depending on the specific action being executed (Churchland et al., 2012). Similar to Mthal "initiation" units, a component of this activity is invariant across potential actions, predicts movement timing but not velocity, and precedes action-specific cortical activity (Kaufman et al., 2016). We speculate that "initiation" units trigger action-invariant components of movement-related cortical dynamics. "Execution" units then invigorate action-specific cortical population-level activity (Churchland et al., 2012). In both cases, Mthal modulations are early and brief relative to movement duration. In fact, many Tone and Nose Out units transiently decrease firing below baseline rates immediately after their event-related firing rate increase (see Figs. 2B and 5) (Tanaka, 2007; Bosch-Bouju et al., 2014). These observations are consistent with the idea that cortical dynamics evolve in a predetermined manner depending on their initial state (Churchland et al., 2010). This is analogous to pushing a pendulum, which behaves as a harmonic oscillator: its kinematics are uniquely determined by its initial state and the force with which it is pushed (unless acted upon again) (Dudman and Krakauer, 2016; Yttri and Dudman,

2018). This hypothesis should be testable by manipulating the timing of Mthal activation with respect to the onset of a ballistic movement. Such a mechanism may be important for pre-planned ballistic movements, as opposed to slower movements that require continuous adjustment (Tanaka, 2005).

The idea that precisely-timed pulses of Mthal activity regulate movement vigor may explain the apparent paradox that BG output lesions and high frequency stimulation slow movement in healthy subjects, speed movement in parkinsonian subjects (Bastian et al., 2003), and improve dyskinesias (Marsden and Obeso, 1994; Ellens and Leventhal, 2013). High frequency, bursty BG output in Parkinson Disease (Ellens and Leventhal, 2013; Galvan et al., 2015) could force persistent Mthal bursting (Zirh et al., 1998; Magnin et al., 2000; Guehl et al., 2003; Molnar et al., 2005; Pessiglione et al., 2005; Rubin et al., 2012; Kim et al., 2017) and prevent the natural evolution of cortical dynamics. Eliminating aberrant BG output would restore baseline corticothalamic function, but not allow vigor modulation by BG-thalamocortical circuits. Critically, tonic BG output imposed by high frequency stimulation would have a similar effect.

It remains unclear how distinct subcortical afferents influence Mthal activity and behavior. One possibility is that "initiation" and "execution" units represent cerebellar- and BG-recipient thalamocortical neurons, respectively. Suppressing deep cerebellar nuclear (DCN) activity prolongs RT (Meyer-Lohman et al., 1977; Trouche and Beaubaton, 1980). Transient increases in DCN activity precede and are time-locked to saccades (Ohmae et al., 2017) or limb movements in a simple RT task (Thach, 1975). Furthermore, Purkinje neuron inhibition releases DCN from tonic inhibition and initiates movement (Heiney et al., 2014). Finally, after pairing Purkinje neuron inhibition with an auditory cue, the auditory stimulus itself is sufficient to

increase DCN activity and initiate movement (Lee et al., 2015). Cerebellum-dependent action initiation could be driven via Mthal, though the DCN also project to the superior colliculus and red nucleus (Teune et al., 2000).

Conversely, the BG are implicated in action selection (Maia and Frank, 2011; Redgrave et al., 2011; Jin et al., 2014) and regulating movement vigor (Panigrahi et al., 2015; Dudman and Krakauer, 2016). In simple RT tasks, BG output lesions/inactivations slow MT, but not RT (Horak and Anderson, 1984a; Mink and Thach, 1991; Desmurget and Turner, 2010). Furthermore, Parkinson Disease patients react and move slower during choice RT tasks than healthy controls (Pullman et al., 1988). In tasks similar to the one used here, striatal dopamine depletion (Carli et al., 1985; Dowd and Dunnett, 2005 Leventhal et al., 2014), striatal inactivation (Leventhal et al., 2014), or subthalamic lesions (Baunez et al., 2001) impair action selection and prolong RT and MT. Single units in striatum, globus pallidus, the subthalamic nucleus, and SNr encode movement direction in this task (Gage et al., 2010; Schmidt et al., 2013). Thus, BG-recipient Mthal is a candidate to convey vigor and action-specific signals from the BG into corticospinal tracts. Alternatively, "initiation" and "execution" units may be distributed across Mthal subregions, with BG- and cerebellum-derived signals mixing through recurrent corticothalamic loops (Bosch-Bouju et al., 2013), disynaptic connections between the BG and cerebellum (Bostan et al., 2010; Chen et al., 2014), or sparse cerebellar projections to BG-recipient thalamus (Deniau et al., 1992; Kuramoto et al., 2011). The latter projections could explain why "execution" units predict RT as well as MT.

The correlation between depressed hold period Mthal activity and RT (Figure 2-5A, B) suggests an attentional mechanism to anticipate the cue. Thalamocortical neurons express T-type Ca^{2+} channels that de-inactivate during hyperpolarization, increasing excitability (Kim et al.,

2017). While extracellular recordings cannot determine if firing rate depressions correspond to membrane hyperpolarization, the correlation between the depth of the hold period depression and the height of the peri-Nose Out peak implies a rebound phenomenon. Mthal hyperpolarization could be caused by enhanced BG output, though SNr hold period activity is not elevated in a similar task (Schmidt et al., 2013, Figure S8). Alternatively, decreased Mthal activity could reflect increased reticular thalamic inhibition (Guo et al., 2017) or decreased cortical excitation (Galvan et al., 2016; Guo et al., 2017). However, it is also possible that network mechanisms account for the correlations between depressed pre-tone firing rate, peri-Nose Out peak firing, and behavior.

Premotor corticothalamic loops can maintain selected actions in working memory when instructive cues precede imperative cues, and disrupting corticothalamic activity reduces task performance to chance (Guo et al., 2017). In our task, the instructive and imperative cues arrive simultaneously, and non-specific RT-correlated action initiation signals precede direction-specific MT-correlated signals (compare Figs. 5A and D). These results suggest that movement may be initiated by subcortical circuits, but action selection (at least in this task) requires corticothalamic communication. The selected action could be maintained in working memory or used immediately to influence ongoing movement (Fig. 5D). Correlations between BG-recipient Mthal activity and action selection also suggest that action-specific "execution" units are part of BG-Mthal-prefrontal circuits.

Most models of choice RT performance suggest that action preparation and movement initiation must occur sequentially to generate accurate movements (Bogacz et al., 2006). Our results apparently contradict these models, and recent data suggest that action preparation and initiation can occur independently (Haith et al., 2016). When choice RT options demand similar

movement trajectories, “intermediate” movements between potential targets are often generated at short RT (Hening et al., 1988). “Prepare-then-move” models interpret intermediate trajectories as errors caused by inadequate preparation. An alternative is that the motor system is efficiently initiating a trajectory that could be adjusted to either target as more data become available or further processing occurs (Hudson et al., 2007; Haith et al., 2016). Our finding that nonspecific “initiation” units are modulated before action-specific “execution” units is consistent with the latter interpretation.

In summary, in a choice RT task, Mthal activity is briefly modulated around movement onset, and correlated with the speed of movement initiation and execution. Instead of a strict rate model of BG-thalamocortical function, our results suggest that pulses of Mthal activity modify the kinematics of impending or ongoing movement. This hypothesis makes specific, testable predictions that will allow current models of BG- and cerebellar-thalamocortical function to be refined.

Materials and Methods

Subjects. All animal procedures were approved by the Institutional Animal Care and Use Committee of the University of Michigan. 5 adult male Long-Evans rats (250-275 g, Charles River Laboratories, Wilmington, MA) were housed in groups of 2-3 on a reverse light/dark cycle prior to electrode implantation. They were subsequently housed individually to protect the implants. Food restriction was imposed on all animals during training and testing for no more than 5 days in a row, with 2 days of free feeding in between. Upon arrival in the laboratory, rats were handled daily for one week to acclimate them to the laboratory environment.

Behavioral task. Operant chambers were outfitted with five illuminated nose-poke holes at the front and a food port at the back (ENV-009 Med Associates). At the beginning of each trial one of three center nose ports was illuminated signaling the rat to poke into that port and hold for a variable delay (0.5-1 s, pulled from a uniform distribution). The rat was then cued with a low (1 kHz) or high (4 kHz) pitched tone lasting 250 ms, instructing them to poke the left or right adjacent port, respectively. Trials completed within 1 second of the tone in the proper direction were deemed "correct" and rewarded with a 45 mg sucrose pellet at the food port. The intertrial interval was 15 seconds. Procedural errors including initiating the trial via an unlit center port, withdrawing from the center port before the tone, or failing to poke a side port within 1 second were unrewarded and the house light was illuminated for the intertrial interval. "Incorrect" trials in which the rat moved to the wrong side port but met the timing criteria were unrewarded, but the house light was not illuminated. No effort was made to track head movement.

Training. Rats began training on the two-alternative forced choice task at six weeks of age, progressing through training levels at an individualized pace. First, all nose ports were lit and the rat was rewarded for poking any port. Next, one of the three central ports was lit and the rat was trained to poke and hold for a progressively longer delay period, with 250 ms of white noise signaling the reward. Finally, a low or high pitch tone (instructing left or right movement) replaced the white noise. The deadline for the rat to enter a side port after the tone was gradually reduced to 1 second as their performance improved. Rats were deemed ready for electrode implantation when their accuracy was 80% for three consecutive days and their body weight exceeded 400 grams.

Implant Preparation. Implants were designed using 3D modeling software (SolidWorks) and printed with biocompatible resins (3D Systems ProJet 3500 HD Max). The electrode

interface board (EIB) was designed using custom software (Advanced Circuits) and assembled by hand. The electrodes were either individual 50 μm tungsten wires (California Fine Wire) or tetrodes made from 12 μm nickel-chrome wire (Sandvik PX000004). The electrodes were separated using a custom matrix made with polyimide tubing (HPC Medical Products 72113300022-039) resulting in 0.3 mm spacing. All electrodes were drivable via a central, mechanical platform controlled with a single drive screw. Tetrodes were gold plated twice according to vendor instructions (Neuralynx) to a final impedance less than 220 kOhm. Electrodes were submerged in mineral oil prior to implantation.

Surgical Procedures. Rats were placed on free feed at least 24 hours prior to surgery. Anesthesia was induced and maintained via isoflurane inhalation at 5% and ~2% (adjusted as needed), respectively. Following induction, atropine (0.05 mg/kg, Henry Schein AtroJect SA) and carprofen (5 mg/kg, Sigma-Aldrich) were administered subcutaneously to reduce bronchial secretions and post-operative pain, respectively. Enrofloxacin (8 mg/kg, VetOne Enrosite) was administered following surgery to prevent wound infections. Body temperature was monitored and maintained via anal thermometer and abdominal heating pad (37°C; Physitemp Instruments Inc. TCAT-2LV).

Rats were secured in a stereotaxic frame using ear bars. The incision site was shaved, cleaned with ethanol and betadine, and injected with lidocaine (Henry Schein LidoJect) as a local anesthetic. A roughly 10 mm anterior-to-posterior incision was made to expose the skull. The pericranium was removed and the skull cleaned with hydrogen peroxide. Bone screws (Fine Science Tools 19010-00) were placed bilaterally along the lateral cranial ridges, and two screws placed in the posterior skull plate over the cerebellum served as ground and reference for electrophysiology. The skull was leveled and a craniotomy was performed over the recording site

(Mthal; AP: -3.1 mm, ML: 1.2 mm, DV: -7.1 mm). The electrodes were lowered into the brain and the gap between the implant base and skull was filled using a biocompatible silicone adhesive (World Precision Instruments Kwik-Sil). The implant was secured using dental cement (Teets Denture Material, #525000). Rats recovered from surgery for at least one week before retraining on the behavioral task.

Electrophysiological Recordings. Electrodes were driven down daily until at the anticipated target depth. At the end of each recording session, electrodes were driven down at least 60 μm so that new units were identified in each session. Wideband signals (0.1 Hz to 10 kHz) from the EIB were transmitted through a digital headstage, motorized commutator, pre-amplifier, data processor, and streamed to storage (Tucker-David Technologies ZD64, AC32, PZ4, RZ2, RS4). Data were filtered in MATLAB (RRID:SCR_001622) (244 Hz – 6.10 kHz) and manually sorted into single units (Offline Sorter, RRID:SCR_000012). Potential duplicate units (i.e., the same unit recorded in multiple sessions) were identified by comparing the spike waveforms, unit autocorrelograms, cross-correlograms, and firing rates between sessions ("Tracking neurons over multiple days", MATLAB Central ID 30113, Fraser and Schwartz, 2012). 53 potential duplicate units were excluded from subsequent analysis. The behavior chambers were controlled by LabVIEW software that stored behavioral data and a video of each session. Digital pulses indicating behavioral events (e.g., cues, nose pokes) and video frames were transmitted from the behavioral control software to the electrophysiology rig to synchronize behavior and electrophysiology.

Data Analysis. Classification of single unit event responsiveness. Peri-event time histograms (PETHs) of Z-scored firing rates were used to determine the task-related modulation of single unit activity. We used a ±1 s window with 20 ms bins smoothed by a 3-point moving

average for all PETH analyses. The mean and standard deviation used in calculating each Z-score was obtained from the 2 seconds period prior to the "Cue" event (Figure 2-1A). We chose this epoch because animals were not engaged in the task, and by observation, were unlikely to be exploring the cage or grooming. Primary unit classes were determined by finding the event for which the absolute value of a unit's Z-score was maximal and exceeded 1 within ±200 ms around the event. Secondary unit classes were determined by finding the next highest absolute peri-event Z-score with the following restrictions. Secondary events could not be immediately before or after a unit's primary event. Second, to ensure at least a moderate degree of modulation, the absolute value of the secondary Z-score had to either exceed 1 or be greater than one-half of the unit's maximum primary Z-score. Units whose activity was not modulated strongly enough to be assigned to an event were classified as non-responsive (N.R.). Only primary task-modulated units could be assigned secondary event classifications (i.e., the secondary classification of primary N.R. units could only be N.R.).

Identification of directionally selective units. Directional coding on a per-unit basis was assessed by creating ±1 second PETHs independently for contralateral and ipsilateral trials. The ipsilateral PETHs were subtracted from the contralateral PETHs, resulting in a time series representing the firing rate difference between the two trial types. Statistical comparisons between PETHs were performed with a shuffle test (Schmidt et al., 2013). We randomly reassigned trial type labels 1,000 times to calculate surrogate PETH differences. P-values were determined as the fraction of surrogate PETH differences greater (or less) than the actual PETH difference. In each time bin, a unit was counted as directionally selective if $p < 0.01$. We labeled any unit that showed sustained selectivity for at least 40 ms around the Nose Out event (-200 to 400 ms) "directionally selective" and exclusively classified them as contralaterally or

ipsilaterally selective. If a unit was selective for both directions at different times, we classified it based on the earliest time when our selection criteria were met. To quantify the magnitude of a unit's directional selectivity, we summed the difference between the ipsilateral and contralateral PETHs for bins in which this difference was significant (-200 to 400 ms around Nose Out, Figure 2-4C). Directional selectivity for incorrect trials was assessed using the same criteria but was limited by the small number of such trials. Directional selectivity at the Side Out event was determined using the same criteria except trials were sorted by the direction the rat moved to the food port based on manual video review.

Correlations between single unit activity, RT, and MT. Visual inspection of our RT distribution revealed distinct early (express), "main", and late components (Figure 2-1C, 5A, B). We empirically identified the main RT distribution (Noorani and Carpenter, 2011) as between 50-350 ms. Similarly, the MT distribution comprised two distinct components (there is no express component of the MT distribution). Empirically, the main MT distribution was identified between 0-400 ms. Consistent with results from similar tasks, our ordinary trials (i.e., those with RT and MT within the main distributions) comprised ~90% of all trials.

The main RT and MT distributions for all trials were divided into 10 quantiles, and average PETHs were generated for directionally and non-directionally selective units. We identified two epochs around the Nose Out event where single unit Z-scores varied systematically with RT or MT (Figure 2-5) for further analysis. The minimum Z-score for each quantile was extracted from between -0.7 and -0.2 s with respect to the Nose Out event (Figure 2-5, black arrows), and the maximum peri-event Z-score was extracted from between -0.2 and 0.3 seconds (Figure 2-5, red arrows). These values were then regressed against RT and MT (Figure 2-5).

All subject data were stored in a MySQL database, analyzed using MATLAB, and versioned using Git.

Anatomic Localization of Recording Sites. Animals were deeply anesthetized and electrolytic lesions were made by passing 15-30 μA between each electrode and the ground wire. Animals were euthanized in accordance with AVMA guidelines by cardiac perfusion with 10% paraformaldehyde (PFA, Sigma-Aldrich P6148). The implant was removed, cleaned with ethanol and stored. The brain was sequentially stored in the following solutions: 10% PFA, 20% sucrose/PBS, 30% sucrose/PBS, 50% OCT, 100% OCT (PBS - phosphate buffered saline, OCT - Fisher Healthcare Tissue-Plus Optimal Cutting Temperature Compound). Brain slices were taken on a cryostat (Leica CM3050 S) at 30 μm intervals, stained using Cresyl Violet Acetate to highlight Nissl substance, and digitally imaged under brightfield illumination. Electrolytic lesions were identified from images in Adobe Photoshop (RRID:SCR_014199) and electrode tracks were followed to the dorsal entry point. The implant (with electrodes intact) was imaged and analyzed to create a three-dimensional electrode map to correlate with the location of electrolytic lesions in the histology images. We morphed the histology images to match standard rat brain maps (Paxinos and Watson, 2007).

Statistics. Directional coding was determined using a shuffle test with 1,000 random permutations (MATLAB *randperm*) of trial labels (i.e., contraversive vs. ipsiversive movement). We used a binomial inverse cumulative distribution (MATLAB *binoinv*) to determine the fraction of units expected to show directional coding by chance (Schmidt et al., 2013) ($p < 0.01$). Statistical significance between fractions of units belonging to a particular class or group was determined using the chi-squared test. RT and MT regressions were fit using a linear polynomial

curve to determine R^2 with p-values computed using Pearson's linear correlation coefficient (MATLAB *fit* and *corr*, respectively). Each fit was reported with 95% confidence intervals (MATLAB *polyconf*). Electrophysiological characteristics were plotted using MATLAB *boxplot*. Unless stated otherwise, numbers are reported as the mean ± standard deviation.

Figures

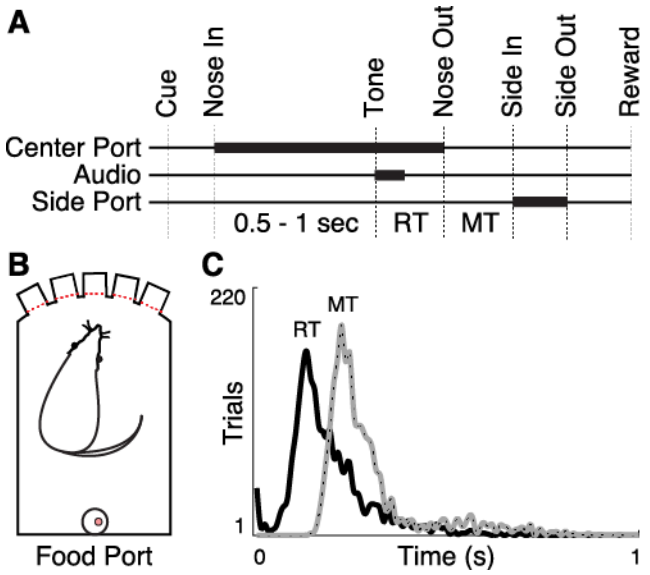

Figure 2-1: Behavioral task

(A) Trials began by illuminating one of the three center ports in a 5-port behavior chamber ("Cue"). The rat poked and held its nose in the lit port ("Nose In") for a variable interval (0.5-1 s, pulled from a uniform distribution) until a 1 or 4 kHz auditory cue played ("Tone") instructing the rat to move one port to the left or right, respectively. "Nose Out", "Side In", and "Side Out" indicate when the rat withdrew from the central port, poked the adjacent port, and withdrew from the adjacent port, respectively. "Reward" indicates the time of reward pellet retrieval. **(B)** schematic diagram of the operant chamber. **(C)** RT and MT distributions (10 ms bins, 5-point smoothed) for all trials.

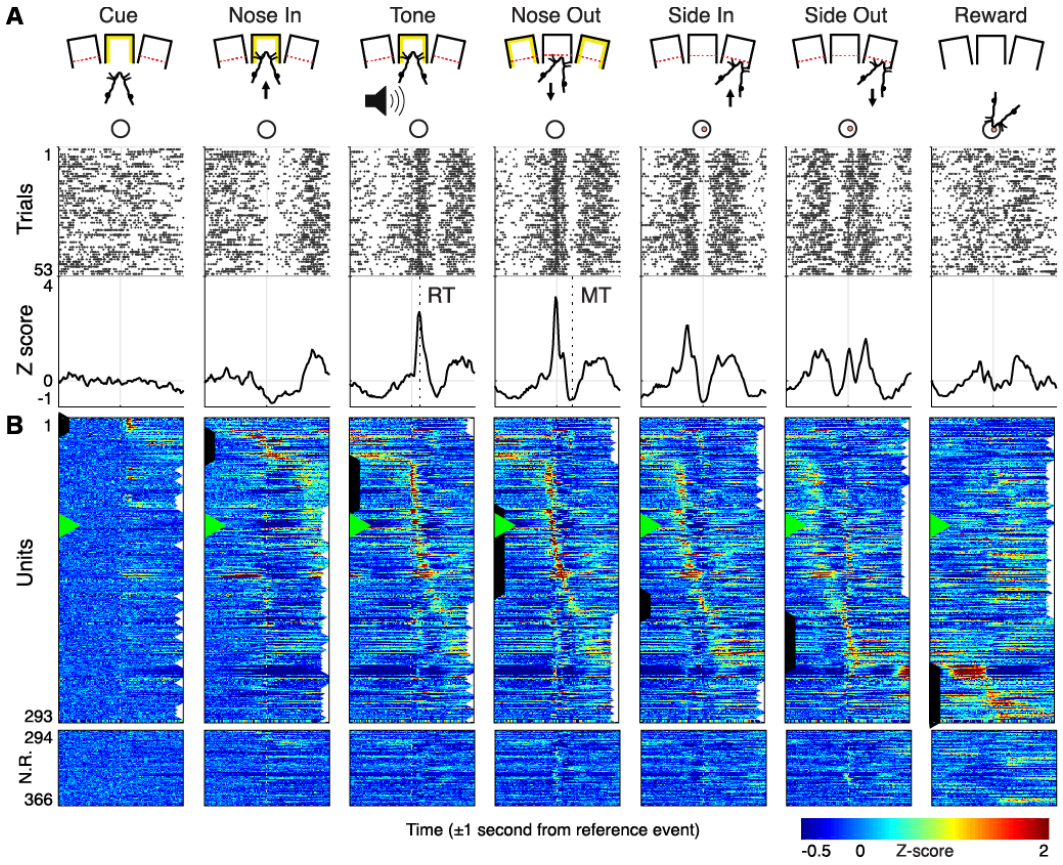

Figure 2-2: Single unit Mthal activity during task performance

(A) Single unit raster (top) and peri-event time histograms (PETHs, bottom) of a Nose Out responsive unit. Vertical dashed lines indicate the median reaction time (RT, 132 ms) and movement time (MT, 249 ms) in this session. **(B)** PETHs for all units sorted by their primary unit class and the timing of their maximal Z-score. Black and white arrows along the column edges indicate the primary and secondary unit classification, respectively. Green triangles in (B) indicate the unit from (A). N.R. – non-responsive units.

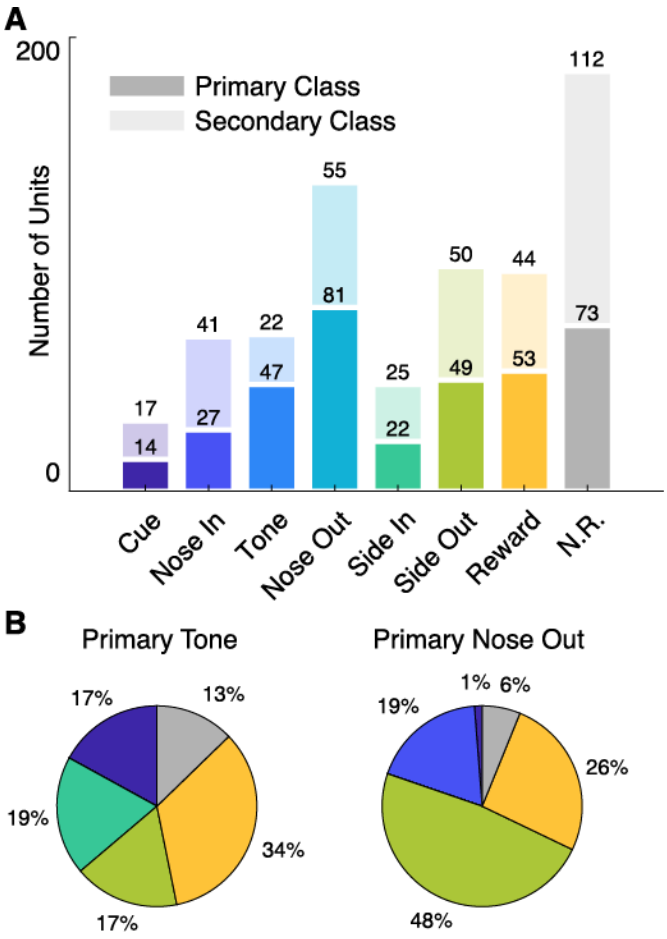

Figure 2-3: Numbers of units with activity time-locked to behavioral events

(A) Distribution of primary (bottom, dark bars) and secondary (top, light bars) unit classes. Numbers above each bar indicate the number of units preferentially locked to each event. **(B)** Distributions of secondary events for primary Tone (left) and Nose Out (right) units. Tone units show an approximately equal preference for firing at other events while Nose Out units are highly modulated at Side Out.

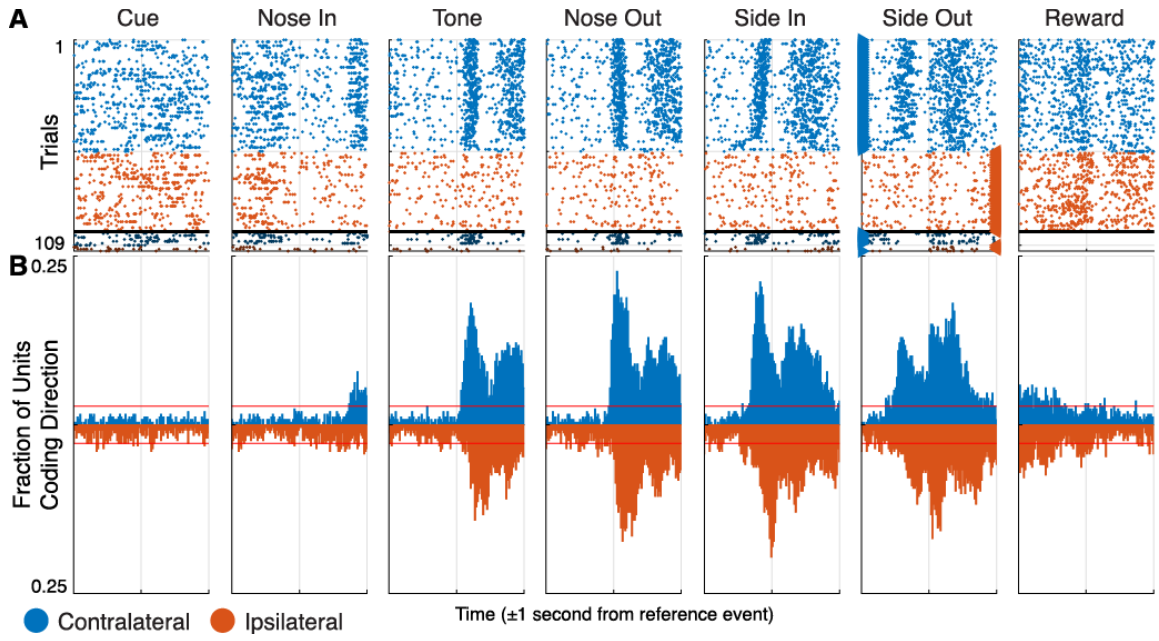

Figure 2-4: Directional selectivity of Mthal units

(A) Peri-event rasters from a single unit sensitive to movement direction. Trials are segregated into 4 groups from top to bottom: cued contralateral, moved contralateral; cued ipsilateral, moved ipsilateral; cued ipsilateral, moved contralateral; and cued contralateral, moved ipsilateral. Trials are sorted by MT within each group. Markers on either side of the Side Out event indicate the direction the rat turned to retrieve the sugar pellet. **(B)** Fraction of units showing directional selectivity on correct trials. Counts above the horizontal axis indicate increased firing for contralateral movement; counts below the axis indicate increased firing for ipsilateral movements. Horizontal red lines indicate a chance level of directional selectivity. **(C)** Histograms of Selectivity Indices (SI) for directionally (red bars) and non-directionally selective (gray bars) units. **(D)** Fraction of units that exhibit directional selectivity (red bars) at the Nose Out event according to their event-responsiveness.

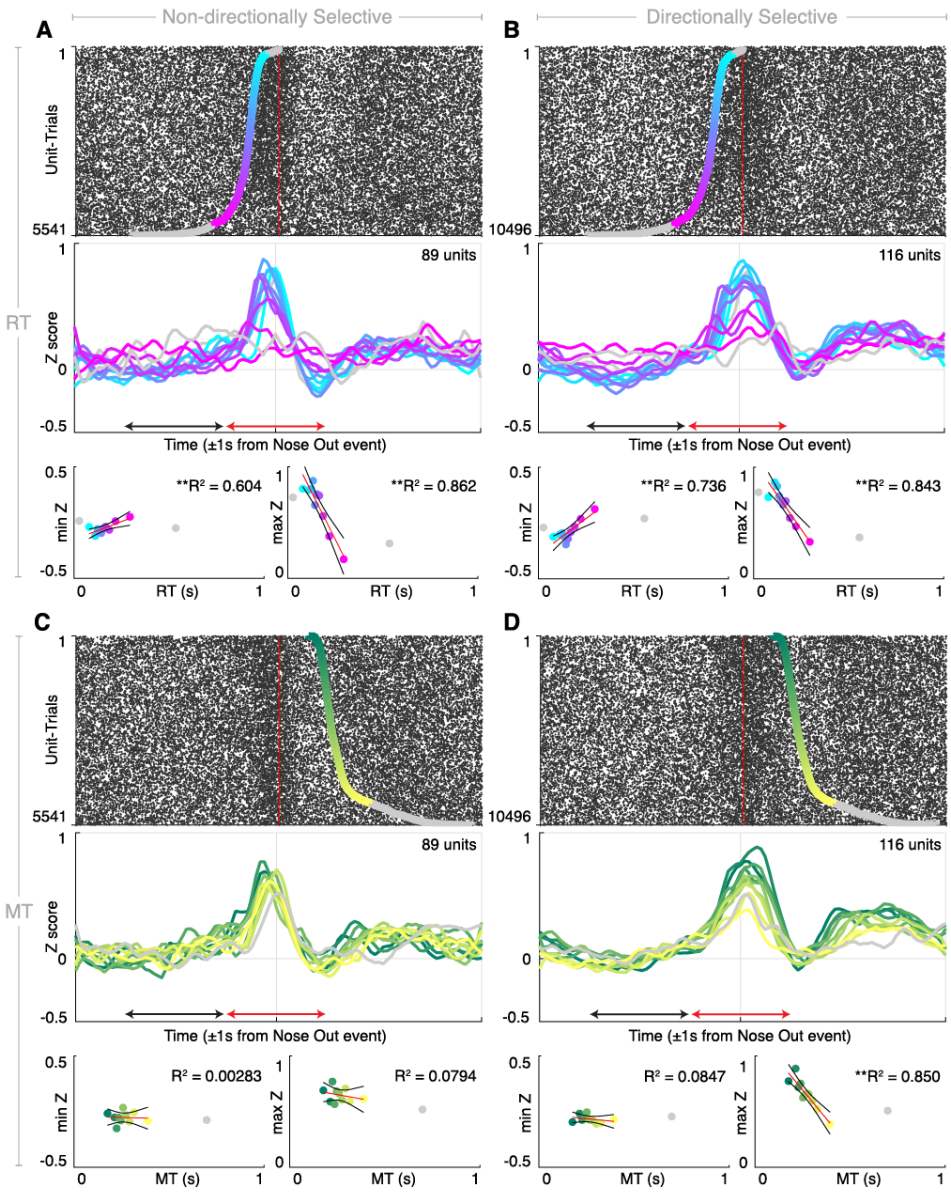

Figure 2-5: Relationships between single unit activity, RT, and MT

Top panels: single trial rasters for each non-directionally selective **(A, C)** or directionally selective **(B, D)** unit sorted by RT **(A, B)** or MT **(C, D)**. Cyan-violet overlays indicate the Tone event for the main RT distribution; green-yellow overlays indicate the Side In event for the main MT distribution. Gray overlays indicate short ("express") RT or long RT/MT. Middle panels: mean peri-event Z-scores for each RT (A, B) or MT (C, D) decile. Colored traces correspond to shading in the raster above. Bottom left panels: linear regressions of minimum Z-score in the pre-Nose Out period (black arrow on the PETHs above) against RT (A, B) or MT (C, D). Bottom right panels: linear regressions of maximum Z-score in the peri-Nose Out period (red arrow on the PETHs above) against RT (A, B) or MT (C, D). * $p < 0.05$, ** $p < 0.01$.

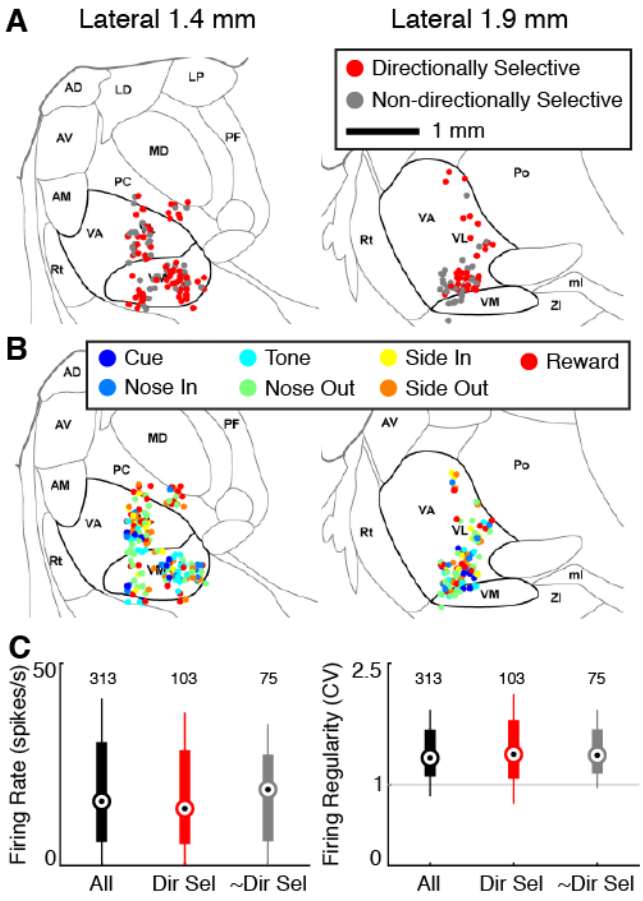

Figure 2-6: Anatomical and electrophysiological characteristics of Mthal units

(A) Location of directionally (red) and non-directionally selective (gray) units superimposed on sagittal rat brain atlas images (Paxinos and Watson, 2007). Mthal nuclei (VA = ventral anterior, VL = ventral lateral, VM = ventromedial) are enclosed within bold lines. AD = anterodorsal thalamus, AM = anteromedial thalamus, AV = anteroventral thalamus, LD = laterodorsal thalamus, LP = lateral posterior thalamus, MD = mediodorsal thalamus, ml = medial lemniscus, PC = paracentral thalamus, PF = parafascicular thalamus, Po = posterior thalamic nuclear group, Rt = reticular thalamus, ZI = zona incerta. **(B)** Anatomical characterization of Mthal units based on event-responsiveness. There was no clear anatomic segregation of units based on directional selectivity or event-responsiveness. **(C)** Left: median firing rates of all, directionally selective (Dir Sel), and non-directionally selective (~Dir Sel) units. Right: median coefficient of variation (CV) for the same units. Thick lines indicate the 10^{th} to 90^{th} percentiles. The whiskers extend to the most extreme data points not considered outliers.

References

Albin RL, Young AB, Penney JB (1989) The functional anatomy of basal ganglia disorders. Trends Neurosci, 12:366–375.

Albin RL, Leventhal DK (2017) The missing, the short, and the long: Levodopa responses and dopamine actions. Ann Neurol,

Anderson ME, Turner RS (1991) Activity of neurons in cerebellar-receiving and pallidal-receiving areas of the thalamus of the behaving monkey. J Neurophysiol, 66:879–893.

Bastian AJ, Kelly VE, Perlmutter JS, Mink JW (2003) Effects of pallidotomy and levodopa on walking and reaching movements in Parkinson's disease. Mov Disord, 18:1008–1017.

Baunez C, Humby T, Eagle DM, Ryan LJ, Dunnett SB, Robbins TW (2001) Effects of STN lesions on simple vs choice reaction time tasks in the rat: preserved motor readiness, but impaired response selection. Eur J Neurosci, 13:1609–1616.

Bogacz R, Brown E, Moehlis J, Holmes P, Cohen JD (2006) The physics of optimal decision making: a formal analysis of models of performance in two-alternative forced-choice tasks. Psychol Rev, 113:700–765.

Bosch-Bouju C, Hyland BI, Parr-Brownlie LC (2013) Motor thalamus integration of cortical, cerebellar and basal ganglia information: implications for normal and parkinsonian conditions. Front Comput Neurosci, 7:163.

Bosch-Bouju C, Smither RA, Hyland BI, Parr-Brownlie LC (2014) Reduced reach-related modulation of motor thalamus neural activity in a rat model of Parkinson's disease. J Neurosci, 34:15836–15850.

Bostan AC, Dum RP, Strick PL (2010) The basal ganglia communicate with the cerebellum. Proc Natl Acad Sci U S A, 107:8452–8456.

Boulet S, Lacombe E, Carcenac C, Feuerstein C, Sgambato-Faure V, Poupard A, Savasta M (2006) Subthalamic stimulation-induced forelimb dyskinesias are linked to an increase in glutamate levels in the substantia nigra pars reticulata. J Neurosci, 26:10768–10776.

Butler EG, Horne MK, Hawkins NJ (1992) The activity of monkey thalamic and motor cortical neurones in a skilled, ballistic movement. J Physiol, 445:25–48.

Carli M, Evenden JL, Robbins TW (1985) Depletion of unilateral striatal dopamine impairs initiation of contralateral actions and not sensory attention. Nature, 313:679–682.

Carpenter RH, Williams ML (1995) Neural computation of log likelihood in control of saccadic eye movements. Nature, 377:59–62.

Chen CH, Fremont R, Arteaga-Bracho EE, Khodakhah K (2014) Short latency cerebellar modulation of the basal ganglia. Nat Neurosci, 17:1767–1775.

Chiken S, Nambu A (2016) Mechanism of Deep Brain Stimulation: Inhibition, Excitation, or Disruption? Neuroscientist, 22:313–322.

Churchland MM, Cunningham JP, Kaufman MT, Foster JD, Nuyujukian P, Ryu SI, Shenoy KV (2012) Neural population dynamics during reaching. Nature, 487:51–56.

Churchland MM, Cunningham JP, Kaufman MT, Ryu SI, Shenoy KV (2010) Cortical preparatory activity: representation of movement or first cog in a dynamical machine? Neuron, 68:387–400.

Cif L, Hariz M (2017) Seventy years of pallidotomy for movement disorders. Mov Disord, 32:972–982.

DeLong MR (1990) Primate models of movement disorders of basal ganglia origin. Trends Neurosci, 13:281–285.

Deniau JM, Kita H, Kitai ST (1992) Patterns of termination of cerebellar and basal ganglia efferents in the rat thalamus. Strictly segregated and partly overlapping projections. Neurosci Lett, 144:202–206.

Desmurget M, Turner RS (2010) Motor sequences and the basal ganglia: kinematics, not habits. J Neurosci, 30:7685–7690.

Dowd E, Dunnett SB (2005) Comparison of 6-hydroxydopamine-induced medial forebrain bundle and nigrostriatal terminal lesions in a lateralised nose-poking task in rats. Behav Brain Res, 159:153–161.

Dudman JT, Krakauer JW (2016) The basal ganglia: from motor commands to the control of vigor. Curr Opin Neurobiol,

Ellens DJ, Leventhal DK (2013) Review: Electrophysiology of Basal Ganglia and Cortex in Models of Parkinson Disease. J Parkinsons Dis, 3:241–254.

Forlano LM, Horne MK, Butler EG, Finkelstein D (1993) Neural activity in the monkey anterior ventrolateral thalamus during trained, ballistic movements. J Neurophysiol, 70:2276–2288.

Fraser GW, Schwartz AB (2012) Recording from the same neurons chronically in motor cortex. J Neurophysiol, 107:1970–1978.

Gage GJ, Stoetzner CR, Wiltschko AB, Berke JD (2010) Selective activation of striatal fast-spiking interneurons during choice execution. Neuron, 67:466–479.

Galvan A, Devergnas A, Wichmann T (2015) Alterations in neuronal activity in basal ganglia-thalamocortical circuits in the parkinsonian state. Front Neuroanat, 9:5.

Galvan A, Hu X, Smith Y, Wichmann T (2016) Effects of Optogenetic Activation of Corticothalamic Terminals in the Motor Thalamus of Awake Monkeys. J Neurosci, 36:3519–3530.

Guehl D, Pessiglione M, François C, Yelnik J, Hirsch EC, Féger J, Tremblay L (2003) Tremor-related activity of neurons in the 'motor' thalamus: changes in firing rate and pattern in the MPTP vervet model of parkinsonism. European Journal of Neuroscience, 17:2388–2400.

Guo ZV, Inagaki HK, Daie K, Druckmann S, Gerfen CR, Svoboda K (2017) Maintenance of persistent activity in a frontal thalamocortical loop. Nature,

Haith AM, Pakpoor J, Krakauer JW (2016) Independence of Movement Preparation and Movement Initiation. J Neurosci, 36:3007–3015.

Hamid AA, Pettibone JR, Mabrouk OS, Hetrick VL, Schmidt R, Vander Weele CM, Kennedy RT, Aragona BJ, Berke JD (2016) Mesolimbic dopamine signals the value of work. Nat Neurosci, 19:117–126.

Hashimoto T, Elder CM, Okun MS, Patrick SK, Vitek JL (2003) Stimulation of the subthalamic nucleus changes the firing pattern of pallidal neurons. J Neurosci, 23:1916–1923.

Heiney SA, Kim J, Augustine GJ, Medina JF (2014) Precise control of movement kinematics by optogenetic inhibition of Purkinje cell activity. J Neurosci, 34:2321–2330.

Hening W, Vicario D, Ghez C (1988) Trajectory control in targeted force impulses. IV. Influences of choice, prior experience and urgency. Exp Brain Res, 71:103–115.

Horak FB, Anderson ME (1984a) Influence of globus pallidus on arm movements in monkeys. I. Effects of kainic acid-induced lesions. J Neurophysiol, 52:290–304.

Horak FB, Anderson ME (1984b) Influence of globus pallidus on arm movements in monkeys. II. Effects of stimulation. J Neurophysiol, 52:305–322.

Hudson TE, Maloney LT, Landy MS (2007) Movement planning with probabilistic target information. J Neurophysiol, 98:3034–3046.

Jin X, Tecuapetla F, Costa RM (2014) Basal ganglia subcircuits distinctively encode the parsing and concatenation of action sequences. Nat Neurosci,

Kaufman MT, Seely JS, Sussillo D, Ryu SI, Shenoy KV, Churchland MM (2016) The Largest Response Component in the Motor Cortex Reflects Movement Timing but Not Movement Type. eNeuro, 3

Kim J, Kim Y, Nakajima R, Shin A, Jeong M, Park AH, Jeong Y, Jo S, Yang S, Park H, Cho S-HH, Cho K-HH, Shim I, Chung JH, Paik S-BB, Augustine GJ, Kim D (2017) Inhibitory Basal Ganglia Inputs Induce Excitatory Motor Signals in the Thalamus. Neuron, 95:1181–1196.e8.

Kravitz AV, Freeze BS, Parker PRL, Kay K, Thwin MT, Deisseroth K, Kreitzer AC (2010) Regulation of parkinsonian motor behaviours by optogenetic control of basal ganglia circuitry. Nature, 466:622–626.

Kuramoto E, Fujiyama F, Nakamura KC, Tanaka Y, Hioki H, Kaneko T (2011) Complementary distribution of glutamatergic cerebellar and GABAergic basal ganglia afferents to the rat motor thalamic nuclei. Eur J Neurosci, 33:95–109.

Lauwereyns J, Watanabe K, Coe B, Hikosaka O (2002) A neural correlate of response bias in monkey caudate nucleus. Nature, 418:413–417.

Lee KH, Mathews PJ, Reeves AMB, Choe KY, Jami SA, Serrano RE, Otis TS (2015) Circuit mechanisms underlying motor memory formation in the cerebellum. Neuron, 86:529–540.

Leventhal DK, Gage GJ, Schmidt R, Pettibone JR, Case AC, Berke JD (2012) Basal Ganglia Beta oscillations accompany cue utilization. Neuron, 73:523–536.

Leventhal DK, Stoetzner CR, Abraham R, Pettibone J, DeMarco K, Berke JD (2014) Dissociable effects of dopamine on learning and performance within sensorimotor striatum. Basal Ganglia, 4:43–54.

Macpherson JM, Rasmusson DD, Murphy JT (1980) Activities of neurons in “motor” thalamus during control of limb movement in the primate. J Neurophysiol, 44:11–28.

Magnin M, Morel A, Jeanmonod D (2000) Single-unit analysis of the pallidum, thalamus and subthalamic nucleus in parkinsonian patients. Neuroscience, 96:549–564.

Maia TV, Frank MJ (2011) From reinforcement learning models to psychiatric and neurological disorders. Nat Neurosci, 14:154–162.

Marsden CD, Obeso JA (1994) The functions of the basal ganglia and the paradox of stereotaxic surgery in Parkinson's disease. Brain, 117:877–897.

McIntyre CC, Grill WM, Sherman DL, Thakor NV (2004) Cellular effects of deep brain stimulation: model-based analysis of activation and inhibition. J Neurophysiol, 91:1457–1469.

Meyer-Lohman J, Hore J, Brooks VB (1977) Cerebellar participation in generation of prompt arm movements. JNeurophysiol, 40:1038–1050.

Mink JW, Thach WT (1991) Basal ganglia motor control. II. Late pallidal timing relative to movement onset and inconsistent pallidal coding of movement parameters. J Neurophysiol, 65:301–329.

Molnar GF, Pilliar A, Lozano AM, Dostrovsky JO (2005) Differences in neuronal firing rates in pallidal and cerebellar receiving areas of thalamus in patients with Parkinson’s disease, essential tremor, and pain. J Neurophysiol, 93:3094–3101.

Nakamura KC, Sharott A, Magill PJ (2014) Temporal coupling with cortex distinguishes spontaneous neuronal activities in identified basal ganglia-recipient and cerebellar-recipient zones of the motor thalamus. Cereb Cortex, 24:81–97.

Nambu A, Yoshida S, Jinnai K (1991) Movement-related activity of thalamic neurons with input from the globus pallidus and projection to the motor cortex in the monkey. Exp Brain Res, 84:279–284.

Niv Y, Daw ND, Joel D, Dayan P (2007) Tonic dopamine: opportunity costs and the control of response vigor. Psychopharmacology (Berl), 191:507–520.

Noorani I, Carpenter RHS (2011) Full reaction time distributions reveal the complexity of neural decision-making. Eur J Neurosci, 33:1948–1951.

Ohmae S, Kunimatsu J, Tanaka M (2017) Cerebellar Roles in Self-Timing for Sub- and Supra-Second Intervals. J Neurosci, 37:3511–3522.

Panigrahi B, Martin KA, Li Y, Graves AR, Vollmer A, Olson L, Mensh BD, Karpova AY, Dudman JT (2015) Dopamine Is Required for the Neural Representation and Control of Movement Vigor. Cell, 162:1418–1430.

Paxinos G, Watson C (2007) The rat brain in stereotaxic coordinates. Elsevier Academic Press.

Pessiglione M, Guehl D, Rolland A-SS, François C, Hirsch EC, Féger J, Tremblay L (2005) Thalamic neuronal activity in dopamine-depleted primates: evidence for a loss of functional segregation within basal ganglia circuits. J Neurosci, 25:1523–1531.

Pullman SL, Watts RL, Juncos JL, Chase TN, Sanes JN (1988) Dopaminergic effects on simple and choice reaction time performance in Parkinson's disease. Neurology, 38:249–254.

Redgrave P, Vautrelle N, Reynolds JNJ (2011) Functional properties of the basal ganglia's re-entrant loop architecture: selection and reinforcement. Neuroscience, 198:138–151.

Rovó Z, Ulbert I, Acsády L (2012) Drivers of the primate thalamus. J Neurosci, 32:17894–17908.

Rubin JE, McIntyre CC, Turner RS, Wichmann T (2012) Basal ganglia activity patterns in parkinsonism and computational modeling of their downstream effects. Eur J Neurosci, 36:2213–2228.

Schmidt R, Leventhal DK, Mallet N, Chen F, Berke JD (2013) Canceling actions involves a race between basal ganglia pathways. Nat Neurosci, 16:1118–1124.

Summerside E, Shadmehr R, Ahmed AA (2018) Vigor of reaching movements: reward discounts the cost of effort. J Neurophysiol,

Tanaka M (2005) Involvement of the central thalamus in the control of smooth pursuit eye movements. J Neurosci, 25:5866–5876.

Tanaka M (2007) Cognitive signals in the primate motor thalamus predict saccade timing. J Neurosci, 27:12109–12118.

Teune TM, Burg JVD, Moer JVD, Voogd J, Ruigrok TJH (2000) Topography of cerebellar nuclear projections to the brain stem in the rat. Prog Brain Res, 124

Thach WT (1975) Timing of activity in cerebellar dentate nucleus and cerebral motor cortex during prompt volitional movement. Brain Res, 88:233–241.

Thorn CA, Atallah H, Howe M, Graybiel AM (2010) Differential dynamics of activity changes in dorsolateral and dorsomedial striatal loops during learning. Neuron, 66:781–795.

Thura D, Cisek P (2017) The Basal Ganglia Do Not Select Reach Targets but Control the Urgency of Commitment. Neuron,

Trouche E, Beaubaton D (1980) Initiation of a goal-directed movement in the monkey. Role of the cerebellar dentate nucleus. Exp Brain Res, 40:311–321.

van Donkelaar P, Stein JF, Passingham RE, Miall RC (1999) Neuronal activity in the primate motor thalamus during visually triggered and internally generated limb movements. J Neurophysiol, 82:934–945.

Xiao Y, Agnesi F, Bello EM, Zhang S, Vitek JL, Johnson MD (2018) Deep brain stimulation induces sparse distributions of locally modulated neuronal activity. Sci Rep, 8:2062.

Yamamoto S, Monosov IE, Yasuda M, Hikosaka O (2012) What and where information in the caudate tail guides saccades to visual objects. J Neurosci, 32:11005–11016.

Yamawaki N, Shepherd GMG (2015) Synaptic circuit organization of motor corticothalamic neurons. J Neurosci, 35:2293–2307.

Yttri EA, Dudman JT (2018) A proposed circuit computation in basal ganglia: History-dependent gain. Mov Disord.

Yttri EA, Dudman JT (2016) Opponent and bidirectional control of movement velocity in the basal ganglia. Nature.

Zirh TA, Lenz FA, Reich SG, Dougherty PM (1998) Patterns of bursting occurring in thalamic cells during parkinsonian tremor. Neuroscience, 83:107–121.

CHAPTER 3: Behavior and Spiking Correlate with the Motor Thalamic Local Field Potential in Rats

Co-authored by Amy Hurst, Christopher Cyr, and Daniel K. Leventhal

Abstract

Interactions between neural oscillations in distinct frequency bands are believed to coordinate brain activity over large spatiotemporal scales. However, it is unknown how cross-frequency interactions in motor thalamus (Mthal), the major interface between the basal ganglia and cortex, are related to neuronal spiking and behavior. We recorded wideband Mthal electrophysiology as healthy rats performed a two-alternative forced choice task. The power of delta (1–4 Hz), beta (13-30 Hz), low gamma (30–70 Hz), and high gamma (70–200 Hz) oscillations were strongly modulated by task performance. As in cortex, delta phase predicted beta/low gamma power and reaction time. Furthermore, delta phase differentially predicted spike timing in functionally distinct populations of Mthal neurons, which also predicted task performance and beta power. These complex relationships suggest mechanisms for commonly observed LFP-LFP and spike-LFP interactions, as well as subcortical influences on motor output.

Introduction

Local field potential (LFP) oscillations represent rhythmic fluctuations in the extracellular potential that emerge from, and may also regulate (Anastassiou, Montgomery, Barahona, Buzsáki, & Koch, 2010), neuronal dynamics over a large spatiotemporal scale (Fries, 2015). Various aspects of the LFP including phase, amplitude and frequency are correlated with sensorimotor phenomena (Friston, Bastos, Pinotsis, & Litvak, 2015; Pesaran et al., 2018; Armstrong, Sale, & Cunnington, 2018). Delta band (~1-4 Hz) oscillations predict movement kinematics (Bansal, Vargas-Irwin, Truccolo, & Donoghue, 2011), reaction time (RT, Lakatos, Karmos, Mehta, Ulbert, & Schroeder, 2008; Stefanics et al., 2010; Hamel-Thibault, Thénault, Whittingstall, & Bernier, 2018), and sensory thresholds (Schroeder & Lakatos, 2009; Fiebelkorn et al., 2013). Beta oscillations (~13-30 Hz) in the cortex and basal ganglia are enhanced under a variety of conditions including pre-movement hold periods (Donoghue, Sanes, Hatsopoulos, & Gaál, 1998; Saleh, Reimer, Penn, Ojakangas, & Hatsopoulos, 2010), isometric contractions (Baker, Olivier, & Lemon, 1997), post-movement "rebound" (Pfurtscheller, Stancák, & Neuper, 1996; Feingold, Gibson, DePasquale, & Graybiel, 2015), and parkinsonism (Brown, 2006; Mallet et al., 2008; Ellens & Leventhal, 2013). Beta oscillations are also correlated with prolonged reaction times (Leventhal et al., 2012; Khanna & Carmena, 2017; Shin, Law, Tsutsui, Moore, & Jones, 2017; van Wijk, 2017; Torrecillos et al., 2018) and slowed movement (Pogosyan, Gaynor, Eusebio, & Brown, 2009; Lofredi et al., 2019). Conversely, movement onset is (usually) associated with decreased beta and increased gamma (~60-100 Hz) power (Feingold et al., 2015; Tan et al., 2019, but see Leventhal et al., 2012).

In addition to correlations with behavior, LFP oscillations exhibit complex spatiotemporal relationships with each other and single unit activity. LFP coherence is common

between brain regions, providing a potential mechanism to coordinate inter-regional activity (Fries, 2015; Wang, Göschl, Friese, König, & Engel, 2019). For example, beta oscillations occur in bursts simultaneously throughout cortical-basal ganglia circuits, with network-wide single unit activity locked to beta phase (Leventhal et al., 2012). Oscillations of different frequencies are commonly coupled to each other, both within and between brain regions. The possibility of an oscillatory "hierarchy" (Lakatos et al., 2005; Canolty et al., 2007) stems in part from observations that delta phase predicts beta oscillation amplitude (Saleh et al., 2010; López-Azcárate et al., 2013; Arnal, Doelling, & Poeppel, 2015; Hamel-Thibault et al., 2018; Grabot et al., 2019), and beta phase predicts the amplitude of higher frequency oscillations (de Hemptinne et al., 2013; Meidahl et al., 2019). These complex correlation patterns provide rich information regarding neural mechanisms of behavior, but also make it difficult to distinguish cause from effect.

The thalamus is a central hub in nearly all motor, sensory, and associative circuits, and therefore well-positioned to regulate circuit-wide neuronal oscillations. Indeed, thalamocortical circuits generate or modulate many well-described LFP oscillations including sleep spindles (Halassa et al., 2011; Mak-McCully et al., 2017), cortical slow (< 1 Hz) oscillations (Neske, 2015), delta rhythms (Fogerson & Huguenard, 2016), alpha (~8-15 Hz) rhythms (Saalmann, Pinsk, Wang, Li, & Kastner, 2012; Crunelli et al., 2018), beta rhythms (Bastos, Briggs, Alitto, Mangun, & Usrey, 2014), and gamma rhythms (McAfee, Liu, Dhamala, & Heck, 2018). Though many of these studies focused on sensory (especially visual) regions, motor thalamic (Mthal) spiking is also phase-locked to delta oscillations under anesthesia (Nakamura, Sharott, & Magill, 2014). Modeling studies suggest that motor system beta oscillations could result from layer-specific thalamocortical inputs (Sherman et al., 2016; Reis et al., 2019), though mechanisms

intrinsic to the basal ganglia have also been proposed as “beta generators” (McCarthy et al., 2011; Tachibana, Iwamuro, Kita, Takada, & Nambu, 2011; Mirzaei et al., 2017). Given the strong associations between thalamic activity and brain rhythms across sensory modalities and brain states, we hypothesized that Mthal, which is reciprocally connected with motor and premotor cortices, mediates many LFP-LFP and LFP-behavior correlations.

To understand the relationship between Mthal spiking, Mthal LFPs, and behavior, we recorded wideband Mthal activity as rats performed a two-alternative forced choice task. Using this data set, we previously found that two distinct, functionally defined populations of Mthal neurons predict dissociable aspects of task performance (see Chapter 2, Gaidica, Hurst, Cyr, & Leventhal, 2018). Here, we describe Mthal LFP-behavior correlations, as well as novel relationships between functionally defined Mthal single units and LFP oscillations. These results have important implications for models of motor system LFP generation, as well as their functional interpretation.

Results

LFP Power and Phase are Modulated by Task Performance in Discrete Frequency Bands. Rats (n = 5) were cued to immediately move left or right from a center nose port based on the pitch of an instructional cue (Figure 3-1, "Tone" event) until a high degree of accuracy was achieved (77 ± 17% over 30 sessions). Reaction times (RT; the time from Tone to Center Out) and movement times (MT; the time from Center Out to Side In) were consistent with similar studies (197 ± 10.3 ms and 302 ± 127 ms, respectively, see Figure 2-1) (Dowd & Dunnett, 2005; Leventhal et al., 2012; Leventhal et al., 2014; Schmidt, Leventhal, Mallet, Chen, & Berke, 2013). Similar to observations in cortex (Saleh et al., 2010; Igarashi, Isomura, Arai, Harukuni, & Fukai, 2013; Murthy & Fetz, 1992) and the BG (Masimore, Schmitzer-Torbert, Kakalios, & Redish, 2005; Berke, Okatan, Skurski, & Eichenbaum, 2004), the awake LFP power spectrum in Mthal had discrete peaks in delta (1–4 Hz), theta (4–7 Hz), beta (13–30 Hz), and low gamma (30–70 Hz) bands (Figure 3-1).

Task-linked Mthal LFP power modulation was nearly identical to prior observations in motor cortex and the BG during a similar task (Figure 3-2) (Leventhal et al., 2012). Beta/low gamma power transiently increased concurrently near the Nose Out and Side Out events, when movement was initiated. Correlations between beta and low gamma power were also present outside of trials (albeit weaker), and nearly disappeared when cross-frequency power-power correlations were recalculated using trial-shuffled data (Figure 3-3). These findings argue that beta/low gamma power correlations do not result solely from independent modulation of these bands by the same task events, and instead are a general feature of Mthal physiology. Delta power also increased at Nose Out, but remained elevated through Side In. Finally, high gamma

power transiently increased at Nose- and Side Out, and exhibited a sustained elevation as the rat moved from the nose ports to the food receptacle (prior to the Reward event).

In addition to LFP power changes, LFP phase in specific bands was strongly modulated by the task. Beta/low gamma phase became sharply aligned at the Tone event (Figure 3-2), as previously observed in the BG (Leventhal et al., 2012). Phase alignment in the delta band was present as early as the Cue event and peaked at the Nose Out and Side Out events. Collectively, these data suggest complex temporal coordination of LFP power and phase in discrete frequency bands.

Delta Phase Predicts Beta and Low Gamma Power. The co-occurrence of a delta phase alignment and beta/low gamma power increase at Nose Out suggests that phase-amplitude coupling (PAC) is a prominent feature of Mthal physiology, as has been observed in other brain regions (Dejean et al., 2011; Belluscio, Mizuseki, Schmidt, Kempter, & Buzsáki, 2012; Cohen, Elger, & Fell, 2009; López-Azcárate et al., 2013; Canolty et al., 2006; Tort et al., 2008). Indeed, delta-beta/low gamma PAC was significantly elevated throughout the task ("in-trial", Figure 3-4), most prominently during movement from the Center to Side nose ports (i.e., Nose Out to Side In, Figure 3-4). Significant delta-beta/low gamma PAC was also present when the rat was not actively engaged in the task ("inter-trial"), and was significantly diminished when recalculated using trial-shuffled data. As for beta/low gamma amplitude-amplitude coupling, these results argue that delta-beta/low gamma PAC does not result simply from common responses to behavioral events.

Delta Phase Predicts Single Unit Mthal Activity. The phase of low frequency oscillations also predicted the timing of single unit activity (Lakatos et al., 2005; Fujisawa & Buzsáki, 2011; Nakamura et al., 2014; Crunelli, David, Lőrincz, & Hughes, 2015). 59% of all

units (n = 366) exhibited a non-uniform delta phase distribution during trials (black line in Figure 3-5; defined as $p < 0.05$ for each unit, Rayleigh test for non-uniformity), which fell to 46% during the inter-trial period. These percentages were significantly greater than chance, as assessed by surrogate firing-rate matched Poisson spike trains. Furthermore, spike-phase entrainment was unique to the delta and theta bands. The average mean resultant length (MRL, a measure of phase uniformity) of spike-LFP phases across units was also significantly greater than chance for low frequencies. These data support the notion that low-frequency oscillations modulate Mthal single neuron excitability in a behaviorally-relevant manner.

We next investigated whether phase preferences differed for two functionally distinct subpopulations of Mthal units previously identified in this data set (Chapter 2, Gaidica et al., 2018). Briefly, "directionally selective" unit activity was tightly linked to the Nose Out event, predicted which direction the rat would move, and predicted both RT and MT. Conversely, "non-directionally selective" units were more tightly locked to the Tone event and predicted RT, but not MT or movement direction (366 total units, 103 directionally selective units, and 75 non-directionally selective units).

These functionally defined populations were differentially entrained to delta oscillations. In-trial, 82% of directionally selective units were significantly entrained to delta phase (Fig. 5), which was the case for only 38% of non-directionally selective units. Between trials, delta entrainment decreased slightly for all units, resulting in entrainment for 61% of directionally selective units and 28% of non-directionally selective units. When compared against Poisson spike trains, it became clear that directionally selective units, but not non-directionally selective units, accounted for most of the single unit delta entrainment.

To determine if Mthal units tended to fire at the same preferred delta phase, we created a spike-phase histogram for each unit (Figure 3-6). Within trials, there was a clear phase preference for both directionally and non-directionally selective units (175.69°, $p = 5.7 \times 10^{-7}$ and 113.86°, $p = 0.0044$, respectively, Rayleigh test for non-uniformity). Between trials, the phase preference for non-directionally selective units disappeared. For directionally selective units, however, the phase preference persisted (191.13°, $p = 9.5 \times 10^{-8}$ Raleigh test for non-uniformity) and was statistically indistinguishable from the in-trial phase preference ($p = 1$ compared with in-trial phase, Kuiper two-sample test against the null hypothesis that the two distributions are identical). These results suggest that the in-trial phase entrainment observed for non-directionally selective units may be an artifact of two physiologic events independently locked to the same behavioral event. Conversely, the phase entrainment of directionally selective units is more likely to be a pervasive feature of Mthal physiology.

Directionally Selective Unit Activity Uniquely Predicts LFP Power. Delta phase predicts both beta/low gamma power and single unit spiking. We therefore hypothesized that spiking and beta/low gamma power are also correlated. To test this, we cross correlated LFP power with a continuous spike density estimate (SDE) of all Mthal single unit activity and compared it to chance using a Poisson spike distribution.

During trials, directionally selective unit activity was maximally correlated with beta power ($r = 0.03$) at a lag of -0.72 s (i.e., Mthal spiking preceded beta power increases on average) (Figures 7 and 8). There was a smaller, yet significant negative correlation ($r = -0.02$) that peaked at -0.4 s, which may reflect decreased Mthal activity preceding the Nose- and Side In events (Figure 3-2, Gaidica et al., 2018) when beta power is enhanced. The cross-correlation pattern was strikingly similar during inter-trial intervals but attenuated ($r = 0.01$ at -0.58 s lag, r =

-0.014 at -0.25 s lag), suggesting that beta power is enhanced following a "pause-fire" pattern of directionally selective Mthal unit spiking. Non-directionally selective unit activity was correlated with beta power slightly earlier, and to a lesser degree in-trial ($r = 0.016$, $t = -0.18$ s lag, $r = -0.017$, $t = -0.52$ s lag), but was not significantly correlated with beta power during the inter-trial period. These results suggest that the relationship between non-directionally selective unit activity and beta power resulted from independent correlations with behavioral events. Conversely, the relationship between directionally selective unit activity and beta power is likely a general feature of Mthal physiology.

Similar patterns were observed for directionally selective unit spike-low gamma power correlations, which were significant during both in-trial and inter-trial epochs. However, non-directionally selective unit activity was not correlated with low gamma power during either epoch. The consistency of these correlations (or lack thereof) across both behavioral epochs supports the notion that directionally selective unit activity is uniquely linked to the LFP.

The pattern of high gamma modulation during the task closely matched single unit Mthal activity patterns (Figure 3-2, Gaidica et al., 2018), consistent with observations that high frequency oscillations are correlated with multi-unit activity. High gamma power best correlated with directionally selective unit activity, exhibiting roughly zero-lag between spiking and power increases. Therefore, as in cortex, Mthal high gamma power may serve as a surrogate for multi-unit activity (Watson, Ding, & Buzsáki, 2018; Ray, Crone, Niebur, Franaszczuk, & Hsiao, 2008; Manning, Jacobs, Fried, & Kahana, 2009).

Mthal single unit activity also showed a small correlation with delta power, which was larger for directionally selective units. Unlike the beta power correlation, the time lag (and pattern, Figure 3-8) of spike-delta power correlations was inconsistent between the in-trial and

inter-trial periods. The peak spike-power correlation occurred at -0.68 s in-trial ($r = 0.035$) but at 0.1 s during the inter-trial interval ($r = 0.019$). Similar but smaller correlations were also observed for non-directionally selective units ($r = 0.032$ at -0.13 s in-trial, $r = 0.015$ at 0.04 inter-trial).

In summary, the consistency of in-trial and inter-trial correlations argues for a unique physiological relationship between directionally selective unit activity and beta/low gamma power in Mthal.

LFP Correlates of Performance. Given the relationships between single unit activity and task performance (Figure 2-5, Gaidica et al., 2018), and single unit activity and LFP features, we next examined relationships between LFP features and task performance.

Delta phase near the Tone event strongly predicted RT ($p < 0.05$) in 19/30 recording sessions (Figure 3-9; session-averaged $r = 0.42$ at $t = 0.53$ s after the event). This suggests that there is a preferred Mthal delta phase for movement initiation (Figure 3-2), and that RT is (at least partially) determined by the distance from that preferred phase when the Tone plays (Lakatos et al., 2008). While we cannot completely rule out the possibility that filtering propagates a delta phase reset at Nose Out back in time to the Tone event (de Cheveigné & Nelken, 2019), similar delta phase-RT correlations have been reported in a range of behavioral paradigms (Stefanics et al., 2010; Hamel-Thibault et al., 2018; Saleh et al., 2010). Furthermore, while phase discontinuities were occasionally observed in the filtered signal (Figure 3-10A, orange marker), they were not consistently present at the Nose Out event (Figure 3-10C). Indeed, delta phase varied smoothly from the Tone through Nose Out events across all trials (Figure 3-10C).

There was a similar delta phase correlation near the Side In event for MT (Figure 3-9B, $p < 0.05$ for 20/30 sessions; session-averaged $r = 0.37$ at $t = 0.07$ s before the event). However, since delta phase was aligned at Nose Out, and MT was approximately the length of a single delta oscillation cycle, one would expect Side In to occur at different delta phases for different MTs. Thus, this delta phase-MT correlation likely does not represent a new finding independent of the Nose Out delta phase alignment.

Beta power also predicted RT in the peri-Tone period ($p < 0.05$ for 21/30 sessions; session-averaged $r = 0.29$ at $t = 0.45$ s after the event) (Leventhal et al., 2012). As for the delta phase-MT correlation, however, this relationship can be explained by event-related beta modulation. Specifically, for short RT, beta power increases earlier after the Tone event because the Nose Out event is closer to the Tone event (by definition). We previously reported a small but significant correlation between striatal beta power and RT in the immediate pre-Nose Out period, but this finding was not replicated in Mthal ($p < 0.05$ in only 4/30 sessions). Whether this is due to subtle differences between BG and Mthal physiology, failure to detect a subtle correlation in the present study, or a false positive result in the prior study, is unclear.

Finally, beta power was anticorrelated with MT just prior to Side In ($p < 0.05$ for 19/30 sessions; session-averaged $r = -0.27$ at $t = 0.04$ s before the event). However, because beta power increases transiently after Nose Out, beta power must be elevated just prior to Side In for short MT. This correlation is also, therefore, unlikely to represent a new effect independent of task-linked beta modulation. In summary, delta phase at the Tone event was the only LFP feature that consistently and independently predicted task performance.

Discussion

We identified several interrelated correlations between Mthal LFPs, Mthal single unit activity, and behavior. First, LFP phase in the delta band, and power in multiple frequency bands (delta, beta, low and high gamma) were modulated by specific behavioral events. Delta phase strongly predicted RT, LFP beta/low gamma power, and single unit spike timing. Given these correlations, it is not surprising that spike timing also predicted beta/low gamma power, though we did not find a consistent, independent relationship between beta power and RT. Interestingly, Mthal single unit subpopulations previously identified on the basis of their behavioral correlations (Chapter 2, Gaidica et al., 2018) exhibited distinct relationships with delta phase and beta power. Many, but not all, of these correlations persisted during the intertrial interval and decreased greatly when analyzed using trial-shuffled data. These findings argue that some of these correlations arise from independent locking of physiological features to task events, while others are a general feature of Mthal physiology (see below). These observations unify prior observations of correlations between delta phase, beta power, and behavior. They also provide new insights into how motor system LFP oscillations may be generated and linked to behavior.

Mthal event-related beta/low gamma power modulations were very similar to patterns in the basal ganglia and motor cortex during a nearly identical task (Leventhal et al., 2012). In both experiments, beta power increased at Nose Out, in apparent conflict with the widely held view that beta power decreases with movement onset. This discrepancy is likely due to task design. When instructive and imperative cues are temporally separated, beta power increases during inter-stimulus “hold” periods and decreases with movement onset (including in our own experiments) (Donoghue et al., 1998; Saleh et al., 2010; Leventhal et al., 2012; Khanna &

Carmena, 2017). Therefore, beta oscillations may be more strongly associated with processing behaviorally relevant stimuli than the presence or absence of movement (Saleh et al., 2010).

Beta oscillations are suggested to represent a stabilized network state during which motor plans are less likely to change (Gilbertson et al., 2005; Pogosyan et al., 2009; Engel & Fries, 2010; Khanna & Carmena, 2017), which may serve the adaptive purpose of preventing distractors from interfering with a recently adopted plan. This interpretation is supported by small, but significant and reproducible, correlations between beta power and RT (Leventhal et al., 2012; Khanna & Carmena, 2017; Shin et al., 2017; van Wijk, 2017; Torrecillos et al., 2018). However, we did not replicate that finding here. This could be due to differences in recording sites, as prior correlations were found in basal ganglia or cortex. However, patterns of event-related beta power modulation were nearly identical in striatum and Mthal (Leventhal et al., 2012), making it less likely that Mthal and cortical-BG beta oscillations differentially predict RT. We suggest instead that beta power is linked to RT indirectly, explaining why weak beta-RT correlations are frequently observed.

Delta phase was more strongly and consistently correlated with RT prior to movement onset than beta power, and similar correlations have been found during tasks in which cortical delta oscillations entrain to rhythmic stimuli (Arnal et al., 2015; Lakatos et al., 2008; Stefanics et al., 2010). LFP oscillations may modulate neuronal excitability through ephaptic interactions (Anastassiou et al., 2010; Tiganj, Chevallier, & Monacelli, 2014), or simply reflect aggregate synaptic drive that influences spiking probability (Pesaran et al., 2018). In either case, active entrainment of LFP oscillations to rhythmic cues is a potential mechanism to optimize neuronal excitability at the time of anticipated salient stimuli (Schroeder & Lakatos, 2009). It remains unclear, however, whether such mechanisms are generalizable to single interval timing (Breska

& Deouell, 2017; Zoefel, Archer-Boyd, & Davis, 2018; Hamel-Thibault et al., 2018). In our task, imperative cue (Tone) timing is somewhat predictable, occurring 0.5–1.0 s after Nose In. The presence of significant delta phase coherence across trials even prior to Nose In (Figure 3-11), and the smooth progression of delta phase at Nose Out (as opposed to an abrupt phase reset, Figure 3-10), support the idea that delta phase actively aligns to increase the probability that the Tone arrives at a favorable phase for quick reactions.

A plausible mechanism for delta phase-RT correlations is that delta phase predicts (perhaps influences) Mthal spike timing, which directly drives motor cortex to initiate movement. Thus, if the Tone arrives just after the optimal phase, a full delta cycle would have to repeat before Mthal neurons are maximally excitable, potentially explaining a source of RT variability. In support of this hypothesis, units whose activity predicted RT, MT, and movement direction ("directionally-selective" units) were most strongly entrained to delta rhythms. Furthermore, this entrainment persisted into the inter-trial interval with the same preferred phase, suggesting that the delta phase-spike timing relationship for these units specifically is a feature of Mthal physiology. A related but slightly different interpretation is that circuit-wide delta oscillations simultaneously reflect thalamic and cortical excitability, with cortical neurons more likely to fire at specific delta phases independently of thalamic input (Lakatos et al., 2005; Rule, Vargas-Irwin, Donoghue, & Truccolo, 2018).

Directionally selective unit activity also predicted beta power increases, both during task performance and the inter-trial interval. This provides a possible mechanism for delta-beta PAC: delta phase predicts Mthal single unit spike timing which in turn predicts, and possibly causes, cortical beta oscillations that are propagated throughout basal ganglia-thalamocortical circuits (Sherman et al., 2016; Reis et al., 2019; Jones et al., 2009). Such a model could explain

frequently observed correlations between beta power and RT, as well as associations between "bursty" Mthal activity and beta oscillations in Parkinson Disease (Kühn et al., 2009; Ellens & Leventhal, 2013; Devergnas et al., 2015; Reis et al., 2019). If delta phase-modulated Mthal single unit activity both initiates movement and drives cortical beta oscillations, one would expect weak correlations between beta power and movement initiation. Note that this model does not exclude the possibility that other sources of beta oscillations (e.g., intrinsic basal ganglia oscillators, McCarthy et al., 2011; Tachibana et al., 2011; Mirzaei et al., 2017) are independently associated with behavior.

It is not clear if directionally- and non-directionally selective units are anatomically distinguishable, which may have important implications for understanding how LFP oscillations are generated and regulated. Mthal comprises two mostly non-overlapping subregions defined by basal ganglia or cerebellar afferents (Deniau, Kita, & Kitai, 1992; Kuramoto et al., 2011). Several pieces of evidence indirectly suggest that directionally-selective units reside in basal ganglia-recipient Mthal. First, directionally selective unit activity predicts features of task performance commonly attributed to the basal ganglia (action selective and movement vigor). Second, directionally selective units were more tightly entrained to delta oscillations during wakefulness, as are basal ganglia-recipient Mthal units (compared to cerebellar-recipient units) under anesthesia (Nakamura et al., 2014). Finally, directionally-selective unit activity predicted increased beta power, which is associated with basal ganglia-thalamocortical circuitry (Leventhal et al., 2012; López-Azcárate et al., 2013; Brittain & Brown, 2014; Feingold et al., 2015). An alternative possibility is that these Mthal populations are defined by layer-specific cortical projections. Thalamic afferent activity in layer 1 near movement onset is correlated with the speed of individual lever pulls performed by mice (Tanaka et al., 2018), consistent with

correlations between directionally-selective unit activity and MT (Figure 2-5, Gaidica et al., 2018). Because basal ganglia- and cerebellar-recipient Mthal thalamocortical neurons tend to project to cortical layers 1 and 3/5 respectively (but not with 100% certainty) (Herkenham, 1980; Kuramoto et al., 2009; Kuramoto et al., 2015; Tanaka et al., 2018), these possibilities may ultimately be indistinguishable.

In summary, we found complex relationships between Mthal LFP oscillations, single unit activity, and performance of a two-alternative forced choice task. These results support a model in which low frequency LFP oscillations either modulate or reflect neuronal excitability, which in turn drives movement initiation and regulates higher frequency (beta/low gamma) oscillations. These results potentially explain previously observed correlations between delta phase, beta power, and behavior. Selective, independent manipulation of neural activity at multiple nodes in basal ganglia-thalamocortical circuits during well-defined behaviors will be needed to test this model.

Materials and Methods

Data Collection. Detailed data collection methods have been previously described in Chapter 2, Materials and Methods. All animal procedures were approved by the Institutional Animal Care and Use Committee of the University of Michigan. 5 adult male Long-Evans rats (Charles River Laboratories, Wilmington, MA) were housed on a reverse light/dark cycle and food restricted on training days. Operant chambers (ENV-009 Med Associates) were outfitted with 5 illuminated nose ports along one side with an opposite-facing reward port (Figure 3-1B). Rats were progressively trained to poke one of three illuminated center ports and then, after a variable delay (0.5–1 s, pulled from a uniform distribution), instructed to poke a neighboring port based on a brief low (1 kHz, "go left") or high (4 kHz, "go right") pitched tone. Correct trials were rewarded with a 45 mg sucrose pellet at the reward port. Rats were required to perform 80% of trials correctly for three sequential 1-hour sessions before being implanted.

Electrophysiological implants were designed in SolidWorks and printed at the University of Michigan 3D Lab using biocompatible resins. Tetrodes spun from 12 μm wire (Sanvik PX000004) or 50 μm single wire electrodes (California Fine Wire) were interfaced with a Tucker Davis Technologies amplifier system (TDT, ZD64, AC32, PZ4, RZ2, and RS4) using a custom printed circuit board (Advanced Circuits). The entire electrode assembly was driven down with a single precision drive screw. Immediately before surgery, the tetrodes (but not single wires) were gold plated according to a third-party protocol (Neuralynx) and impedances for all electrodes were recorded using a nanoZ (White Matter) impedance tester. All implants were surgically placed with the electrodes residing above the final recording site (Mthal; AP: -3.1 mm, ML: 1.2 mm, DV: -7.1 mm) with a ground and reference screw placed over the cerebellum contacting cerebral spinal fluid. Rats recovered for one week before retraining.

Electrodes were driven roughly 60 μm after each recording day. Wideband (0.1−10 kHz) neural signals were recorded with the TDT system, which was interfaced with custom LabVIEW behavioral software to record behavior timestamps. Single units were sorted in Offline Sorter (Plexon).

Data Analysis. All data analysis was performed using MATLAB software which was routinely versioned using Git. Only correct trials that did not contain wideband artifacts were included in our analysis (n = 2,248 from 30 sessions) using the following exclusion criteria. The signal was converted to a z-score based on the mean and standard deviation from all trials in that session. If the z-score exceeded 5 for more than 5% of the trial length, the trial was excluded. We used the same single unit population (n = 366) from Chapter 2, that did not consider LFP interactions within neuronal firing.

Power Spectrum. We visually inspected the raw data from all electrodes from each session and ranked their recording quality to select electrodes with no high amplitude artifacts. This enabled us to use a single, high quality LFP signal from each session for our analyses. In addition, for spike-power and spike-phase correlations, we selected LFP signals from wires where the spikes were not recorded, minimizing the possible influence of the spike waveform itself on the LFP. The LFP was consistent across electrodes, which has been observed by others performing high-density, single-site electrophysiology (Buzsáki, Anastassiou, & Koch, 2012).

We separately analyzed epochs during which the rat was engaged in the task ("in-trial", between the Cue to Reward) and between trials ("inter-trial", after the Reward and before the Cue). We created the in-trial power spectrum by concatenating the wideband LFP from all in-trial time periods from a single session. Next, we performed a Fourier transform (*fft* in MATLAB) to obtain the power-frequency spectrum. In order to obtain an average spectrum for

all sessions, we normalized the spectrum using the 70-150 Hz segment as a reference, which accounted for the variability associated with using different types of electrodes. We present the average spectrum using a conservative smoothing window (*smooth* in MATLAB, Figure 3-1C). We created the inter-trial power spectrum in the same way but selected inter-trial segments of the LFP equaling the in-trial duration.

LFP Correlates of Behavior. A complex scalogram (1–200 Hz, 30 steps log-scale) was computed for each trial by applying a bank of Gabor filters to the raw data (Wallisch et al., 2013). The peri-event (± 1 s) window was extracted from a buffered data series to eliminate filter edge effects. LFP power was calculated by taking the squared magnitude of the complex spectrum. For each session, we determined the mean ($\mu_{baseline}$) and standard deviation ($\sigma_{baseline}$) of baseline power using a window (2 s) leading up to the Cue event. The average $\mu_{baseline}$ and $\sigma_{baseline}$ for each session ($\mu_{session}$ and $\sigma_{session}$, respectively) allowed us to z-score the peri-event power of each trial.

$$trial_{z-score} = \frac{trial_{power} - \mu_{session}}{\sigma_{session}}$$

LFP phase was determined using the *angle* function in MATLAB on the complex scalogram. The mean resultant vector length (MRL) for phase data was computed using the *circ_r* function from the Circular Statistics Toolbox (CircStat) for MATLAB (Berens, 2009). Z-scored power and the raw MRL values were calculated for each session and reported as the mean for all sessions (Figure 3-2).

Power Comodulation. Power 3grams were generated using the *corr* function in MATLAB (Pearson's correlation). For each session, the power from all trials for each event (± 0.5 s) was concatenated and used to calculate the correlation coefficient for all frequency pairs (1–200 Hz, 30 steps log-scale). Trial-shuffled 3grams used a random trial order and were

reported as the mean correlation coefficient from repeating the calculation 100 times. Both 3grams are presented as the average over all sessions (Figure 3-3).

Phase-amplitude Coupling (PAC). We quantified the strength of PAC based on established methods (Canolty et al., 2006). A complex scalogram (1–200 Hz, 30 steps log-scale) was computed for a peri-event time window (± 0.5s) for each trial. For each session, we concatenated data from all trials for each event. Thus, we obtained a complex time series for all events that was *n*-seconds long, where *n* is the number of trials in a session. We then obtained the time-series phase (Φ_t) by applying the *angle* function in MATLAB and amplitude (A_t) by taking the squared magnitude. These data were used to determine the PAC between pairs of frequencies (*m*,*n*) across all events, with the constraint that the amplitude frequency was always greater than or equal to the phase frequency. We achieved this by first creating a composite phase-amplitude signal (z_t) from the session-wide time series data:

$$z_{t(m,n)} = A_{t(m,n)} e^{i\phi_{t(m,n)}}$$

The mean ($M_{m,n}$) of $z_{t(m,n)}$ quantifies the deviation of $z_{t(m,n)}$ from a radially symmetric distribution of high frequency LFP amplitudes across low frequency phases. To account for the possibility that Φ_t is not uniformly distributed, we normalized $M_{m,n}$ for each session using 200 surrogates generated by adding a random lag τ to A_t.

$$z_{t(m,n)+\tau} = A_{t(m,n)+\tau} e^{i\phi_{t(m,n)}}$$

M_{surr} is the mean of $z_{t(m,n)+\tau}$ and is calculated separately for each surrogate phase-amplitude analysis. The mean (μ_{Msurr}) and standard deviation (σ_{Msurr}) of the surrogate distribution were calculated using *normfit* in MATLAB (where the input was all 200 M_{surr} values). We report the modulation index ($MI_{m,n}$) as the magnitude of the normalized $M_{m,n}$ (Figure 3-4).

$$MI_{m,n} = \left| \frac{M_{m,n} - \mu_{M_{surr}}}{\sigma_{M_{surr}}} \right|$$

A p-value was obtained for each phase-amplitude pair in the MI matrix using *normcdf* in MATLAB with the 'upper' option to compute right-tailed probabilities. We corrected for multiple comparisons (Bonferroni method) by multiplying the p-values by the number of elements in $MI_{m,n}$ ($N = 30 \times 30$). For example, using $\alpha = 0.05$, the z-score contained in MI must exceed 3.87 to reach significance (determined using *norminv* function in MATLAB on $\alpha \div N$).

To determine if PAC was present independent of correlations between LFP features and behavior, we recalculated surrogate MIs 1,000 times from a composite signal where the trial order of A_t was shuffled (Stark & Abeles, 2005). This allowed us to generate a statistical measure for the fraction of shuffled MIs greater or less than the true MI.

Single Unit Entrainment. We extracted the instantaneous phase of the LFP from the complex spectrum (using the MATLAB *angle* function) for each spike timestamp within equal duration in-trial and inter-trial periods. Next, we performed a Rayleigh test for non-uniformity of circular data (CircStat *circ_rtest* function) (Berens, 2009) for the compiled phases to obtain a p-value to reject the null hypothesis that spike timing is uniformly distributed from -180° to 180° (Figure 3-5A). To determine if the number of units significantly entrained was greater than chance, we generated firing rate matched, Poisson distributed spike trains for each unit and recalculated the p-values 1,000 times. We used the same data to calculate the mean MRL of LFP phase at each spike timestamp for each unit population (Figure 3-5B), and similarly compared it against Poisson spikes.

To determine if a phase preference was consistent across all units, we used the spike-phase data from above to generate spike histograms for each unit across 12 bins linearly spaced between -180° and 180° (Figure 3-6). Each unit histogram was normalized by dividing each bin

count by the total number of spikes for that unit to account for spike rate. We used the same method described above to generate surrogate Poisson spike-phase histograms, which were used to assess the significance of single unit phase preferences.

Spike-power Cross Correlations. We used a cross correlation to determine the relationship between LFP power and single unit activity for equal duration in-trial and inter-trial periods. First, we generated a session-wide continuous spike density estimate (SDE) for each unit and trial by convolving the vector of discrete spiking events with a 50 ms Gaussian kernel (Wallisch et al., 2013). Next, we extracted the relevant SDE segments for the in-trial and inter-trial periods. We cross correlated these data with LFP power (1–200 Hz, 30 steps log-scale) on a per-trial basis using the *xcorr* function in MATLAB with the 'coeff' option so that the autocorrelations at zero lag equal 1. Cross correlation matrices are presented as the mean over all trials and sessions (Figure 3-7). We recalculated each cross correlation using a firing rate matched, Poisson distributed spike train 20 times, giving us a distribution of correlation values across time for each frequency. The maximum and minimum of that distribution are where we considered values significantly different from chance (Figure 3-8).

LFP Correlates of Performance. To determine relationships between LFP features, reaction time (RT), and movement time (MT), we used peri-event (± 1s) power and phase data for each frequency (1–200 Hz, 30 steps log-scale) and all trials. For each time point and frequency, we created a 1-by-*n* array of power (or phase) values, where *n* was the number of trials in that session, along with a 1-by-*n* array of the RT (or MT) values for each trial. We used these two arrays as inputs to the *corr* function in MATLAB to calculate Spearman's correlation coefficient for power-RT/MT, and the *circ_corrcl* function (CircStat toolbox, Berens, 2009) for

phase-RT/MT correlations. Therefore, each time-frequency pair generated a single p-value for the correlation between power/phase and RT/MT (Figure 3-9).

Figures

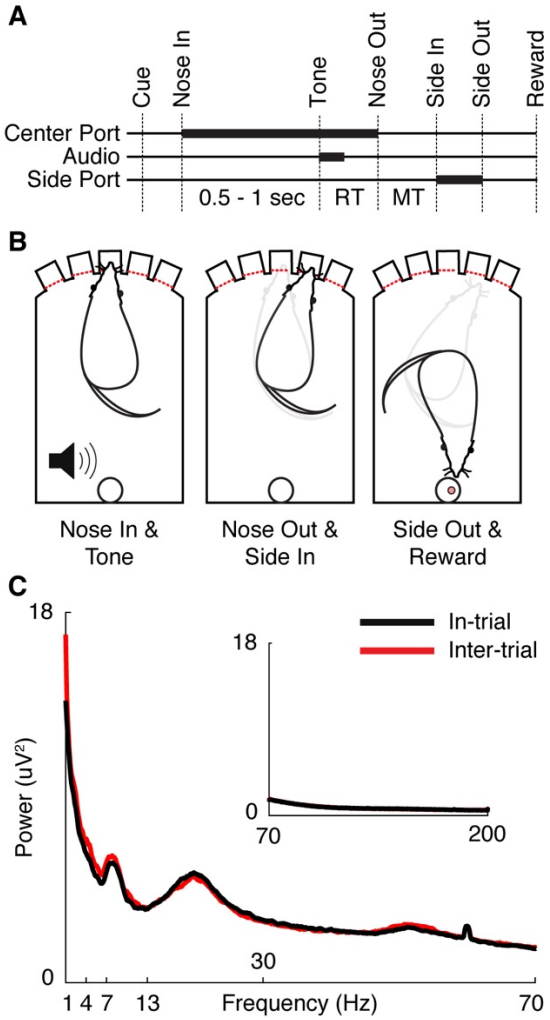

Figure 3-1: Behavioral task and physiology

(A) Trials began by illuminating one of the three center ports in a five-port behavior chamber ("Cue"). The rat poked and held its nose in the lit port ("Nose In") for a variable interval (0.5–1 s, pulled from a uniform distribution) until a 1 or 4 kHz auditory cue ("Tone") instructed the rat to move one port to the left or right, respectively. Nose Out, Side In, and Side Out indicate when the rat withdrew from the central port, poked the adjacent port, and withdrew from the adjacent port, respectively. "Reward" indicates the time of reward pellet retrieval. Reaction time (RT) and movement time (MT) intervals are labelled. **(B)** Schematic of the rat operant chamber during key behavioral epochs. **(C)** Session-averaged power spectrum of low (1–70 Hz) and high (inset, 70–200 Hz) frequencies for in-trial (black) and inter-trial (red) periods.

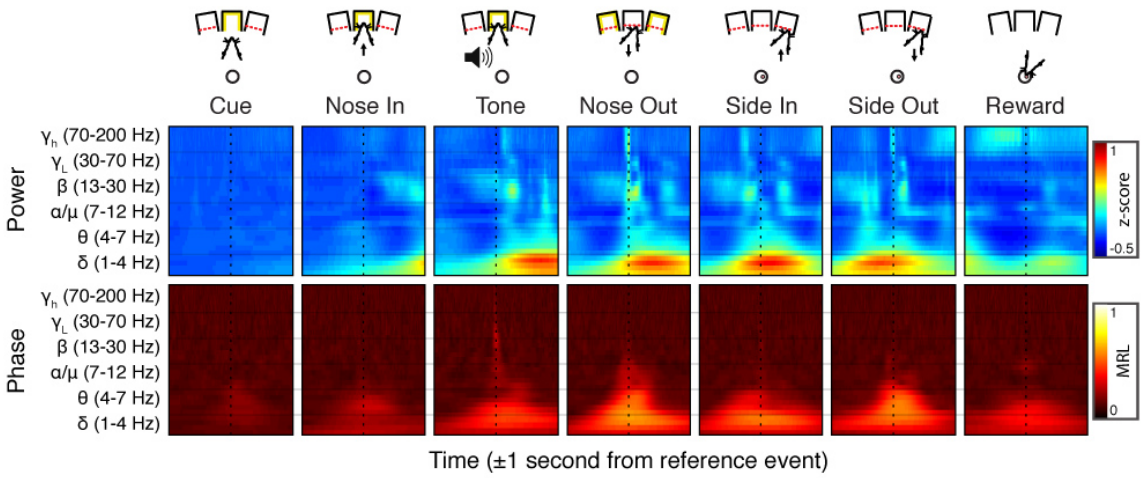

Figure 3-2: Peri-event LFP power and phase modulation

(Top) behavioral schematic for a rightward-cued successful trial. (Middle) Mean gabor spectrograms for each event. (Bottom) Mean resultant length (MRL) of event-locked LFP phase. Higher values indicate more consistent phase alignment at each time-frequency point.

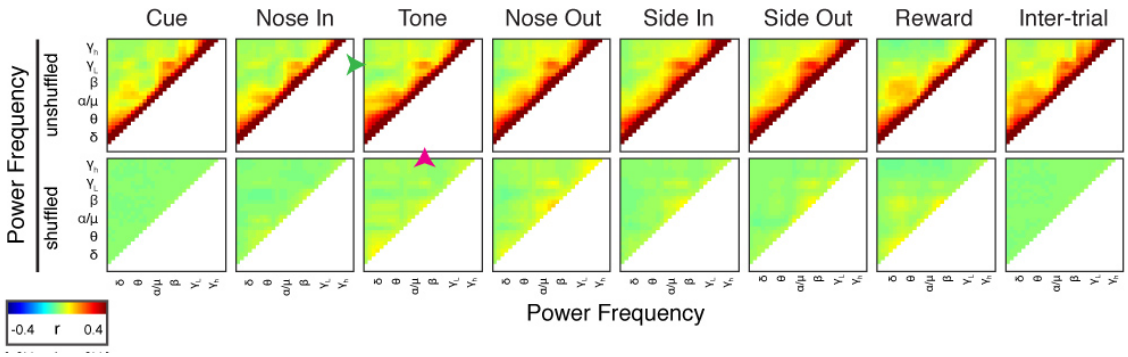

Figure 3-3: Mthal LFP power in discrete frequency bands is comodulated during and between trials.

(Top) power-power comodugrams locked to each behavioral event and during the inter-trial interval. Note the consistent positive correlation between continuous beta (20 Hz, magenta arrow at Tone) and low gamma (55 Hz, green arrow at Tone) power. (Bottom) comodugrams for the same events but calculated using trial-shuffled data.

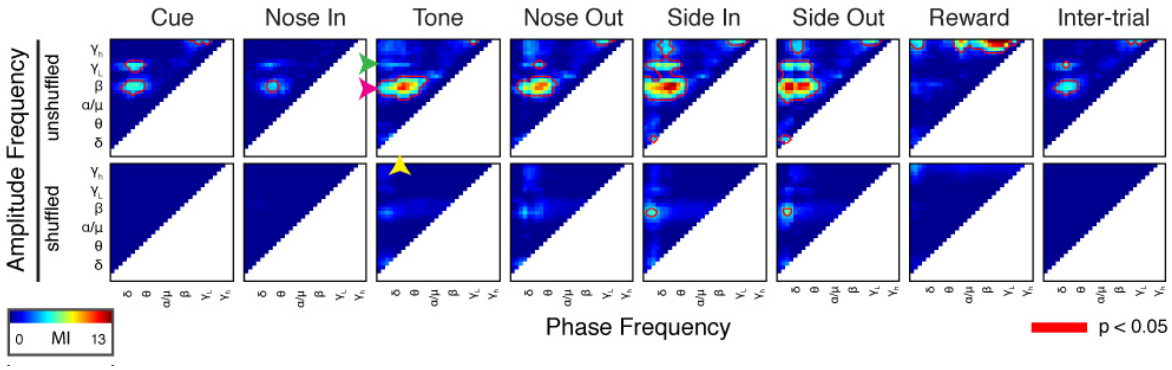

Figure 3-4: Phase-amplitude coupling (PAC) is dynamically modulated by task events

(Top) Peri-event PAC as assessed by the modulation index (MI, see Materials and Methods). (Bottom) same calculation using trial shuffled data. Red outlines highlight areas where PAC is significant ($p < 0.05$).

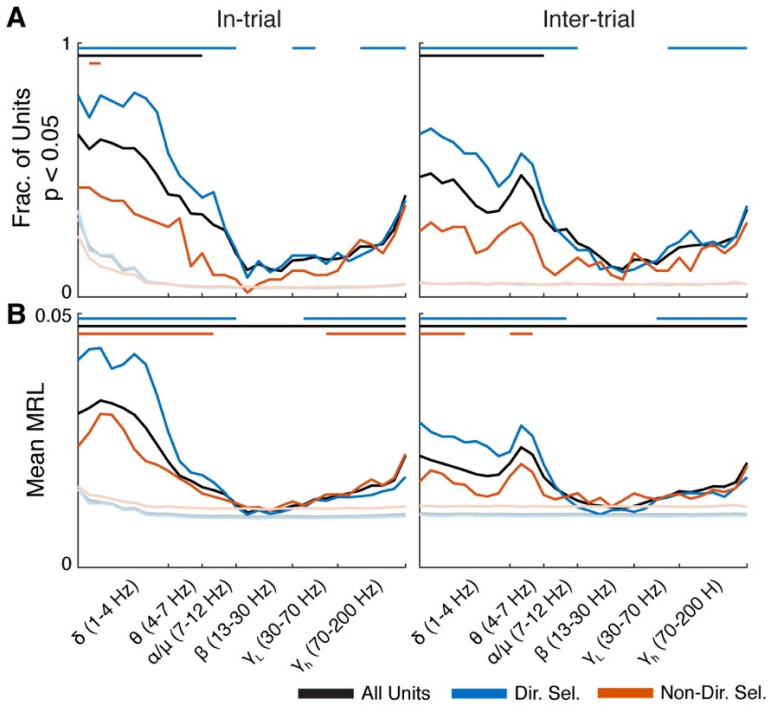

Figure 3-5: Single unit activity is selectively entrained to low frequency oscillations

(A) The fraction of units from each population that were significantly entrained to the delta oscillation ($p < 0.05$, Rayleigh test for non-uniformity) during task engagement ("in-trial") and during the inter-trial interval ("inter-trial"). **(B)** Average mean resultant length (MRL) for each unit population.

Colored lines at the top of each plot indicate frequencies at which the values significantly exceed ($p < 0.001$) those from firing-rate matched, Poisson-distributed spike trains (muted colored lines).

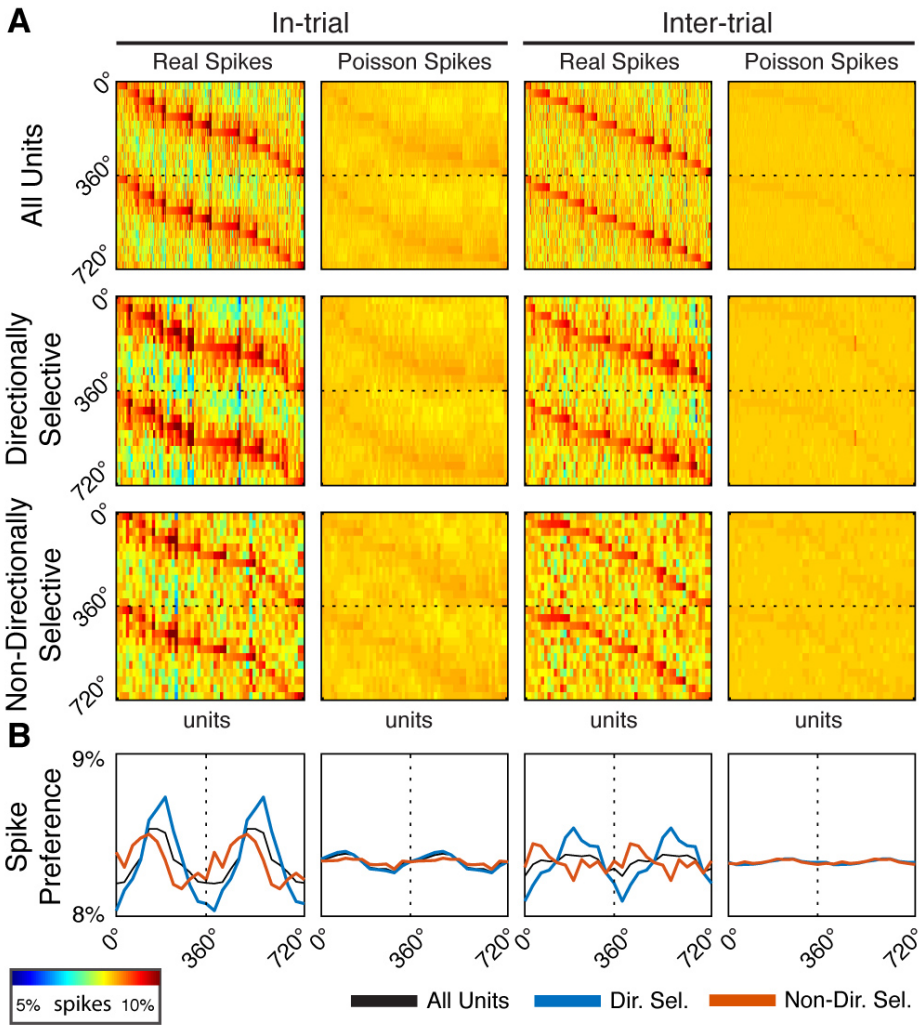

Figure 3-6: Single unit entrainment occurs at preferred delta phases specifically for directionally-selective units

(A) Spike-phase histograms for functionally-defined single unit populations and surrogate Poisson-distributed spike trains. Each column within the individual phase histograms represents a single unit. Colors indicate the percentage of spikes within a phase bin (12 bins from 0° to 360°, repeated to 720° for clarity). Units are sorted by their preferred phase separately for each plot. **(B)** Mean spike-phase histograms for each unit population.

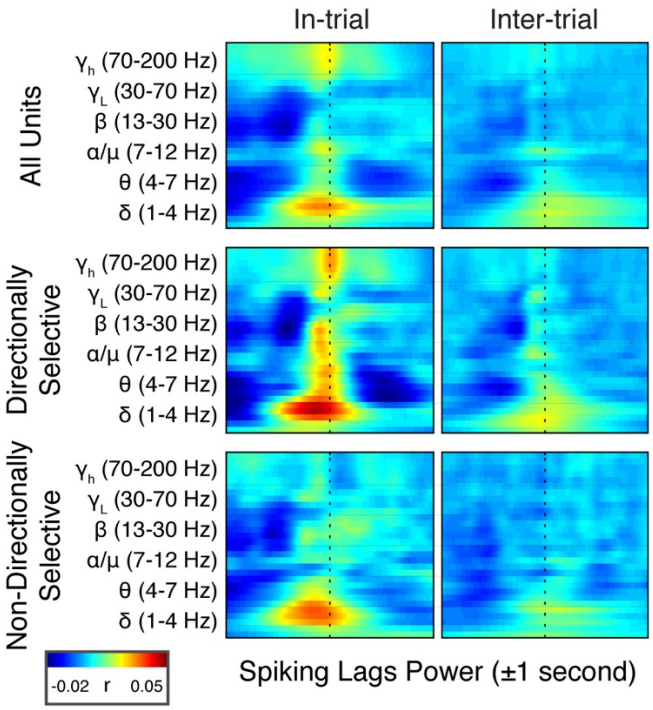

Figure 3-7: Spike timing is correlated with power modulation in specific frequency bands

Spike-power cross correlations for in-trial and inter-trial epochs (±1 s). Positive correlations prior to t = 0 indicate that spiking led (i.e., came before) power increases.

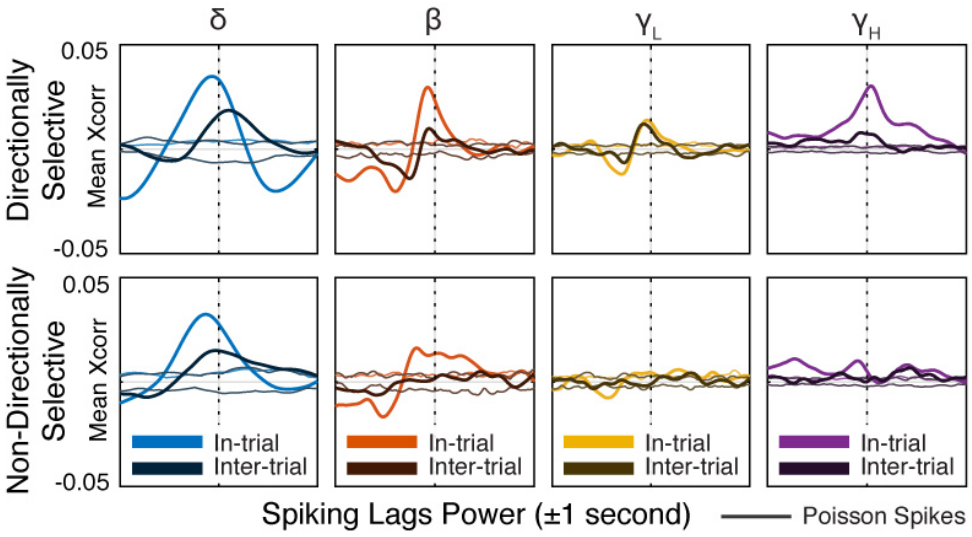

Figure 3-8: Beta power lags directionally-selective unit spiking during and between trials

Band-specific cross correlations (±1 s) in specific frequency bands for directionally selective (top) and non-directionally selective (bottom) units. Thick lines represent the actual correlations; thin lines represent thresholds for significance (see Materials and Methods).

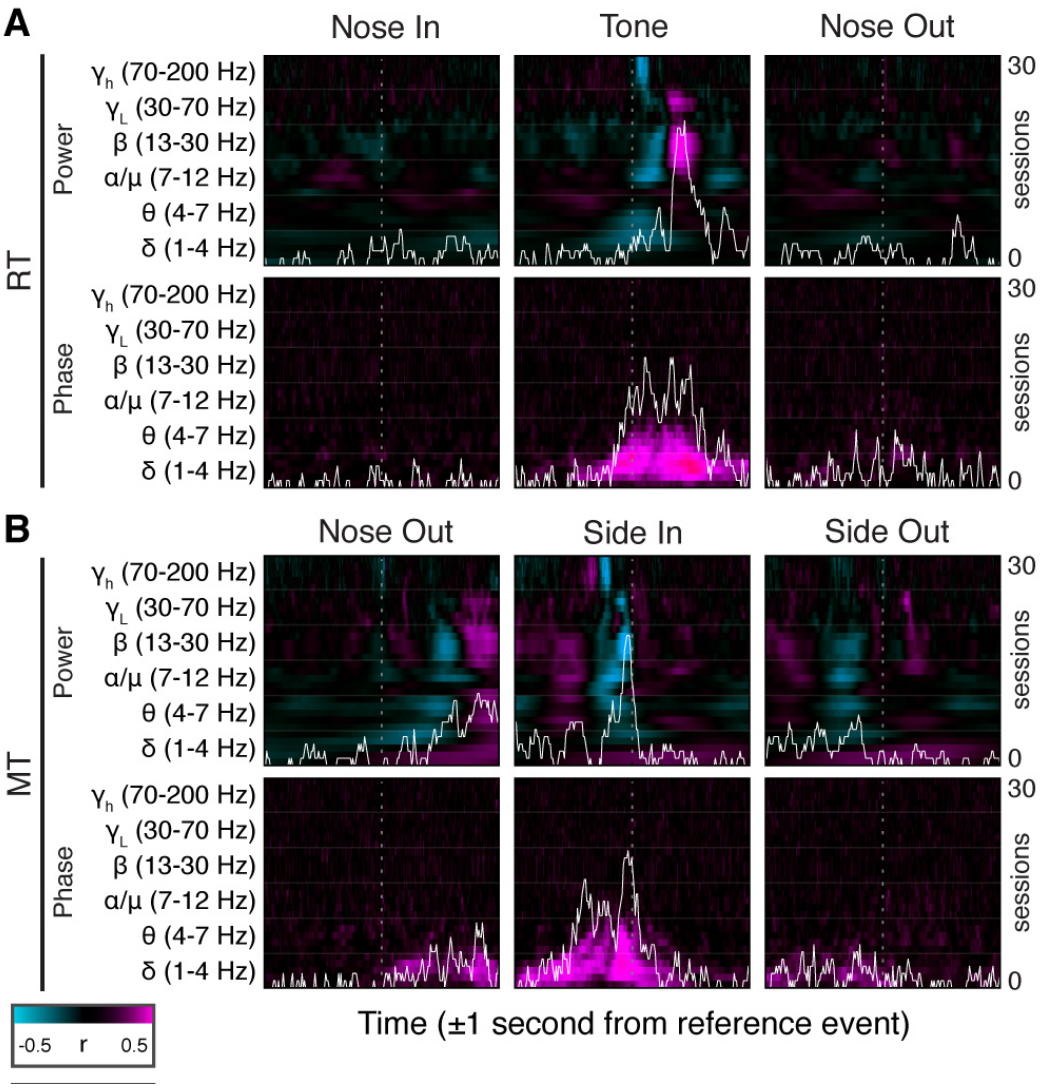

Figure 3-9: LFP oscillations predict task performance

(A) Peri-event (±1 s) reaction time (RT) correlations for power (top) and phase (bottom) for the Nose In, Tone, and Nose out events. Correlation values are session-averaged. The white line indicates how many sessions reached significance ($p < 0.05$) at each time point. **(B)** Same data as (A) for movement time (MT) from the Nose Out, Side In, and Side Out events.

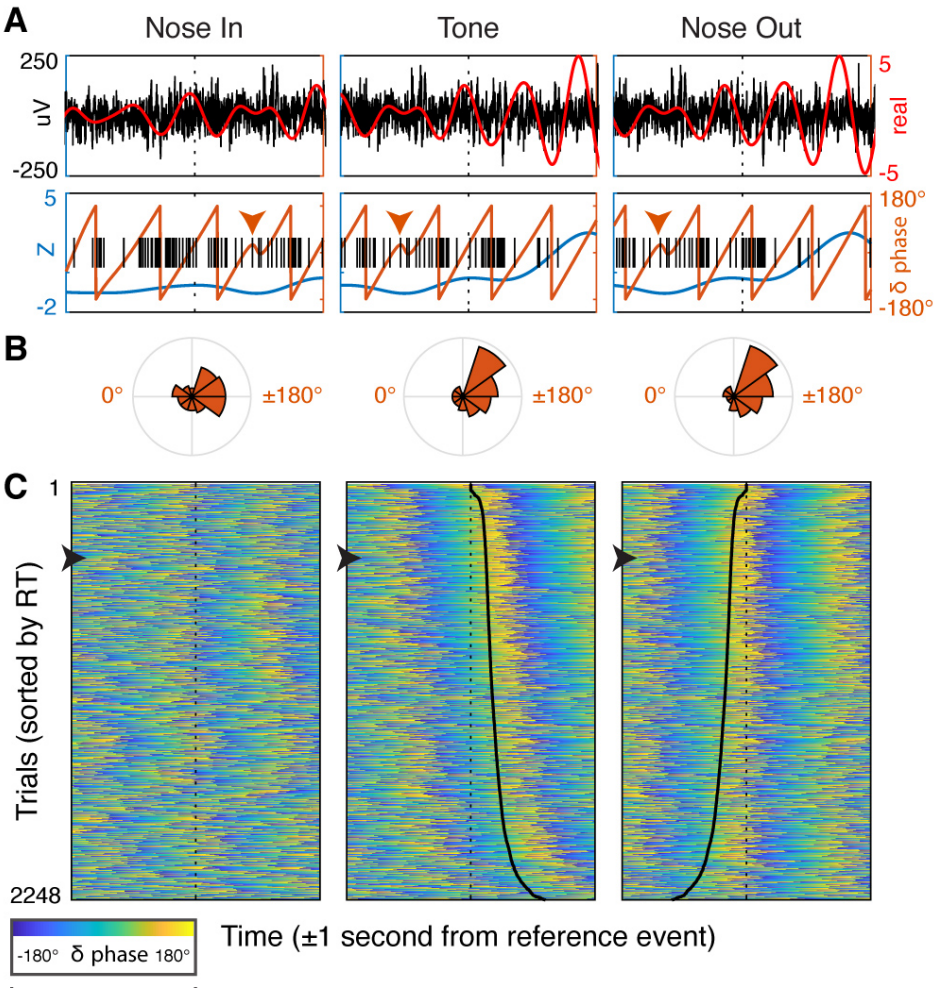

Figure 3-10: Delta phase predicts spiking and becomes aligned at Nose Out.

(A) Peri-event (±1 s) data from a single trial. Top - the unfiltered, wideband signal (black) and real component of the analytic signal (red) in the delta band. Bottom - delta power (blue) and phase (orange line, orange marker highlights phase discontinuity), and single unit spike timing (black, directionally selective unit #319, bottom). **(B)** Normalized, single unit spike-phase histograms for the data in (A). **(C)** Peri-event delta phase from all trials sorted by reaction time (RT, trial from A marked with black arrow along left border). Black lines in the Tone and Nose Out panels indicate the Nose Out and Tone events, respectively (i.e., time from event to the black line is RT).

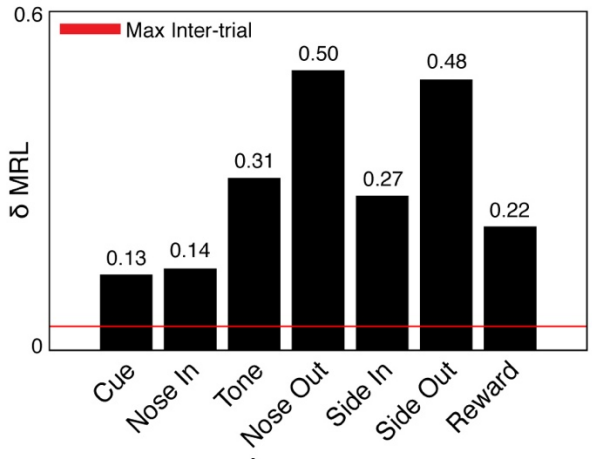

Figure 3-11: Delta phase syncs to task before Nose Out.

The mean resultant length (MRL) for delta phase (~2.5 Hz) at the time of each event. The red line indicates the maximum inter-trial MRL obtained by resampling delta phase during the inter-trial period (see Materials and Methods).

References

Anastassiou, C. A., Montgomery, S. M., Barahona, M., Buzsáki, G., & Koch, C. (2010). The effect of spatially inhomogeneous extracellular electric fields on neurons. *J Neurosci*, *30*(5), 1925-1936.

Armstrong, S., Sale, M. V., & Cunnington, R. (2018). Neural Oscillations and the Initiation of Voluntary Movement. *Front Psychol*, *9*, 2509.

Arnal, L. H., Doelling, K. B., & Poeppel, D. (2015). Delta-Beta Coupled Oscillations Underlie Temporal Prediction Accuracy. *Cereb Cortex*, *25*(9), 3077-3085.

Baker, S. N., Olivier, E., & Lemon, R. N. (1997). Coherent oscillations in monkey motor cortex and hand muscle EMG show task-dependent modulation. *J Physiol*, *501*, 225-241.

Bansal, A. K., Vargas-Irwin, C. E., Truccolo, W., & Donoghue, J. P. (2011). Relationships among low-frequency local field potentials, spiking activity, and three-dimensional reach and grasp kinematics in primary motor and ventral premotor cortices. *J Neurophysiol*, *105*(4), 1603-1619.

Bastos, A. M., Briggs, F., Alitto, H. J., Mangun, G. R., & Usrey, W. M. (2014). Simultaneous recordings from the primary visual cortex and lateral geniculate nucleus reveal rhythmic interactions and a cortical source for γ-band oscillations. *J Neurosci*, *34*(22), 7639-7644.

Belluscio, M. A., Mizuseki, K., Schmidt, R., Kempter, R., & Buzsáki, G. (2012). Cross-Frequency Phase-Phase Coupling between Theta and Gamma Oscillations in the Hippocampus. *J Neurosci*, *32*, 423-435.

Berens, P. (2009). CircStat: a MATLAB toolbox for circular statistics. *J Stat Softw*, *31*(10), 1-21.

Berke, J. D., Okatan, M., Skurski, J., & Eichenbaum, H. B. (2004). Oscillatory entrainment of striatal neurons in freely moving rats. *Neuron*, *43*, 883-896.

Breska, A., & Deouell, L. Y. (2017). Neural mechanisms of rhythm-based temporal prediction: Delta phase-locking reflects temporal predictability but not rhythmic entrainment. *PLoS Biol*, *15*(2), e2001665.

Brittain, J.-S. S., & Brown, P. (2014). Oscillations and the basal ganglia: motor control and beyond. *Neuroimage*, *85 Pt 2*, 637-647.

Brown, P. (2006). Bad oscillations in Parkinson's disease. *J Neural Transm Suppl*, 27-30.

Buzsáki, G., Anastassiou, C. A., & Koch, C. (2012). The origin of extracellular fields and currents--EEG, ECoG, LFP and spikes. *Nat Rev Neurosci*, *13*, 407-420.

Canolty, R. T., Edwards, E., Dalal, S. S., Soltani, M., Nagarajan, S. S., Kirsch, H. E. et al. (2006). High gamma power is phase-locked to theta oscillations in human neocortex. *Science*, *313*, 1626-1628.

Canolty, R. T., Soltani, M., Dalal, S. S., Edwards, E., Dronkers, N. F., Nagarajan, S. S. et al. (2007). Spatiotemporal dynamics of word processing in the human brain. *Front Neurosci*, *1*, 185-196.

Cohen, M. X., Elger, C. E., & Fell, J. (2009). Oscillatory activity and phase-amplitude coupling in the human medial frontal cortex during decision making. *J Cogn Neurosci*, *21*, 390-402.

Crunelli, V., David, F., Lőrincz, M. L., & Hughes, S. W. (2015). The thalamocortical network as a single slow wave-generating unit. *Curr Opin Neurobiol*, *31*, 72-80.

Crunelli, V., Lőrincz, M. L., Connelly, W. M., David, F., Hughes, S. W., Lambert, R. C. et al. (2018). Dual function of thalamic low-vigilance state oscillations: rhythm-regulation and plasticity. *Nat Rev Neurosci*, *19*(2), 107-118.

de Cheveigné, A., & Nelken, I. (2019). Filters: When, Why, and How (Not) to Use Them. *Neuron*, *102*(2), 280-293.

de Hemptinne, C., Ryapolova-Webb, E. S., Air, E. L., Garcia, P. A., Miller, K. J., Ojemann, J. G. et al. (2013). Exaggerated phase-amplitude coupling in the primary motor cortex in Parkinson disease. *Proc Natl Acad Sci U S A*, *110*, 4780-4785.

Dejean, C., Arbuthnott, G., Wickens, J. R., Le Moine, C., Boraud, T., & Hyland, B. I. (2011). Power Fluctuations in Beta and Gamma Frequencies in Rat Globus Pallidus: Association with Specific Phases of Slow Oscillations and Differential Modulation by Dopamine D1 and D2 Receptors. *J Neurosci*, *31*, 6098-6107.

Deniau, J. M., Kita, H., & Kitai, S. T. (1992). Patterns of termination of cerebellar and basal ganglia efferents in the rat thalamus. Strictly segregated and partly overlapping projections. *Neurosci Lett*, *144*, 202-206.

Devergnas, A., Chen, E., Ma, Y., Hamada, I., Pittard, D., Kammermeier, S. et al. (2015). Anatomical Localization of CaV3.1 Calcium Channels and Electrophysiological Effects of T-type Calcium Channel Blockade in the Thalamus of MPTP-Treated Monkeys. *J Neurophysiol*, jn.00858.2015.

Donoghue, J. P., Sanes, J. N., Hatsopoulos, N. G., & Gaál, G. (1998). Neural discharge and local field potential oscillations in primate motor cortex during voluntary movements. *J Neurophysiol*, *79*, 159-173.

Dowd, E., & Dunnett, S. B. (2005). Comparison of 6-hydroxydopamine-induced medial forebrain bundle and nigrostriatal terminal lesions in a lateralised nose-poking task in rats. *Behav Brain Res*, *159*, 153-161.

Ellens, D. J., & Leventhal, D. K. (2013). Review: electrophysiology of basal ganglia and cortex in models of Parkinson disease. *J Parkinsons Dis*, *3*, 241-254.

Engel, A. K., & Fries, P. (2010). Beta-band oscillations--signalling the status quo? *Curr Opin Neurobiol*, *20*, 156-165.

Feingold, J., Gibson, D. J., DePasquale, B., & Graybiel, A. M. (2015). Bursts of beta oscillation differentiate postperformance activity in the striatum and motor cortex of monkeys performing movement tasks. *Proc Natl Acad Sci U S A*, *112*, 13687-13692.

Fiebelkorn, I. C., Snyder, A. C., Mercier, M. R., Butler, J. S., Molholm, S., & Foxe, J. J. (2013). Cortical cross-frequency coupling predicts perceptual outcomes. *Neuroimage*, *69*, 126-137.

Fogerson, P. M., & Huguenard, J. R. (2016). Tapping the Brakes: Cellular and Synaptic Mechanisms that Regulate Thalamic Oscillations. *Neuron*, *92*, 687-704.

Fries, P. (2015). Rhythms for Cognition: Communication through Coherence. *Neuron*, *88*, 220-235.

Friston, K. J., Bastos, A. M., Pinotsis, D., & Litvak, V. (2015). LFP and oscillations-what do they tell us. *Curr Opin Neurobiol*, *31*, 1-6.

Fujisawa, S., & Buzsáki, G. (2011). A 4 Hz oscillation adaptively synchronizes prefrontal, VTA, and hippocampal activities. *Neuron*, *72*(1), 153-165.

Gaidica, M., Hurst, A., Cyr, C., & Leventhal, D. K. (2018). Distinct Populations of Motor Thalamic Neurons Encode Action Initiation, Action Selection, and Movement Vigor. *J Neurosci*, *38*(29), 6563-6573.

Gilbertson, T., Lalo, E., Doyle, L., Di Lazzaro, V., Cioni, B., & Brown, P. (2005). Existing motor state is favored at the expense of new movement during 13-35 Hz oscillatory synchrony in the human corticospinal system. *J Neurosci*, *25*, 7771-7779.

Grabot, L., Kononowicz, T. W., Dupré la Tour, T., Gramfort, A., Doyère, V., & van Wassenhove, V. (2019). The strength of alpha-beta oscillatory coupling predicts motor timing precision. *J Neurosci*.

Halassa, M. M., Siegle, J. H., Ritt, J. T., Ting, J. T., Feng, G., & Moore, C. I. (2011). Selective optical drive of thalamic reticular nucleus generates thalamic bursts and cortical spindles. *Nat Neurosci*, *14*(9), 1118-1120.

Hamel-Thibault, A., Thénault, F., Whittingstall, K., & Bernier, P. M. (2018). Delta-Band Oscillations in Motor Regions Predict Hand Selection for Reaching. *Cereb Cortex*, *28*(2), 574-584.

Herkenham, M. (1980). Laminar organization of thalamic projections to the rat neocortex. *Science*, *207*, 532-535.

Igarashi, J., Isomura, Y., Arai, K., Harukuni, R., & Fukai, T. (2013). A $λ$-$γ$ Oscillation Code for Neuronal Coordination during Motor Behavior. *J Neurosci*, *33*, 18515-18530.

Jones, S. R., Pritchett, D. L., Sikora, M. A., Stufflebeam, S. M., Hämäläinen, M., & Moore, C. I. (2009). Quantitative analysis and biophysically realistic neural modeling of the MEG mu rhythm: rhythmogenesis and modulation of sensory-evoked responses. *J Neurophysiol*, *102*, 3554-3572.

Khanna, P., & Carmena, J. M. (2017). Beta band oscillations in motor cortex reflect neural population signals that delay movement onset. *Elife*, *6*.

Kühn, A. A., Tsui, A., Aziz, T., Ray, N., Brücke, C., Kupsch, A. et al. (2009). Pathological synchronisation in the subthalamic nucleus of patients with Parkinson's disease relates to both bradykinesia and rigidity. *Exp Neurol*, *215*, 380-387.

Kuramoto, E., Fujiyama, F., Nakamura, K. C., Tanaka, Y., Hioki, H., & Kaneko, T. (2011). Complementary distribution of glutamatergic cerebellar and GABAergic basal ganglia afferents to the rat motor thalamic nuclei. *Eur J Neurosci*, *33*, 95-109.

Kuramoto, E., Furuta, T., Nakamura, K. C., Unzai, T., Hioki, H., & Kaneko, T. (2009). Two types of thalamocortical projections from the motor thalamic nuclei of the rat: a single neuron-tracing study using viral vectors. *Cereb Cortex*, *19*, 2065-2077.

Kuramoto, E., Ohno, S., Furuta, T., Unzai, T., Tanaka, Y. R., Hioki, H. et al. (2015). Ventral medial nucleus neurons send thalamocortical afferents more widely and more preferentially to layer 1 than neurons of the ventral anterior-ventral lateral nuclear complex in the rat. *Cereb Cortex*, *25*, 221-235.

Lakatos, P., Karmos, G., Mehta, A. D., Ulbert, I., & Schroeder, C. E. (2008). Entrainment of neuronal oscillations as a mechanism of attentional selection. *Science*, *320*, 110-113.

Lakatos, P., Shah, A. S., Knuth, K. H., Ulbert, I., Karmos, G., & Schroeder, C. E. (2005). An oscillatory hierarchy controlling neuronal excitability and stimulus processing in the auditory cortex. *J Neurophysiol*, *94*, 1904-1911.

Leventhal, D. K., Gage, G. J., Schmidt, R., Pettibone, J. R., Case, A. C., & Berke, J. D. (2012). Basal Ganglia Beta oscillations accompany cue utilization. *Neuron*, *73*, 523-536.

Leventhal, D. K., Stoetzner, C. R., Abraham, R., Pettibone, J., DeMarco, K., & Berke, J. D. (2014). Dissociable effects of dopamine on learning and performance within sensorimotor striatum. *Basal Ganglia*, *4*, 43-54.

Lofredi, R., Tan, H., Neumann, W.-J., Yeh, C.-H., Schneider, G.-H., Kühn, A. A. et al. (2019). Beta bursts during continuous movements accompany the velocity decrement in Parkinson's disease patients. *Neurobiology of Disease*.

López-Azcárate, J., Nicolás, M. J., Cordon, I., Alegre, M., Valencia, M., & Artieda, J. (2013). Delta-mediated cross-frequency coupling organizes oscillatory activity across the rat cortico-basal ganglia network. *Front Neural Circuits*, *7*, 155.

Mak-McCully, R. A., Rolland, M., Sargsyan, A., Gonzalez, C., Magnin, M., Chauvel, P. et al. (2017). Coordination of cortical and thalamic activity during non-REM sleep in humans. *Nat Commun*, *8*, 15499.

Mallet, N., Pogosyan, A., Márton, L. F., Bolam, J. P., Brown, P., & Magill, P. J. (2008). Parkinsonian beta oscillations in the external globus pallidus and their relationship with subthalamic nucleus activity. *J Neurosci*, *28*, 14245-14258.

Manning, J. R., Jacobs, J., Fried, I., & Kahana, M. J. (2009). Broadband shifts in local field potential power spectra are correlated with single-neuron spiking in humans. *J Neurosci*, *29*, 13613-13620.

Masimore, B., Schmitzer-Torbert, N. C., Kakalios, J., & Redish, A. D. (2005). Transient striatal gamma local field potentials signal movement initiation in rats. *Neuroreport*, *16*, 2021-2024.

McAfee, S. S., Liu, Y., Dhamala, M., & Heck, D. H. (2018). Thalamocortical Communication in the Awake Mouse Visual System Involves Phase Synchronization and Rhythmic Spike Synchrony at High Gamma Frequencies. *Front Neurosci*, *12*, 837.

McCarthy, M. M., Moore-Kochlacs, C., Gu, X., Boyden, E. S., Han, X., & Kopell, N. (2011). Striatal origin of the pathologic beta oscillations in Parkinson's disease. *Proc Natl Acad Sci U S A*.

Meidahl, A. C., Moll, C. K. E., van Wijk, B., Gulberti, A., Tinkhauser, G., Westphal, M. et al. (2019). Synchronised spiking activity underlies phase amplitude coupling in the subthalamic nucleus of Parkinson's disease patients. *Neurobiol Dis*.

Mirzaei, A., Kumar, A., Leventhal, D., Mallet, N., Aertsen, A., Berke, J. et al. (2017). Sensorimotor Processing in the Basal Ganglia Leads to Transient Beta Oscillations during Behavior. *37*, 11220-11232.

Murthy, V. N., & Fetz, E. E. (1992). Coherent 25- to 35-Hz oscillations in the sensorimotor cortex of awake behaving monkeys. *Proc Natl Acad Sci U S A*, *89*, 5670-5674.

Nakamura, K. C., Sharott, A., & Magill, P. J. (2014). Temporal coupling with cortex distinguishes spontaneous neuronal activities in identified basal ganglia-recipient and cerebellar-recipient zones of the motor thalamus. *Cereb Cortex*, *24*(1), 81-97.

Neske, G. T. (2015). The Slow Oscillation in Cortical and Thalamic Networks: Mechanisms and Functions. *Front Neural Circuits*, *9*, 88.

Pesaran, B., Vinck, M., Einevoll, G. T., Sirota, A., Fries, P., Siegel, M. et al. (2018). Investigating large-scale brain dynamics using field potential recordings: analysis and interpretation. *Nat Neurosci*, *21*(7), 903-919.

Pfurtscheller, G., Stancák, A., & Neuper, C. (1996). Post-movement beta synchronization. A correlate of an idling motor area? *Electroencephalogr Clin Neurophysiol*, *98*, 281-293.

Pogosyan, A., Gaynor, L. D., Eusebio, A., & Brown, P. (2009). Boosting cortical activity at Beta-band frequencies slows movement in humans. *Curr Biol*, *19*, 1637-1641.

Ray, S., Crone, N. E., Niebur, E., Franaszczuk, P. J., & Hsiao, S. S. (2008). Neural correlates of high-gamma oscillations (60-200 Hz) in macaque local field potentials and their potential implications in electrocorticography. *J Neurosci*, *28*(45), 11526-11536.

Reis, C., Sharott, A., Magill, P. J., van Wijk, B. C. M., Parr, T., Zeidman, P. et al. (2019). Thalamocortical dynamics underlying spontaneous transitions in beta power in Parkinsonism. *Neuroimage*, *193*, 103-114.

Rule, M. E., Vargas-Irwin, C., Donoghue, J. P., & Truccolo, W. (2018). Phase reorganization leads to transient β-LFP spatial wave patterns in motor cortex during steady-state movement preparation. *J Neurophysiol*, *119*(6), 2212-2228.

Saalmann, Y. B., Pinsk, M. A., Wang, L., Li, X., & Kastner, S. (2012). The pulvinar regulates information transmission between cortical areas based on attention demands. *Science*, *337*(6095), 753-756.

Saleh, M., Reimer, J., Penn, R., Ojakangas, C. L., & Hatsopoulos, N. G. (2010). Fast and slow oscillations in human primary motor cortex predict oncoming behaviorally relevant cues. *Neuron*, *65*, 461-471.

Schmidt, R., Leventhal, D. K., Mallet, N., Chen, F., & Berke, J. D. (2013). Canceling actions involves a race between basal ganglia pathways. *Nat Neurosci*, *16*, 1118-1124.

Schroeder, C. E., & Lakatos, P. (2009). Low-frequency neuronal oscillations as instruments of sensory selection. *Trends Neurosci*, *32*(1), 9-18.

Sherman, M. A., Lee, S., Law, R., Haegens, S., Thorn, C. A., Hämäläinen, M. S. et al. (2016). Neural mechanisms of transient neocortical beta rhythms: Converging evidence from humans, computational modeling, monkeys, and mice. *Proceedings of the National Academy of Sciences*, *113*(33), E4885-E4894.

Shin, H., Law, R., Tsutsui, S., Moore, C. I., & Jones, S. R. (2017). The rate of transient beta frequency events predicts behavior across tasks and species. *Elife*, *6*.

Stark, E., & Abeles, M. (2005). Applying resampling methods to neurophysiological data. *J Neurosci Methods*, *145*, 133-144.

Stefanics, G., Hangya, B., Hernádi, I., Winkler, I., Lakatos, P., & Ulbert, I. (2010). Phase entrainment of human delta oscillations can mediate the effects of expectation on reaction speed. *J Neurosci*, *30*, 13578-13585.

Tachibana, Y., Iwamuro, H., Kita, H., Takada, M., & Nambu, A. (2011). Subthalamo-pallidal interactions underlying parkinsonian neuronal oscillations in the primate basal ganglia. *Eur J Neurosci*, *34*, 1470-1484.

Tan, H., Debarros, J., He, S., Pogosyan, A., Aziz, T. Z., Huang, Y. et al. (2019). Decoding voluntary movements and postural tremor based on thalamic LFPs as a basis for closed-loop stimulation for essential tremor. *Brain Stimul*.

Tanaka, Y. H., Tanaka, Y. R., Kondo, M., Terada, S. I., Kawaguchi, Y., & Matsuzaki, M. (2018). Thalamocortical Axonal Activity in Motor Cortex Exhibits Layer-Specific Dynamics during Motor Learning. *Neuron*, *100*(1), 244-258.e12.

Tiganj, Z., Chevallier, S., & Monacelli, E. (2014). Influence of extracellular oscillations on neural communication: a computational perspective. *Front Comput Neurosci*, *8*, 9.

Torrecillos, F., Tinkhauser, G., Fischer, P., Green, A. L., Aziz, T. Z., Foltynie, T. et al. (2018). Modulation of Beta Bursts in the Subthalamic Nucleus Predicts Motor Performance. *J Neurosci*, *38*(41), 8905-8917.

Tort, A. B. L., Kramer, M. A., Thorn, C., Gibson, D. J., Kubota, Y., Graybiel, A. M. et al. (2008). Dynamic cross-frequency couplings of local field potential oscillations in rat striatum and hippocampus during performance of a T-maze task. *Proc Natl Acad Sci U S A*, *105*, 20517-20522.

van Wijk, B. C. M. (2017). Is Broadband Gamma Activity Pathologically Synchronized to the Beta Rhythm in Parkinson's Disease. *J Neurosci*, *37*(39), 9347-9349.

Wallisch, P., Lusignan, M. E., Benayoun, M. D., Baker, T. I., Dickey, A. S., & Hatsopoulos, N. G. (2013). *MATLAB for Neuroscientists: An Introduction to Scientific Computing in MATLAB* (2 ed.). Academic Press.

Wang, P., Göschl, F., Friese, U., König, P., & Engel, A. K. (2019). Long-range functional coupling predicts performance: Oscillatory EEG networks in multisensory processing. *Neuroimage*.

Watson, B. O., Ding, M., & Buzsáki, G. (2018). Temporal coupling of field potentials and action potentials in the neocortex. *Eur J Neurosci*, *48*(7), 2482-2497.

Zoefel, B., Archer-Boyd, A., & Davis, M. H. (2018). Phase entrainment of brain oscillations causally modulates neural responses to intelligible speech. *Current Biology*, *28*(3), 401-408. e5.

CHAPTER 4: Pathway-Specific Optogenetics in the Motor Thalamus

Co-authored by Alexandra Falkenberg, Maximilian Wagner, and Daniel K. Leventhal

Introduction

Optogenetics enables temporally precise control of genetically targeted cellular subpopulations using light ({Boyden et al., 2005, #27579}{Yizhar et al., 2011, #97772}) and has played an increasingly important role in the dissection of the neural circuitry involved in movement since its introduction ({Gradinaru et al., 2009, #89852}{Kravitz et al., 2010, #27834}). More interesting to the focus of my aims is the ability to control specific neural pathways ({Fenno et al., 2011, #26582}), including the primary subcortical afferents to Mthal, the BG and cerebellum, which remain relatively well delineated ({Kuramoto et al., 2011, #35386}{Deniau et al., 1992, #103216}). In this chapter, I review the methods we explored to achieve such an effect, including a histological characterization of optogenetic virus expression and preliminary behavioral results.

The basal ganglia (BG) has been particularly amicable to pathway-specific manipulation due to the physiological and molecular characterizations that led to simplified 'standard model' schematic ({Albin et al., 1989, #65207}{DeLong, 1990, #86836}). Cell-type specific neurotoxins and modulators first enabled spatial precision, but the advent of optogenetics, usually paired with transgenic animals, added a temporal dimension key to investigating complex behavior ({Gradinaru et al., 2009, #89852}{Kreitzer and Berke, 2011, #63677}). Early work utilized the Cre-recombinase system to selectively express an adeno-associated virus (AAV) with channelrhodopsin-2 (ChR2) in either D1 (direct pathway) or D2 (indirect pathway)

medium spiny neurons (MSNs) with striking agreement to standard model predictions ({Kravitz et al., 2010, #27834}). These experiments were extended to investigate how the pathway-specific MSNs influenced the BG-output projecting to Mthal to either initiate or suppress movement ({Freeze et al., 2013, #90097}). Several studies have endeavored to directly modulate the BG-recipient thalamus. Using normal mice, an AAV5/1-ChR2 construct attached to a synapsin (Syn) promoter was injected into the BG-output which reliably expressed in ventral medial (VM) thalamus ({Edgerton and Jaeger, 2014, #14278}). Subsequent stimulation of VM thalamus agreed with previous findings that tonic SNr firing would suppress Mthal firing, and only bursty or fast trains of nigral input could evoke rebound spike bursts in Mthal. This study played an important role in establishing that Mthal burst firing is likely a consequence of dysregulated nigral firing, which is characteristic of several movement disorders ({Wichmann and Soares, 2006, #21016}{Devetiarov et al., 2017, #24779}). The use of a synapsin promoter links the virus to neuronal presynaptic vesicles destined for postsynaptic release, thereby carrying the virus anterogradely from origin to destination ({Piñol et al., 2012, #524}{Kügler et al., 2003, #37577}). However, specific serotypes promote retrograde transmission ({Salegio et al., 2013, #82974}, also see Appendix A). Similar techniques have been used to optogenetically target the cerebellar-recipient thalamus by injecting AAV2-Syn-ChR2 into the dentate nucleus of mice ({Chen et al., 2014, #21312}). Other approaches targeting Mthal use complex genetic techniques not easily implemented in rats ({Morrissette et al., 2018, #30734}{Guo et al., 2017, #57220}{Libbrecht et al., 2017, #82430}), making an approach that leverages “off the shelf” viruses ideal. It is also worth noting a blunt-force approach, which is to directly inject a virus into specific anatomical regions of Mthal and rely on histological analysis to verify regional

specificity ({Sizemore et al., 2016, #19052}), however, this creates substantial interpretational challenges.

Introduction

Optogenetics enables temporally precise control of genetically targeted cellular subpopulations using light (Boyden, Zhang, Bamberg, Nagel, & Deisseroth, 2005; Yizhar, Fenno, Davidson, Mogri, & Deisseroth, 2011) and has played an increasingly important role in the dissection of the neural circuitry involved in movement since its introduction (Gradinaru, Mogri, Thompson, Henderson, & Deisseroth, 2009; Kravitz et al., 2010). More interesting to the focus of my aims is the ability to control specific neural pathways (Fenno, Yizhar, & Deisseroth, 2011), including the primary subcortical afferents to Mthal, the BG and cerebellum, which remain relatively well delineated (Kuramoto et al., 2011; Deniau, Kita, & Kitai, 1992). In this chapter, I review the methods we explored to achieve such an effect, including a histological characterization of optogenetic virus expression and preliminary behavioral results.

The basal ganglia (BG) has been particularly amicable to pathway-specific manipulation due to the physiological and molecular characterizations that led to simplified 'standard model' schematic (Albin, Young, & Penney, 1989; DeLong, 1990). Cell-type specific neurotoxins and modulators first enabled spatial precision, but the advent of optogenetics, usually paired with transgenic animals, added a temporal dimension key to investigating complex behavior (Gradinaru et al., 2009; Kreitzer & Berke, 2011). Early work utilized the Cre-recombinase system to selectively express an adeno-associated virus (AAV) with channelrhodopsin-2 (ChR2) in either D1 (direct pathway) or D2 (indirect pathway) medium spiny neurons (MSNs) with striking agreement to standard model predictions (Kravitz et al., 2010). These experiments were extended to investigate how the pathway-specific MSNs influenced the BG-output projecting to Mthal to either initiate or suppress movement (Freeze, Kravitz, Hammack, Berke, & Kreitzer, 2013). Several studies have endeavored to directly modulate the BG-recipient thalamus. Using

normal mice, an AAV5/1-ChR2 construct attached to a synapsin (Syn) promoter was injected into the BG-output which reliably expressed in ventral medial (VM) thalamus (Edgerton & Jaeger, 2014). Subsequent stimulation of VM thalamus agreed with previous findings that tonic SNr firing would suppress Mthal firing, and only bursty or fast trains of nigral input could evoke rebound spike bursts in Mthal. This study played an important role in establishing that Mthal burst firing is likely a consequence of dysregulated nigral firing, which is characteristic of several movement disorders (Wichmann & Soares, 2006; Devetiarov et al., 2017). The use of a synapsin promoter links the virus to neuronal presynaptic vesicles destined for postsynaptic release, thereby carrying the virus anterogradely from origin to destination (Piñol, Bateman, & Mendelowitz, 2012; Kügler, Kilic, & Bähr, 2003). However, specific serotypes promote retrograde transmission (Salegio et al., 2013, also see Appendix A). Similar techniques have been used to optogenetically target the cerebellar-recipient thalamus by injecting AAV2-Syn-ChR2 into the dentate nucleus of mice (Chen, Fremont, Arteaga-Bracho, & Khodakhah, 2014). Other approaches targeting Mthal use complex genetic techniques not easily implemented in rats (Morrissette et al., 2018; Guo et al., 2017; Libbrecht, den Haute, Malinouskaya, Gijsbers, & Baekelandt, 2017), making an approach that leverages "off the shelf" viruses ideal. It is also worth noting a blunt-force approach, which is to directly inject a virus into specific anatomical regions of Mthal and rely on histological analysis to verify regional specificity (Sizemore, Seeger-Armbruster, Hughes, & Parr-Brownlie, 2016), however, this creates substantial interpretational challenges.

Results

BG-recipient Mthal. In rats, the two major BG outputs are the SNr and entopeduncular nucleus (EP) (Deniau et al., 1992). Given the anatomical difficulties in target the EP (the injection occurs in extreme proximity to Mthal) along with the profound functional significance of the SNr (Schmidt, Leventhal, Mallet, Chen, & Berke, 2013), we chose to focus on only the SNr for these studies. Before understanding how AAV serotypes affect expression, we used an AAV6-hSyn-hChR2(H134R)-EYFP virus. Unfortunately, the type 6 serotype acts in a retrograde fashion, so instead of traveling to Mthal, it would have gone upstream to the STN and striatum. This, however, was a good explanation for why we observed no expression of the EYFP marker protein in Mthal. Our second attempt (n = 3 rats) used a similar virus with a serotype well-suited for anterograde trafficking (AAV5-hSyn-hChR2(H134R)-mCherry). This method, when imaged under native fluorescence (i.e., no antibody), showed clear expression at the injection site and in VM thalamus (Figures 4-1, 4-2, 4-3).

We performed a limited behavioral assessment on these rats using a 473 nm laser (Figure 4-4) attached to a fiber optic over Mthal in an open field (Figure 4-5). We observed no overt effects from a variety of stimulation protocols (see Materials and Methods). Previous experiments where ChR2 was expressed in the subthalamic nucleus evoked stereotyped turning during light stimulation, making equipment an unlikely factor.

Cerebellar-recipient Mthal. The dentate nucleus is part of the deep cerebellar nuclei (DCN) and projects directly to the ventrolateral (VL) aspect of Mthal (Bostan, Dum, & Strick, 2010). Similar to the previous experiment in the BG, we wanted to determine the efficacy of DCN injections of the expression of an optogenetic virus (AAV5-hSyn-hChR2(H134R)-mCherry) in Mthal. In our first round of experiments (n = 3 rats), we used a single site injection

targeting the center of the DCN (Paxinos & Watson, 2007; Paxinos, Watson, Pennisi, & Topple, 1985). Virus expression was considerable throughout the cerebellum (suggesting that the injection was well positioned) but was not visible in Mthal. The DCN extends over several millimeters medial-to-lateral, suggesting that our single site injection did not transfect the necessary volume of cerebellar tissue to impact Mthal. Therefore, we performed a second round of experiments (n = 3 rats) to determine if dual injections to the DCN were more effective. Our preliminary results show virus expression extending from the DCN into anteriorly directed axon collaterals with appreciable transfection in Mthal. However, this has only been confirmed for one rat, whereas another rat did not have expression in Mthal (Figure 4-6). No behavioral changes were observed in the rat with little Mthal expression, whereas the rat with good expression was not tested.

Discussion

In this chapter, I explore the possibility of using an optogenetic toolset to gain precise spatiotemporal control over Mthal afferents. Given research findings from previous chapters, the effective modulation of BG and cerebellar inputs to Mthal have the potential to answer several unsolved mysteries concerning the precise role of each structure, and how Mthal acts to integrate their activity in producing movement and supporting behavior. In following, I discuss potential behavioral and physiological outcomes resulting from pathway-specific control of Mthal.

In Chapter 2, we postulate that non-directionally selective units are of cerebellar origin and are linked to movement initiation. Therefore, stimulating cerebellar afferents in Mthal might increase the probability of movement initiation, which has multiple well-established methods of assessment (Kravitz et al., 2010; da Silva, Tecuapetla, Paixão, & Costa, 2018). *Would simulation elicit movement every time?* If the movement initiation signal is coursing through Mthal and directly modulating corticospinal circuits, movement would be expected nearly on each stimulation pulse. However, even in the case where the light sensitive opsins are perfectly located on cerebellar afferents, the nature of the optogenetic stimulation is still a blunt force tool and therefore the type of movement being provoked may take several forms. This may include coordinated locomotion (Koblinger et al., 2018), turning (Magno et al., 2019), eliciting kinematic 'primitives' (Bollu et al., 2018), or orofacial ticks (Heiney, Kim, Augustine, & Medina, 2014). I do not, however, believe this would be the case. Considerable evidence pointing to motor-thalamic regulation of cortical states suggest that even a strong pulse of Mthal activity to cortex may not result in movement. In an open field context, stimulation might only elicit movement when the animal has established a cortical state near a movement initiation threshold (Zimnik, Lara, & Churchland, 2019). This is why the probability of movement is the critical evaluation.

Ideally, future studies can leverage a two-alternative choice task and directly investigate if the stimulation of cerebellar afferents around the tone event (before *and* after) affect RT (in an experiment similar to Figure 3, Horak & Anderson, 1984). Although harder to implement, I show distinct neural dynamics during the movement preparation phase, suggesting a near-threshold state is achieved following task engagement at the Nose In event (Figure 2-5). The most straight forward hypothesis is that early stimulation leading up to the tone would speed RT, with a higher stimulation power enhancing the effect (Anderson & Horak, 1985). An alternative hypothesis, based on the notion that delta oscillations may cyclically regulate the preparatory state through modulating neuronal excitability, is that pre-tone stimulation only speeds RT at specific and 'optimal' delta phases, and has no, or even a negative affect otherwise.

A similar line of thought can be applied to directionally selective units, but specific to BG afferents based on their possible connection with action selection and invigoration. However, it remains unknown whether the method we used expressed opsins specifically to the pre-synaptic sites, or if the virus goes on to transfect the thalamocortical cell itself. This is an important consideration because of the sign reversal that occurs along the BG-Mthal pathway, since BG afferents signal using GABA ("inhibitory") and thalamocortical cells signal using glutamate ("excitatory"). Speculation becomes even less certain given the possibility that hyperpolarizing thalamocortical cells can cause 'paradoxical' excitation through burst mechanisms (see Introduction and Figure 1-3). For the sake of this discussion, I will speak in terms of stimulation having a positive affect (i.e., eliciting more spiking) on Mthal neurons themselves, as this is likely achievable given similar viral strategies or by adjusting the timing and patterns of stimulation.

In Chapter 2, I characterized the directionally selective firing of Mthal units, showing a near equal proportion of ipsilateral vs. contralateral preferring units (based on the peri-movement firing rate, see Figure 2-4). While this knowledge is salient to any hypothesis regarding action selection (i.e., which way to move), it is problematic given the optogenetic tools I propose using. Even if BG afferents in Mthal were effectively targeted, my data suggest that movement direction (i.e., choice) reflects the enhancement of only a particular subpopulation of Mthal units depending on the intended direction of movement. Therefore, a barrage of Mthal activity induced by optogenetic stimulation to BG afferents may, in essence, paralyze the execution of the choice behavior. An interesting addition to such experiments would be to monitor the electromyogram (EMG) from various muscles during stimulation to assess the possible coherence between Mthal and muscles, and if movement were inhibited, determine if that is due to muscular co-activation. Targeting ipsi- or contra-specific populations in Mthal may be possible through more advanced techniques. For example, transgenic animals have been produced in such a manner that *c-fos* (an activity-dependent early gene) inhibits the expression of an optogenetic construct in the presence of doxycycline (Dox) (Liu et al., 2012). Therefore, specific behavioral regimes can be associated with active neurons in the absence of Dox. In the context of my task, animals could be trained to proficiency on Dox, and then subject to a training session where they are only cued to move in one direction off Dox to optogenetically label those neurons specifically. The resulting hypothesis follows that subsequent light stimulation (once again, on Dox) would only bias movement direction in one direction, and scale movement based on the stimulation intensity.

The last consideration concerns the preparatory neuronal activity observed in Chapter 2. Given that neuronal firing is decreased prior to movement, and the extent of that 'pause' correlated with RT (Figure 2-5), inhibiting Mthal during that time may provide a causal

mechanism by which to bias RT. This hypothesis could be easily tested. If the viral strategies I present for targeting BG afferents are indeed limited to the pre-synaptic terminals in Mthal, it is likely that stimulating those would inhibit thalamocortical neurons and thus decrease Mthal activity. If RT is based on post-inhibitory rebound bursting, then it would be expected that stimulation intensity leading up to the tone, but ending before it, would speed RTs. Alternatively, the decrease in Mthal activity could reflect attentional or motivational resources, which may or may not be causally influenced by Mthal. The uncertainty regarding the effects of BG afferent stimulation could be solved using an alternative strategy that leverages inhibitory light sensitive opsins (Kim, Adhikari, & Deisseroth, 2017) expressed directly in thalamocortical cells. Doing this with pathway specificity, again, requires an extended toolset, but it could easily be achieved without such precision by directly injecting the virus into Mthal (Seeger-Armbruster et al., 2015).

The characterization of our virus transfection, while accurate, can be enhanced by using immunohistochemistry (IHC). We piloted the use of an antibody to amplify the fluorescent tag on the virus which greatly decreased background fluorescence and made it easier to distinguish where the virus spread (Figure 4-7). Second, using a cell body stain to determine if the virus was only transfecting synapses, or actual thalamocortical cells, is an important consideration should these techniques be used in the future. Lastly, using GABAergic and glutamatergic antibodies to delineate BG and cerebellar regions of Mthal would have been useful (Nakamura, Sharott, & Magill, 2014; Kuramoto et al., 2011).

Materials and Methods

Animals. All animal procedures were approved by the Institutional Animal Care and Use Committee of the University of Michigan. Adult male Long-Evans rats (250-275 g, Charles

River Laboratories, Wilmington, MA) were housed in groups of 3 on a reverse light/dark cycle prior to virus injections and fiber optic implants. They were subsequently housed individually to protect the implant. Upon arrival in the laboratory, rats were handled daily for one week to acclimate them to the laboratory environment.

Surgical procedures. Surgical preparation, anesthesia, and post-operative care were similar to those described in Chapter 2, Materials and Methods. Rats were injected virus constructs made by Deisseroth Lab (Stanford University, CA) and distributed by the UNC Vector Core (Chapel Hill, NC). Viruses were aliquoted into 10 μL batches upon arrival and stored at -40° C. Each site was injected with 1 μL of virus by a precision syringe (Hamilton Company, Reno, NV, #80016) connected to small tubing and a cannula (Plastics 1, Roanoke, VA, 30 gauge supplies) using an automated pump (Harvard Apparatus, Holliston, MA, #70-4505) set to an injection rate of 0.1 μL/min. The cannula was aligned and lowered by hand on a stereotaxic frame, then raised 5 minutes after the injection was complete. Bilateral SNr injections relative to bregma were located at: AP = -5.4 mm, ML = ±2.4 mm, DV = 8.0 mm. Bilateral single-site DCN injections relative to the interaural line were located at: AP = -2.5 mm, ML = ±2.4 mm, DV = 5.7 mm. Bilateral dual-site DCN injections relative to the interaural line were located at: AP = -2.5 mm, ML = ±1.5/3 mm, DV = 5.7 mm. Following virus injections, a custom-made fiber optic cannula (ThorLabs, Newton, NJ) was placed unilaterally, over the right-hemisphere Mthal (from bregma, AP = -3.1 mm, ML = 1.3 mm, DV = 6.7 mm) and attached to the skull using dental cement and surgical screws. Prior to implantation, all fiber optic cannulas are tested for transmission efficiency which was later used to calculate stimulation power input.

Open field behavior. Rats were attached to a fiber optic cable that ran through a commutator (ThorLabs) to a 473 nm DPSS laser (LaserGlow Technologies, Toronto, ON,

Canada, SKU: R472005GX) then placed into a custom made open field chamber dimensionally equal to a commercially available product (see Med Associates Inc, Fairfield, VA, ENV-515S-A). Predicted irradiance values (i.e., light transmission) through tissue can be calculated using a tool from the Deisseroth Lab, and suggested our stimulation settings were capable of reaching and activating opsins throughout Mthal. Light stimulation was tested using a combination of frequencies (0 Hz, 20 Hz, 50 Hz, 150 Hz) and power (1 mW, 2.34 mW, 5.48 mW, 12.82 mW, 30 mW) that were 30 seconds interspaced with a 30 second interval in between. Stimulation pulses were perfectly square, achieved by an optical shutter and shutter controller (ThorLabs, SH05). Each test session was recorded using two video cameras (overhead and to the side) and behavior was visually monitored and logged in a text file. A sync LED was placed outside of the open field chamber, out of view from the rat, but in view of both cameras, and was directly wired to the signal that turned on the laser so that the cameras could be synced with the stimulation pulse.

Histology. Euthanizing and slicing protocols were described in Chapter 2, Materials and Methods. All slides were imaged under native fluorescence unless otherwise stated with slight changes to image contrast in Photoshop. IHC protocols for mCherry have been adequately documented and archived. Slides processed using a primary anti-mCherry antibody (Abcam, ab125096) and goat anti-mouse secondary (Abcam, ab175473).

Figures

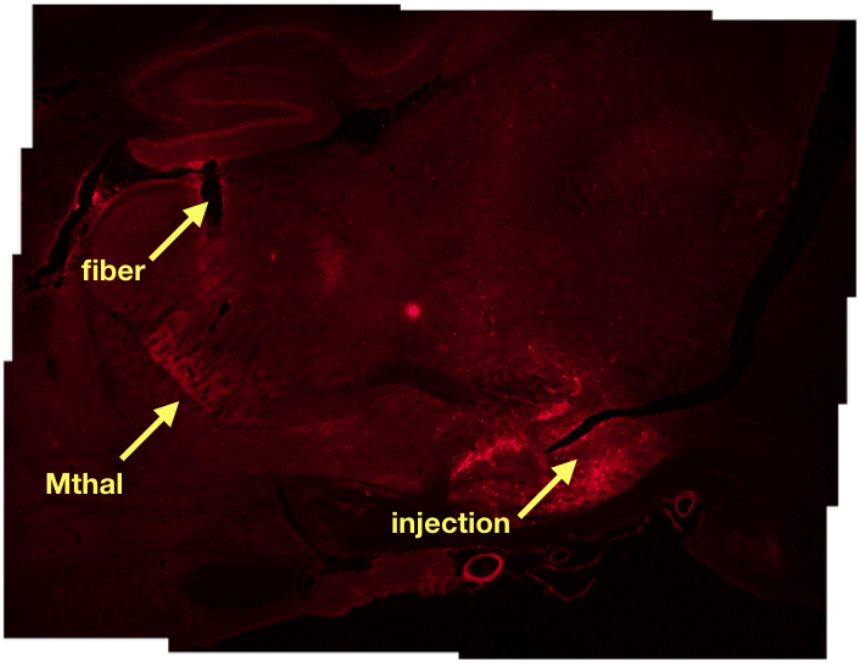

Figure 4-1: Injection of optogenetic virus into SNr of rat 257

The injection site and Mthal are labelled in a slide roughly 1.5 mm medial-lateral after 25 days of expression using AAV5-hSyn-ChR2(H134)-mCherry. A fiber was placed over Mthal and also marked. Imaging was performed using native fluorescence of the mCherry protein marker.

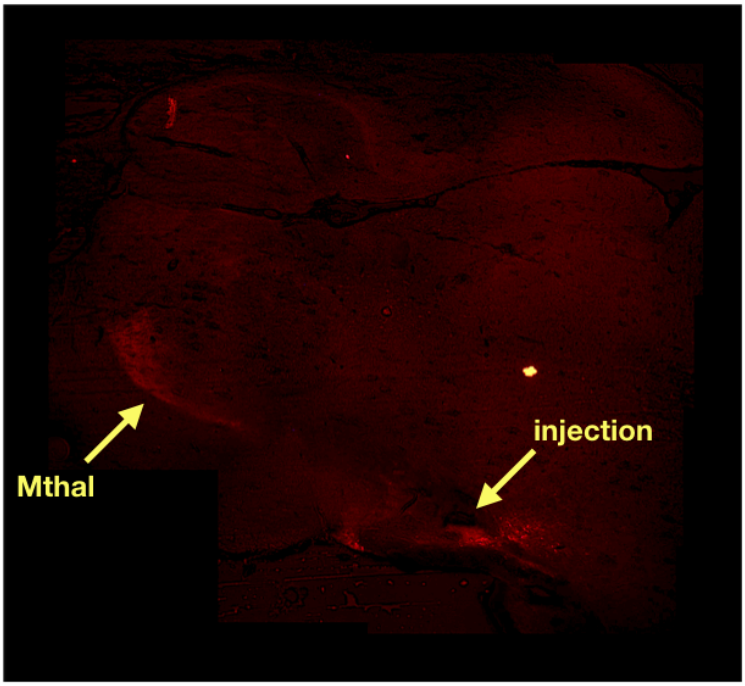

Figure 4-2: Injection of optogenetic virus into SNr of rat 258

The injection site and Mthal are labelled in a slide roughly 1.5 mm medial-lateral after 26 days of expression using AAV5-hSyn-ChR2(H134)-mCherry. The optical fiber is not visible in this slice. Imaging was performed using native fluorescence of the mCherry protein marker.

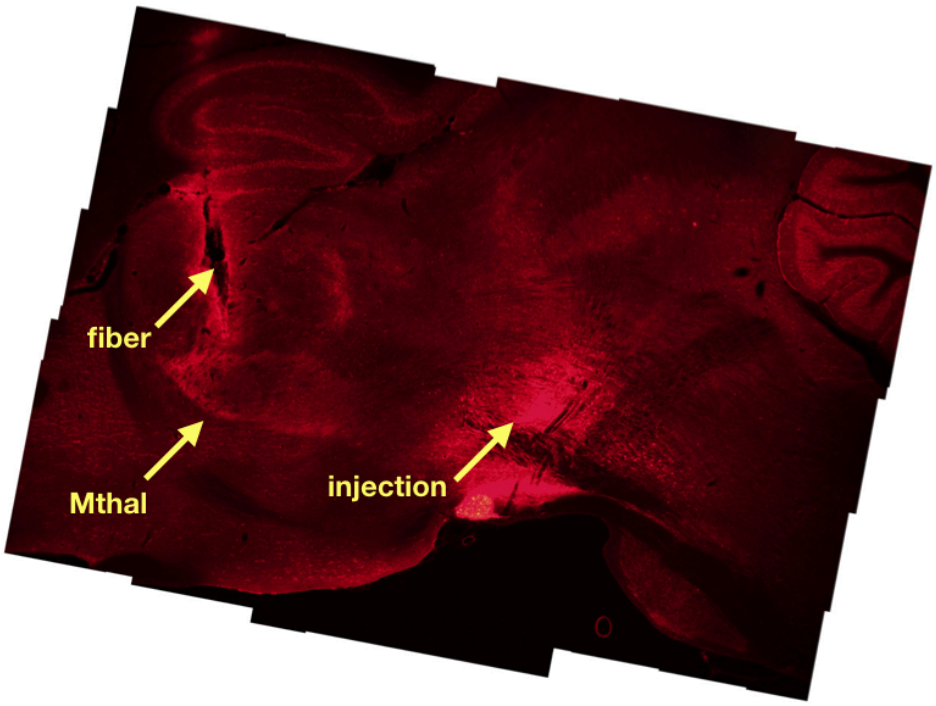

Figure 4-3: Injection of optogenetic virus into SNr of rat 259

The injection site and Mthal are labelled in a slide roughly 1.5 mm medial-lateral after 31 days of expression using AAV5-hSyn-ChR2(H134)-mCherry. A fiber was placed over Mthal and also marked. Imaging was performed using native fluorescence of the mCherry protein marker.

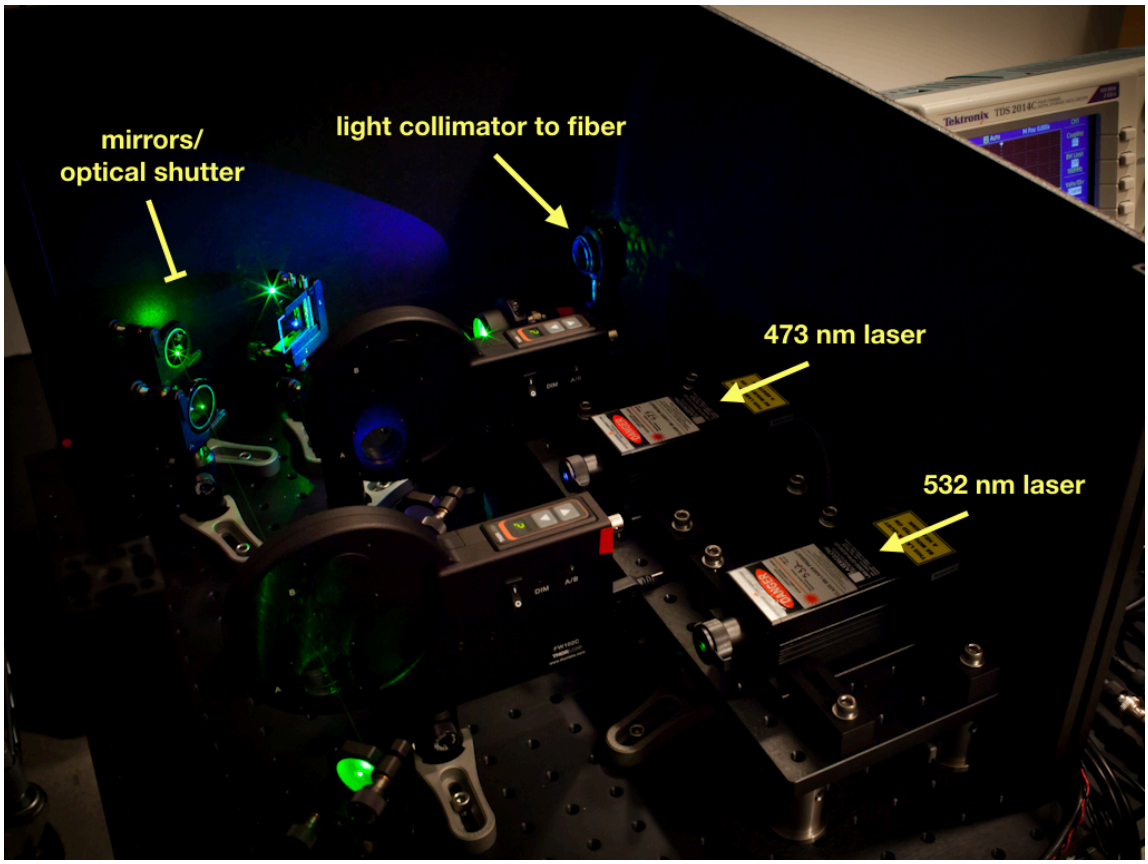

Figure 4-4: Optogenetics laser table

Two lasers with 473 nm (blue) and 532 nm (green) wavelengths were combined into a single fiber optic using a collimator lens. An optical shutter was placed in the path if the laser beam to produce precise square-wave pulses (50% duty cycle) at selectable frequencies.

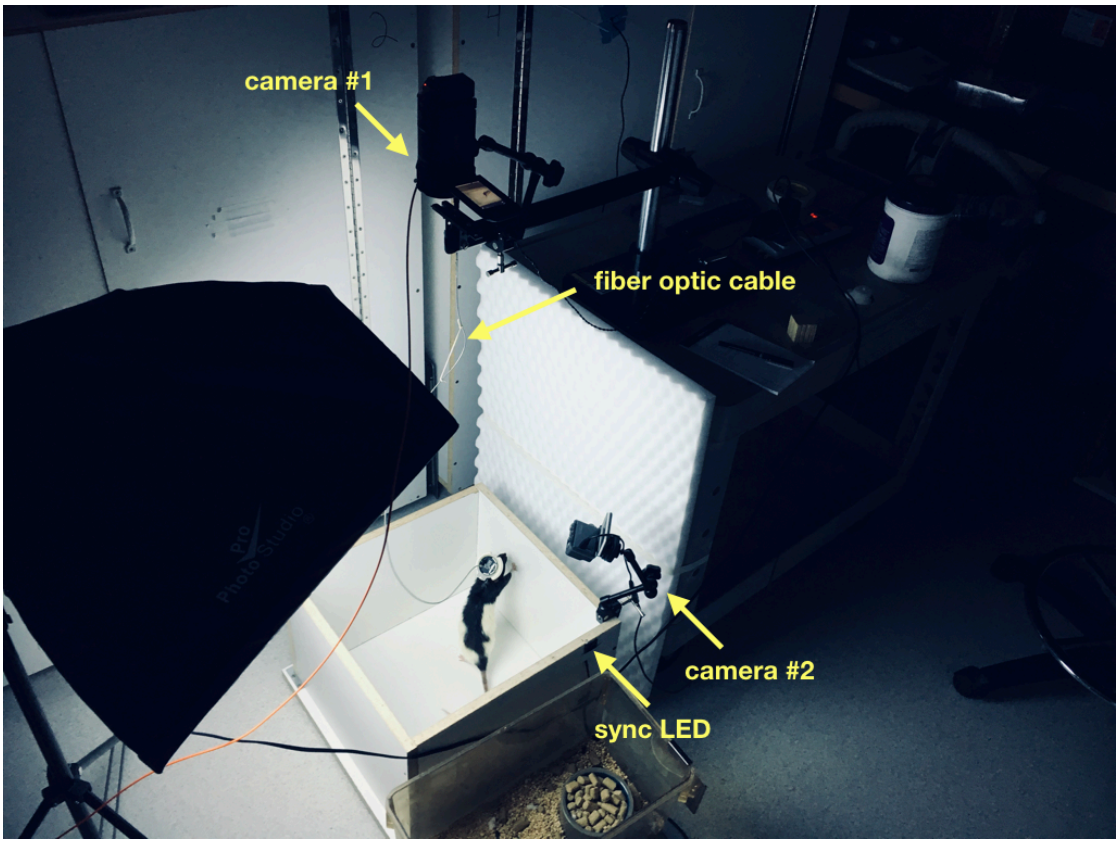

Figure 4-5: Open-field behavior

Two cameras monitored the behavioral status of the rat (shown in box) while laser stimulation was delivered from the optogenetics table through the fiber optic patch cable and optical commutator connected to the fiber optic cable that interfaced with the rat. A sync LED on the side of the open-field enclosure was kept outside of the rat's view, but within the view of both cameras and mirrored the signal that activated the laser.

Figure 4-6: Injection of optogenetic virus into DCN of rat 267

The injection site and Mthal are labelled in a slide roughly 2.0 mm medial-lateral after 38 days of expression using AAV5-hSyn-ChR2(H134)-mCherry. The optical fiber is not visible in this slice. Imaging was performed using native fluorescence of the mCherry protein marker.

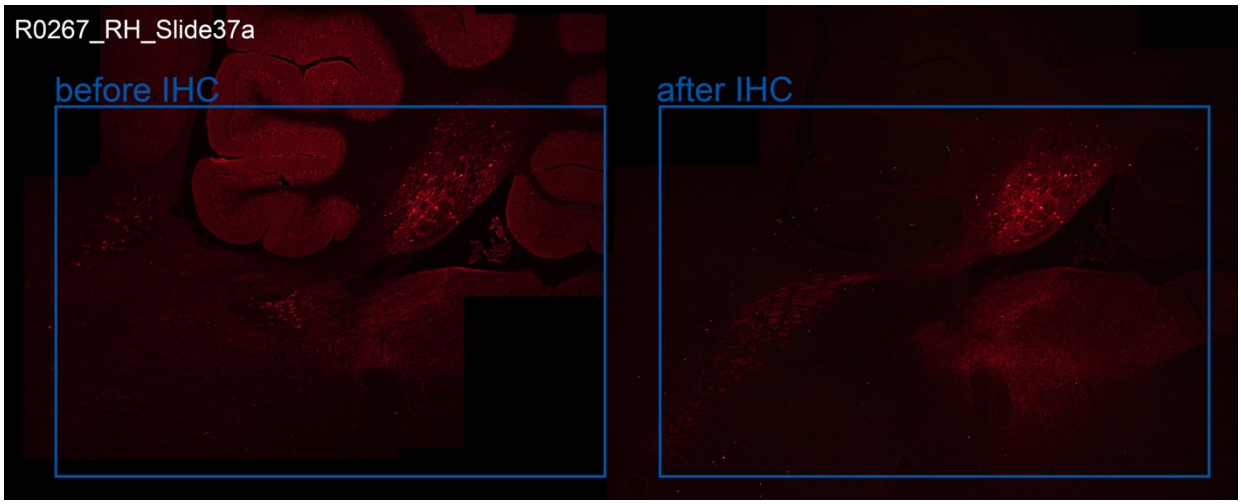

Figure 4-7: Immunohistochemistry on Cerebellar Injection Site

An injection was performed into the deep cerebellar nuclei (upper right in the image) using AAV5-hSyn-ChR2(H134)-mCherry. Immunohistochemistry was performed (see Materials and Methods) resulting in a higher signal to noise ratio where the virus was expected to be expressed.

References

Albin, R. L., Young, A. B., & Penney, J. B. (1989). The functional anatomy of basal ganglia disorders. *Trends Neurosci*, *12*, 366-375.

Anderson, M. E., & Horak, F. B. (1985). Influence of the globus pallidus on arm movements in monkeys. III. Timing of movement-related information. *J Neurophysiol*, *54*, 433-448.

Bollu, T., Whitehead, S. C., Prasad, N., Walker, J. R., Shyamkumar, N., Subramaniam, R. et al. (2018). Motor cortical inactivation reduces the gain of kinematic primitives in mice performing a hold-still center-out reach task. *BioRxiv*, 304907.

Bostan, A. C., Dum, R. P., & Strick, P. L. (2010). The basal ganglia communicate with the cerebellum. *Proc Natl Acad Sci U S A*, *107*, 8452-8456.

Boyden, E. S., Zhang, F., Bamberg, E., Nagel, G., & Deisseroth, K. (2005). Millisecond-timescale, genetically targeted optical control of neural activity. *Nat Neurosci*, *8*, 1263-1268.

Chen, C. H., Fremont, R., Arteaga-Bracho, E. E., & Khodakhah, K. (2014). Short latency cerebellar modulation of the basal ganglia. *Nat Neurosci*, *17*, 1767-1775.

da Silva, J. A., Tecuapetla, F., Paixão, V., & Costa, R. M. (2018). Dopamine neuron activity before action initiation gates and invigorates future movements. *Nature*, *554*(7691), 244-248.

DeLong, M. R. (1990). Primate models of movement disorders of basal ganglia origin. *Trends Neurosci*, *13*, 281-285.

Deniau, J. M., Kita, H., & Kitai, S. T. (1992). Patterns of termination of cerebellar and basal ganglia efferents in the rat thalamus. Strictly segregated and partly overlapping projections. *Neurosci Lett*, *144*, 202-206.

Devetiarov, D., Semenova, U., Usova, S., Tomskiy, A., Tyurnikov, V., Nizametdinova, D. et al. (2017). Neuronal activity patterns in the ventral thalamus: Comparison between Parkinson's disease and cervical dystonia. *Clin Neurophysiol*, *128*, 2482-2490.

Edgerton, J. R., & Jaeger, D. (2014). Optogenetic activation of nigral inhibitory inputs to motor thalamus in the mouse reveals classic inhibition with little potential for rebound activation. *Front Cell Neurosci*, *8*, 36.

Fenno, L., Yizhar, O., & Deisseroth, K. (2011). The development and application of optogenetics. *Annual review of neuroscience*, *34*.

Freeze, B. S., Kravitz, A. V., Hammack, N., Berke, J. D., & Kreitzer, A. C. (2013). Control of basal ganglia output by direct and indirect pathway projection neurons. *J Neurosci*, *33*(47), 18531-18539.

Gradinaru, V., Mogri, M., Thompson, K. R., Henderson, J. M., & Deisseroth, K. (2009). Optical deconstruction of parkinsonian neural circuitry. *Science*, *324*, 354-359.

Guo, Z. V., Inagaki, H. K., Daie, K., Druckmann, S., Gerfen, C. R., & Svoboda, K. (2017). Maintenance of persistent activity in a frontal thalamocortical loop. *Nature*.

Heiney, S. A., Kim, J., Augustine, G. J., & Medina, J. F. (2014). Precise control of movement kinematics by optogenetic inhibition of Purkinje cell activity. *J Neurosci*, *34*, 2321-2330.

Horak, F. B., & Anderson, M. E. (1984). Influence of globus pallidus on arm movements in monkeys. II. Effects of stimulation. *J Neurophysiol*, *52*, 305-322.

Kim, C. K., Adhikari, A., & Deisseroth, K. (2017). Integration of optogenetics with complementary methodologies in systems neuroscience. *Nature Reviews Neuroscience*, *18*(4), 222.

Koblinger, K., Jean-Xavier, C., Sharma, S., Fuzesi, T., Young, L., Eaton, S. et al. (2018). Optogenetic activation of A11 region increases motor activity. *Frontiers in neural circuits*, *12*, 86.

Kravitz, A. V., Freeze, B. S., Parker, P. R. L., Kay, K., Thwin, M. T., Deisseroth, K. et al. (2010). Regulation of parkinsonian motor behaviours by optogenetic control of basal ganglia circuitry. *Nature*, *466*, 622-626.

Kreitzer, A. C., & Berke, J. D. (2011). Investigating striatal function through cell-type-specific manipulations. *Neuroscience*.

Kügler, S., Kilic, E., & Bähr, M. (2003). Human synapsin 1 gene promoter confers highly neuron-specific long-term transgene expression from an adenoviral vector in the adult rat brain depending on the transduced area. *Gene therapy*, *10*(4), 337.

Kuramoto, E., Fujiyama, F., Nakamura, K. C., Tanaka, Y., Hioki, H., & Kaneko, T. (2011). Complementary distribution of glutamatergic cerebellar and GABAergic basal ganglia afferents to the rat motor thalamic nuclei. *Eur J Neurosci*, *33*, 95-109.

Libbrecht, S., den Haute, C., Malinouskaya, L., Gijsbers, R., & Baekelandt, V. (2017). Evaluation of WGA-Cre-dependent topological transgene expression in the rodent brain. *Brain Struct Funct*, *222*, 717-733.

Liu, X., Ramirez, S., Pang, P. T., Puryear, C. B., Govindarajan, A., Deisseroth, K. et al. (2012). Optogenetic stimulation of a hippocampal engram activates fear memory recall. *Nature*, *484*(7394), 381.

Magno, L. A. V., Tenza-Ferrer, H., Collodetti, M., Aguiar, M. F. G., Rodrigues, A. P. C., da Silva, R. S. et al. (2019). Optogenetic stimulation of the M2 cortex reverts motor dysfunction in a mouse model of Parkinson's Disease. *Journal of Neuroscience*, 2277-2218.

Morrissette, A., Chen, P.-H., Bhamani, C., Borden, P. Y., Waiblinger, C., Stanley, G. B. et al. (2018). Unilateral optogenetic inhibition and excitation of basal ganglia output show opposing effects on directional lick choices and movement initiation in mice.

Nakamura, K. C., Sharott, A., & Magill, P. J. (2014). Temporal coupling with cortex distinguishes spontaneous neuronal activities in identified basal ganglia-recipient and cerebellar-recipient zones of the motor thalamus. *Cereb Cortex*, *24*(1), 81-97.

Paxinos, G., & Watson, C. (2007). *The rat brain in stereotaxic coordinates* (6 ed.). Elsevier Academic Press.

Paxinos, G., Watson, C., Pennisi, M., & Topple, A. (1985). Bregma, lambda and the interaural midpoint in stereotaxic surgery with rats of different sex, strain and weight. *Journal of neuroscience methods*, *13*(2), 139-143.

Piñol, R. A., Bateman, R., & Mendelowitz, D. (2012). Optogenetic approaches to characterize the long-range synaptic pathways from the hypothalamus to brain stem autonomic nuclei. *Journal of neuroscience methods*, *210*(2), 238-246.

Salegio, E. A., Samaranch, L., Kells, A. P., Mittermeyer, G., San Sebastian, W., Zhou, S. et al. (2013). Axonal transport of adeno-associated viral vectors is serotype-dependent. *Gene Ther*, *20*(3), 348-352.

Schmidt, R., Leventhal, D. K., Mallet, N., Chen, F., & Berke, J. D. (2013). Canceling actions involves a race between basal ganglia pathways. *Nat Neurosci*, *16*, 1118-1124.

Seeger-Armbruster, S., Bosch-Bouju, C., Little, S. T. C., Smither, R. A., Hughes, S. M., Hyland, B. I. et al. (2015). Patterned, but not tonic, optogenetic stimulation in motor thalamus improves reaching in acute drug-induced parkinsonian rats. *J Neurosci*, *35*, 1211-1216.

Sizemore, R. J., Seeger-Armbruster, S., Hughes, S. M., & Parr-Brownlie, L. C. (2016). Viral vector-based tools advance knowledge of basal ganglia anatomy and physiology. *J Neurophysiol*, *115*(4), 2124-2146.

Wichmann, T., & Soares, J. (2006). Neuronal firing before and after burst discharges in the monkey basal ganglia is predictably patterned in the normal state and altered in parkinsonism. *J NEUROPHYSIOL*, *95*, 2120-2133.

Yizhar, O., Fenno, L. E., Davidson, T. J., Mogri, M., & Deisseroth, K. (2011). Optogenetics in neural systems. *Neuron*, *71*, 9-34.

Zimnik, A. J., Lara, A. H., & Churchland, M. M. (2019). Perturbation of macaque supplementary motor area produces context-independent changes in the probability of movement initiation. *J Neurosci*.

CHAPTER 5: Research Synthesis

The coordination of neural activity through Mthal, which is anatomically and functionally central to primary motor circuits, is critical to the emergence of effective motor behaviors (Gu, van Rijn, & Meck, 2015). In Chapter 2, I show that two functionally distinct neuronal populations in Mthal are briefly modulated around movement (Gaidica, Hurst, Cyr, & Leventhal, 2018). Units that do not encode movement direction ("non-directionally selective) respond primarily to the "go" cue and their activity correlated with RT, while "directionally selective" units respond primarily to the Nose Out event and correlate with reaction time (RT) and movement time (MT). These results imply a role for Mthal in mediating movement initiation, execution, and invigoration. In Chapter 3, I use the same data set to identify how spiking and behavior associate with the Mthal local field potential (LFP). Delta phase appeared to play a critical role during behavior, as it was coupled to beta (and low gamma) power and predicted spike timing. These relationships were also present during the inter-trial period, but to a lesser degree. Motor performance was predicted by delta phase at critical moments, suggesting a model whereby delta phase regulates neuronal excitability (Fries, 2005; Arnal, Doelling, & Poeppel, 2015) leading to transient states of high beta/low gamma power. In Chapter 4, I use an adeno-associated virus (AAV) to selectively express a light-gated ion channel in basal ganglia (BG) and cerebellar recipient areas of Mthal. When injected into the BG, the virus reliably expressed in region Mthal known to receive BG efferents. The same technique in the cerebellum was less efficacious, as we could only identify virus expression exiting the cerebellum, but not in Mthal. No changes in behavior were observed when animals were optogenetically stimulated in an open

field, suggesting that viral expression was either too weak, or the stimulation effect has subtle or nuanced influences on behavior. Nonetheless, these techniques work towards a method of testing several hypotheses regarding the anatomical origins of neural signals that regulate movement.

The Neural Basis of Movement

Skilled movements can be broken into component pieces, namely, movement preparation, initiation, and execution. Competing hypotheses suggest that these stages occur in order, to entirely independently (Haith, Pakpoor, & Krakauer, 2016), but this depends largely on the behavior being examined (Wong, Haith, & Krakauer, 2015). There are several lines of evidence that support the notion that well-learned and optimal motor behaviors indeed use a 'divide and conquer' approach, differentially leveraging simple/fast, and complex/slow brain circuits in parallel (Haith, Huberdeau, & Krakauer, 2015). Clearly, movements classified as reflexes and even basic components of locomotion can occur with minimal to no preparation, however, that is not to say, however, that they cannot participate in more complex motor motifs (Valls-Solé, Rothwell, Goulart, Cossu, & Munoz, 1999). For example, Purkinje neurons in the cerebellum can evoke low-latency orofacial movements (Heiney, Kim, Augustine, & Medina, 2014) and rapid forelimb movements (Lee et al., 2015), possibly by modulating motoneurons through the brainstem (Ito, 1984). Therefore, learned behaviors like skilled reaching (Ellens et al., 2016) may emerge as an amalgamation of neural activity coordinating between multiple, specialized brain regions. Even in the context of 'simple' motor tasks, like the two-alternative choice task used in my studies, I found distinct neuronal correlates of each movement stage in Mthal (Figure 2-3) supporting the possibility that Mthal acts as a "super integrator" of signals from multiple sources (Bosch-Bouju, Hyland, & Parr-Brownlie, 2013). On one hand, this makes Mthal an ideal structure to probe while asking questions about the neural basis of movement, as a

motor-thalamic worldview is by definition one that is all-inclusive, representing neuronal activity from many disparate nuclei. However, until precise functional-anatomical relationships can be determined (see Chapter 4), some interpretations remain speculative. In following, I synthesize my results with these caveats in mind using movement preparation, initiation, and execution as central points of focus.

Movement preparation. As early as a half-second before movement onset, neuronal activity in Mthal is significantly depressed in a manner that correlates with RT, but not MT (Figure 2-5, Gaidica et al., 2018). These findings are highly suggestive of a preparatory state engaged by Mthal—*what purpose does this serve?* One possibility is that Mthal is being primed to deliver a spike volley in response to the imperative cue (i.e., the tone). Thalamocortical neurons express T-type calcium channels that when hyperpolarized, de-inactivate, become more excitable, and mediate low-threshold spiking (LTS) (Llinás, Ribary, Jeanmonod, Kronberg, & Mitra, 1999; Llinás & Steriade, 2006). Although the intracellular potential is not always available (e.g., when recording extracellularly) burst spiking in Mthal is often and primarily attributed to LTS mechanisms (Bosch-Bouju, Smither, Hyland, & Parr-Brownlie, 2014) partly because T-type calcium channel blockers drastically reduce thalamic bursting (Devergnas et al., 2015). Several neuromodulatory inputs to Mthal could provide a hyperpolarizing signal through inhibitory, GABAergic transmission, including the BG, reticular thalamus, and cortex (Ilinsky, Toga, & Kultas-Ilinsky, 1993). This hyper-excitable configuration makes Mthal particularly well-suited for generating a rapid spike volley in the presence of a depolarizing stimulus.

Interestingly, when thalamocortical (*and* corticothalamic) cells are photoinhibited during the preparation stage, choice performance is reduced to chance (Guo et al., 2017). In Chapter 2, I argue for a "state space" cortical model (Churchland, Yu, Sahani, & Shenoy, 2007) that is

regulated by Mthal spiking. The implications are such that Mthal activity is only potent if the cortical state space is operating near threshold, outside the "null space," where preparation, but not movement are permitted (Kaufman, Churchland, Ryu, & Shenoy, 2014). Supporting the state space model, Mthal activity during anesthesia/immobility (Nakamura, Sharott, & Magill, 2014) is comparable to wakefulness (Bosch-Bouju et al., 2014), suggesting a gating mechanism, although it is unclear if this is necessarily cortically based.

In addition to Mthal single unit activity, the low-frequency (~delta) phase of the LFP correlates with RT prior to movement (Figure 3-9). Although it did not predict RT at earlier events, delta phase was aligned to each event above chance levels (peaking at Nose Out, Figure 11) suggesting a role in syncing (or being reactive) to the task structure even at non-movement related events. These observations are consistent with the role for delta oscillations in establishing a sense of time (Scharnowski, Rees, & Walsh, 2013) and syncing or entraining to regularly paced stimuli (Stefanics et al., 2010; Wyart, de Gardelle, Scholl, & Summerfield, 2012).

Typically, the task employed in my studies would be considered "high vigilance" because although it is structured, the key behavioral epochs hinge on the random delay between the Nose In and Tone events (Figure 2-1). Much like a cat waiting for a mouse, high vigilance tasks are hypothesized to suppress delta oscillations in exchange for gamma oscillations, engaging a more reactive, but energy inefficient brain state (Schroeder & Lakatos, 2009). My data contradict this notion and support a role for delta oscillations in non-rhythmic tasks (Breska & Deouell, 2017).

Movement initiation. In Chapter 2, I describe the classification of non-directionally selective units that are modulated around movement onset, but do not encode the ensuing movement direction in their firing rate. The contrast between non-directionally selective units,

which correlate with only RT, and directionally selective units, which correlate with both RT and MT, hints at the possibility that these unit populations are modulated by distinct motor thalamic afferents.

I hypothesize that non-directionally selective units reflect cerebellar inputs to Mthal, and several lines of behavioral evidence support this notion. Reversible cooling (acting as a lesion) to the cerebellar dentate nucleus prolonged RTs by about 80 ms in healthy primates (Miller & Brooks, 1982), suggesting an optimal but not essential pathway for initiating movements. Indeed, lesions to the GPi of healthy primates had no effect on RT, but did slow MT (Horak & Anderson, 1984). The specific anatomy of the cerebellothalamocortical pathway also supports the role for low-latency movement (Thach, 1975) (Figure 1-1). Although cerebellar and BG projections remain relatively separate through Mthal into cortical motor nuclei (Hintzen, Pelzer, & Tittgemeyer, 2017; Kuramoto et al., 2011; Nakamura et al., 2014) tracer studies suggest that cerebellar efferents travel through the VL thalamus and directly innervate layer 5 pyramidal tract neurons of primary motor cortex (Yamawaki & Shepherd, 2015).

Alternative models suggest that the BG are responsible for initiating movement (Kravitz et al., 2010). The possibility that the BG and cerebellum coordinate to optimally initiate movement is likely (Bostan, Dum, & Strick, 2013; Schubert et al., 2002) and so is the notion that their overlapping function and anatomy (largely through Mthal) allow them to act as fail-safes. Several arguments draw a causal link between parkinsonism and the behavioral correlates of BG function (including RT) (Brown & Robbins, 1991 Baunez, Nieoullon, & Amalric, 1995 Jankovic et al., 1999 Schubert et al., 2002), however they are tenuous given that the condition affects wide-scale brain circuits (Schubert et al., 2002).

Challenging the cerebellar-centric model for movement initiation is the finding that in a similar task, but with an added "stop" signal, SNr activity correlated with the successful cancellation of movement (Schmidt, Leventhal, Mallet, Chen, & Berke, 2013). These data suggest that SNr efferents to Mthal have considerable influence over cerebellar efferents, capable of suppressing signals that would normally initiate movement. Activity of the STN also correlates with the stop cue but occurs irrespective of whether the movement was actually inhibited (i.e., it was present on unsuccessful 'stop' trials). STN-derived stop signals could arrive in the cerebellar cortex through the pontine nucleus, a low-latency disynaptic subcortical route (Caligiore et al., 2017), but that would require that the cerebellum also be involved in the final deliberation of whether or not to initiate movement. If the BG is indeed involved, a more likely scenario is that the dentate nucleus of the cerebellum sends an initiating signal to the striatum through the centrolateral thalamus, thus modulating the SNr through the direct pathway (Bostan, Dum, & Strick, 2010). The idea that the cerebellum leverages subcortical, brainstem circuits to influence movement cannot be denied (Ito, 1984), but how and why Mthal receives such a low-latency initiation command, as is present in my data, adds skepticism to this as a mechanism in the context of my studies.

If movement is initiated by cortical mechanisms, then the incoming signal from Mthal, which encodes RT in its firing rate, could either act directly on motor output (as previously mentioned), but may also regulate (or depend on) cortical dynamics to influence movement. The supplementary motor area (SMA) of the cortex receives transthalamic input from the BG and cerebellum (Rouiller, Liang, Babalian, Moret, & Wiesendanger, 1994). When the SMA is stimulated, RT but not movement kinematics are affected for self-paced and externally cued movements (Zimnik, Lara, & Churchland, 2019). These observations can be explained using a

state space model, where specific stimulation patterns modulate the movement initiation threshold within the SMA. Therefore, a reasonable hypothesis is that Mthal firing acts as the stimulus to the SMA but that the potency of Mthal input is context dependent.

An alternative viewpoint is that the initiating signal from Mthal is gated by the cortical state, begging the question, *how are optimal states established and coordinated?* I observed that delta oscillations become phase-locked to the task structure and correlate with RT even before the tone. Given that single units are phase-locked to the delta oscillation, delta phase may influence spiking by modulating neuronal excitability (Schroeder & Lakatos, 2009). Importantly, this effect may extend into connected brain regions within, or associated with the BG-thalamocortical loop (Leventhal et al., 2012). Therefore, a specific delta phase that enhances inter-regional coherence may be deemed 'optimal' (Fries, 2015). Although the delta band is an ideal low-energy, long-range coordination mechanism (Buzsaki, 2006), the observation of a brief, but considerable phase reset in the beta and low gamma bands at the tone event (Figure 3-2) suggest an alternative mechanism by which the stimulus itself alters neural states. Phase-resetting is powerful way by which uncoupled oscillators can sync (Li, Chen, & Aihara, 2006) and permit information flow between different brain regions (Canavier, 2015). While it clearly represents sensory input, the Mthal phase reset at the tone, which also occurs in the BG (Schmidt et al., 2013; Leventhal et al., 2012), may act to synchronize the BG-thalamocortical network by 'brute force'.

Movement execution. In my studies, I used MT as a surrogate window to describe the neural dynamics of movement execution. Thus, it was the component of the task where the choice to move left or right was enacted by the rat. I found that directionally selective units predicted MT (and RT), which was not true for non-directionally selective units (only RT), *why*

was this so? I hypothesize that directionally selective units are preferentially modulated by BG inputs to Mthal. Firstly, the BG are known to be involved in action/choice selection (Graybiel & Grafton, 2015; Leventhal et al., 2014) and therefore well poised to control Mthal firing to bias the rat in the correct direction following the tone. Secondly, the BG scale, or "invigorate" movement (Dudman & Krakauer, 2016) consistent with correlations between directionally selective units and RT/MT. The pathways involved in this phenomenon have been meticulously studied (Kravitz et al., 2010; Freeze, Kravitz, Hammack, Berke, & Kreitzer, 2013). Direct modulation of the striatal direct and indirect pathways affects movement velocity, but not action selection or motivation (Yttri & Dudman, 2016). These data are consistent with the notion that dopaminergic input to the striatum critically influences RT and MT in a lateralized choice task (Heuer, Smith, & Dunnett, 2013; Leventhal et al., 2014). In fact, action and choice may themselves simply reflect motivation and movement gain (i.e., "vigor") which are computed by the BG (Turner & Desmurget, 2010).

The considerable entrainment of directionally selective units to delta phase may be easily explained if they are taken to be co-localized. That is, if directionally selective unit activity is regulated by the BG, and the BG-thalamocortical loop is carrying (or generating) the delta rhythm (see Chapter 3), one reasonable outcome is that those two phenomena are coherent. This argument is made more persuasive by the observation that entrainment persists outside of trials, suggesting a task-independent physiological mechanism.

Another possibility is that neuronal firing is causal to the oscillatory patterns I observed. I investigate this hypothesis in Chapter 3, finding considerable evidence that beta (and low gamma) power is specifically linked to directionally selective unit firing during and outside of

trials. Spiking consistently lags beta power, suggesting a causal relationship that has is supported by thalamocortical spiking models (Reis et al., 2019; Jones et al., 2009).

The unique delta phase and beta (and low gamma) power correlations with directionally selective unit activity suggest a potential cross-frequency relationship. My peri-event investigation into the phase-amplitude coupling (PAC) dynamics reveal that PAC is elevated around the movement epochs (Figure 3-4). Delta-beta PAC has been previously observed in motor tasks (Arnal et al., 2015) although its physiologic origin remains a matter of debate. My work culminates in a model whereby delta oscillations modulate Mthal excitability and Mthal activity regulates beta (and low gamma) states. Several aspects of this model could be directly tested using modern optogenetic approaches described in Chapter 4.

Relation to Movement Disorders

I found electrophysiological correlates of movement preparation, initiation, and execution in Mthal, suggesting that it plays a critical role in the timing and shaping of normal motor function. Therefore, it is unsurprising that movement disorders such as chorea, ataxia, dystonia, tremor and PD have been associated with Mthal (Ellens & Leventhal, 2013). One major question, potentially addressing the nature of Mthal dysregulation, has been why surgical lesions and DBS upstream and within Mthal have been extremely efficacious routes of therapy for movement disorders with non-overlapping symptoms, despite them being drastically different interventions (Johnson, Vitek, & McIntyre, 2009; Okun & Vitek, 2004). In PD, patients move faster after lesions that remove (Jankovic et al., 1999) or DBS procedures that regulate (Schubert et al., 2002) neuronal firing of the BG-output to Mthal. In contrast, the same procedures reduce involuntary movements observed in dystonia and chorea (Mink, 2003) and when targeting cerebellar-receiving nuclei of Mthal, reduce tremor (Benabid et al., 1996). One potential

explanation is that Mthal is required for optimal movement (Bosch-Bouju et al., 2014) but not necessary altogether. My data support this hypothesis, in that trials with very long RTs and MTs show little modulation of activity in Mthal, suggesting an alternative mechanism by which movement was initiated and executed.

A physiological hallmark of PD irregular and "burst" firing in Mthal as evidenced from human (Magnin, Morel, & Jeanmonod, 2000), primate (Devergnas et al., 2015), and rodent (Bosch-Bouju et al., 2013) studies. This has contributed to a change in focus towards the role of neuronal firing patterns rather than firing rates alone (Devetiarov et al., 2017; Galvan, Devergnas, & Wichmann, 2015; Goldberg, Farries, & Fee, 2013) which may be regulated by T-type calcium channels in Mthal (Devergnas et al., 2015). T-type calcium conductance of thalamocortical neurons are regulated by the BG and motor cortical afferents (Tai, Yang, Pan, Huang, & Kuo, 2011; Goldberg, Farries, & Fee, 2012; Sherman, 2016) and control tonic and burst mode transitions thought to underlie important gating and relaying functions of Mthal (Sherman, 2001). I found that long pauses followed by high frequency, burst-like firing precedes normal, ballistic movements. Therefore, the conclusion must be drawn that it is not necessarily the presence of burst firing, but the regulation of such a mode, along with employing it in a coordinated manner, that is important to manifesting normal behavior.

An interesting consequence concerning the anatomical loci of thalamocortical bursting is how it may affect downstream cortical regulation of movement. Dysregulation of BG-recipient cells, which are thought to project preferentially to premotor centers (Bosch-Bouju et al., 2013), may interfere with movement by disrupting complex, state space dynamics. Bursting could disrupt movement plans before they can be implemented, or implement them prematurely and unformed. Symptomatically, this could result in akinesia, cogwheel movements, or dyskinesias.

On the other hand, dysregulation cerebellar-recipient cells, which preferentially project directly to motor cortex, may directly reflect the rhythmic nature of burst firing and expose as tremor.

Slowness of movement is correlated with the presence of beta oscillations in the BG-thalamocortical circuit (Brown, 2006). I hypothesize that beta power is only an 'echo' of Mthal firing, but also recognize that burst firing would necessarily enhance beta power. The observation that Mthal firing correlates with delta oscillations may be a more salient point and explain why delta phase and beta power are linked by PAC (Figure 3-4). The motor delta rhythm is attenuated in PD (Güntekin et al., 2018; Serizawa et al., 2008; Parker, Chen, Kingyon, Cavanagh, & Narayanan, 2015) and delta oscillations have been identified as being dopamine-sensitive in other contexts (Cheng, Tipples, Narayanan, & Meck, 2016). In fact, delta-band optogenetic stimulation of dopamine receptors in a mouse model of PD improves deficits in motor timing (Kim et al., 2017). The dysregulation of delta oscillations may therefore directly affect Mthal, resulting in characteristic transient or uncoordinated beta states often observed in parkinsonism (Sherman et al., 2016; Shin, Law, Tsutsui, Moore, & Jones, 2017). Again, this model could be easily tested by directly manipulating the firing of Mthal neurons using optogenetics while recording from BG-thalamocortical structures (Chapter 4).

Study Limitations

My studies investigate Mthal physiology in isolation from other brain regions. However, previous work in an identical task was utilized to study the BG (Leventhal et al., 2012) and task variants have been employed by our collaborators (Schmidt et al., 2013; Hamid et al., 2016; Mallet et al., 2016; Gage, Stoetzner, Wiltschko, & Berke, 2010) considerably adding to our ability to interpret and discuss our results in a broader context. Future experiments should endeavor to simultaneously record from BG structures such as the striatum and SNr as well as

the cerebellum to understand how motor signals are modified in route to Mthal. In the same vein, technical difficulties due to new recording equipment and hardware contributed to a low subject count for our final data set (n = 5), however, the number of units (n = 366), sessions (n = 30), and trials (n = 2,248) recorded was substantial.

Recording electrophysiology during sleep could have been a strong addition to Chapter 3, as we are left to speculate about single unit entrainment to the delta oscillation during sleep, citing limited existing literature on the topic (Nakamura et al., 2014). At the beginning of my studies, I attempted this. My observations suggested that rather than sleep, these recordings only reflected a state of immobility, which were equally available during inter-trial intervals from the primary recordings that had accompanying video. At the time, it was also unclear what hypothesis the extra effort was contributing towards. In the future, sleep should be considered as part of the specific aims, thereby supporting the additional resources required to collect and analyze the data.

Delta oscillations are a considerable component of the results and discussion in Chapter 3. However, analyzing low-frequency oscillations in the delta band can be fraught due to filtering effects (de Cheveigné & Nelken, 2019). Evoked or event related potentials (ERPs) are large fluctuations that occur in the extracellular field potential in response to a stimulus or action taken (Güntekin & Başar, 2016), and have similar time-frequency characteristics to canonical delta oscillations. In this manner, ERPs are likely the result of coordinated, transient spiking. In contrast, oscillations are thought to wax and wane, or ‘synchronize’ and ‘desynchronize’, which influences the observed electrophysiological phenomena (Harmony, 2013). As our task is event-based, it was initially difficult to assess whether the effects in the delta band were ERPs or oscillations. Therefore, I performed two auxiliary analyses. Firstly, I searched for epochs of

enhanced delta power during the inter-trial period to understand if delta oscillations were ubiquitous, or only found in-trial. Using a bootstrapped algorithm in MATLAB, I found many epochs of enhanced delta power in the inter-trial period, and upon reviewing the synchronized behavioral video, found that this could occur both during movement and complete immobility. These results roughly suggested that the low-frequency signal I recorded in-trial was an oscillation rather than an ERP. Secondly, in Chapter 3 we make a point to show how the delta signal evolves around the Nose In event (Figure 3-10), prior to movement initiation and where correlations between delta phase and RT begin to emerge (Figure 3-9). Even during this early period where movement is minimal, I found many instances where a delta oscillation emerged from the raw electrophysiological data well before movement. In sum, we became confident that our recordings represent real delta oscillations, not ERPs.

Concluding Remarks

Serendipity landed me on a project that was ideally suited for an electrical engineer, with a mentor who was capable of utilizing and pushing my talents. Early on, before Mthal was deemed my primary focus, the mysteries surrounding PD kept me highly motivated. It is a disease that when one component is removed (dopamine) the system goes completely awry, much like removing a small gear from a clock. In engineering, these problems are typically called ‘transfer functions’, where the nature of the output is described by the nature of the input, and they are a central topic of circuit analysis. The standard model (Figure 1-2) is in essence a simplified wiring diagram, directly speaking to such a problem. Additionally, physiological inconsistencies associated with the standard model suggested that, as a field, the translation of input to output was misunderstood. This became especially important as I was encouraged by my mentor to investigate Mthal, which remains an understudied and oversimplified node in the BG-

thalamocortical circuit. Despite a long history of being deemed a ‘relay’, evidence has been accumulating suggesting that Mthal has a more complex role in integrating motor signals. That Mthal represents a quintessential ‘black box’ problem has continually inspired my work, which I hope has added some transparency. The technical challenges of my research have always been subservient to the ultimate purpose, which is to address the suffering of those afflicted with disorders of the central nervous system. PD represents one of many chronic, neurodegenerative diseases that is outright crippling, but also represents one of the few that are amenable to therapies based on insights from circuit-level physiology. It has given me a great sense of purpose to connect with and inform the PD community, patients and researchers alike.

References

Arnal, L. H., Doelling, K. B., & Poeppel, D. (2015). Delta-Beta Coupled Oscillations Underlie Temporal Prediction Accuracy. *Cereb Cortex*, *25*(9), 3077-3085.

Baunez, C., Nieoullon, A., & Amalric, M. (1995). Dopamine and complex sensorimotor integration: further studies in a conditioned motor task in the rat. *Neuroscience*, *65*, 375-384.

Benabid, A. L., Pollak, P., Gao, D., Hoffmann, D., Limousin, P., Gay, E. et al. (1996). Chronic electrical stimulation of the ventralis intermedius nucleus of the thalamus as a treatment of movement disorders. *J Neurosurg*, *84*, 203-214.

Bosch-Bouju, C., Hyland, B. I., & Parr-Brownlie, L. C. (2013). Motor thalamus integration of cortical, cerebellar and basal ganglia information: implications for normal and parkinsonian conditions. *Front Comput Neurosci*, *7*, 163.

Bosch-Bouju, C., Smither, R. A., Hyland, B. I., & Parr-Brownlie, L. C. (2014). Reduced reach-related modulation of motor thalamus neural activity in a rat model of Parkinson's disease. *Journal of Neuroscience*, *34*(48), 15836-15850.

Bostan, A. C., Dum, R. P., & Strick, P. L. (2010). The basal ganglia communicate with the cerebellum. *Proc Natl Acad Sci U S A*, *107*, 8452-8456.

Bostan, A. C., Dum, R. P., & Strick, P. L. (2013). Cerebellar networks with the cerebral cortex and basal ganglia. *Trends Cogn Sci*, *17*, 241-254.

Breska, A., & Deouell, L. Y. (2017). Neural mechanisms of rhythm-based temporal prediction: Delta phase-locking reflects temporal predictability but not rhythmic entrainment. *PLoS Biol*, *15*(2), e2001665.

Brown, P. (2006). Bad oscillations in Parkinson's disease. *J Neural Transm Suppl*, 27-30.

Brown, V. J., & Robbins, T. W. (1991). Simple and choice reaction time performance following unilateral striatal dopamine depletion in the rat. Impaired motor readiness but preserved response preparation. *Brain*, *114*, 513-525.

Buzsaki, G. (2006). *Rhythms of the Brain*. Oxford University Press.

Caligiore, D., Pezzulo, G., Baldassarre, G., Bostan, A. C., Strick, P. L., Doya, K. et al. (2017). Consensus Paper: Towards a Systems-Level View of Cerebellar Function: the Interplay Between Cerebellum, Basal Ganglia, and Cortex. *Cerebellum*, *16*, 203-229.

Canavier, C. C. (2015). Phase-resetting as a tool of information transmission. *Curr Opin Neurobiol*, *31*, 206-213.

Cheng, R.-K., Tipples, J., Narayanan, N. S., & Meck, W. H. (2016). Clock Speed as a Window into Dopaminergic Control of Emotion and Time Perception. *Timing & Time Perception*, *4*(1), 99-122.

Churchland, M. M., Yu, B. M., Sahani, M., & Shenoy, K. V. (2007). Techniques for extracting single-trial activity patterns from large-scale neural recordings. *Curr Opin Neurobiol*, *17*(5), 609-618.

de Cheveigné, A., & Nelken, I. (2019). Filters: When, Why, and How (Not) to Use Them. *Neuron*, *102*(2), 280-293.

Devergnas, A., Chen, E., Ma, Y., Hamada, I., Pittard, D., Kammermeier, S. et al. (2015). Anatomical Localization of CaV3.1 Calcium Channels and Electrophysiological Effects of T-type Calcium Channel Blockade in the Thalamus of MPTP-Treated Monkeys. *J Neurophysiol*, jn.00858.2015.

Devetiarov, D., Semenova, U., Usova, S., Tomskiy, A., Tyurnikov, V., Nizametdinova, D. et al. (2017). Neuronal activity patterns in the ventral thalamus: Comparison between Parkinson's disease and cervical dystonia. *Clin Neurophysiol*, *128*, 2482-2490.

Dudman, J. T., & Krakauer, J. W. (2016). The basal ganglia: from motor commands to the control of vigor. *Curr Opin Neurobiol*.

Ellens, D. J., Gaidica, M., Toader, A., Peng, S., Shue, S., John, T. et al. (2016). An automated rat single pellet reaching system with high-speed video capture. *Journal of Neuroscience Methods*, *271*, 119-127.

Ellens, D. J., & Leventhal, D. K. (2013). Review: electrophysiology of basal ganglia and cortex in models of Parkinson disease. *J Parkinsons Dis*, *3*, 241-254.

Freeze, B. S., Kravitz, A. V., Hammack, N., Berke, J. D., & Kreitzer, A. C. (2013). Control of Basal Ganglia output by direct and indirect pathway projection neurons. *J Neurosci*, *33*, 18531-18539.

Fries, P. (2005). A mechanism for cognitive dynamics: neuronal communication through neuronal coherence. *Trends Cogn Sci*, *9*, 474-480.

Fries, P. (2015). Rhythms for Cognition: Communication through Coherence. *Neuron*, *88*, 220-235.

Gage, G. J., Stoetzner, C. R., Wiltschko, A. B., & Berke, J. D. (2010). Selective activation of striatal fast-spiking interneurons during choice execution. *Neuron*, *67*, 466-479.

Gaidica, M., Hurst, A., Cyr, C., & Leventhal, D. K. (2018). Distinct Populations of Motor Thalamic Neurons Encode Action Initiation, Action Selection, and Movement Vigor. *J Neurosci*, *38*(29), 6563-6573.

Galvan, A., Devergnas, A., & Wichmann, T. (2015). Alterations in neuronal activity in basal ganglia-thalamocortical circuits in the parkinsonian state. *Front Neuroanat*, *9*, 5.

Goldberg, J. H., Farries, M. A., & Fee, M. S. (2013). Basal ganglia output to the thalamus: still a paradox. *Trends Neurosci*.

Goldberg, J. H., Farries, M. A., & Fee, M. S. (2012). Integration of cortical and pallidal inputs in the basal ganglia-recipient thalamus of singing birds. *J Neurophysiol*.

Graybiel, A. M., & Grafton, S. T. (2015). The striatum: where skills and habits meet. *Cold Spring Harb Perspect Biol*, *7*, a021691.

Gu, B. M., van Rijn, H., & Meck, W. H. (2015). Oscillatory multiplexing of neural population codes for interval timing and working memory. *Neurosci Biobehav Rev*, *48*, 160-185.

Güntekin, B., & Başar, E. (2016). Review of evoked and event-related delta responses in the human brain. *Int J Psychophysiol*, *103*, 43-52.

Güntekin, B., Hanoğlu, L., Güner, D., Yılmaz, N. H., Çadırcı, F., Mantar, N. et al. (2018). Cognitive Impairment in Parkinson's Disease Is Reflected with Gradual Decrease of EEG Delta Responses during Auditory Discrimination. *Front Psychol*, *9*, 170.

Guo, Z. V., Inagaki, H. K., Daie, K., Druckmann, S., Gerfen, C. R., & Svoboda, K. (2017). Maintenance of persistent activity in a frontal thalamocortical loop. *Nature*.

Haith, A. M., Huberdeau, D. M., & Krakauer, J. W. (2015). Hedging your bets: intermediate movements as optimal behavior in the context of an incomplete decision. *PLoS Comput Biol*, *11*, e1004171.

Haith, A. M., Pakpoor, J., & Krakauer, J. W. (2016). Independence of Movement Preparation and Movement Initiation. *J Neurosci*, *36*, 3007-3015.

Hamid, A. A., Pettibone, J. R., Mabrouk, O. S., Hetrick, V. L., Schmidt, R., Vander Weele, C. M. et al. (2016). Mesolimbic dopamine signals the value of work. *Nat Neurosci*, *19*, 117-126.

Harmony, T. (2013). The functional significance of delta oscillations in cognitive processing. *Front Integr Neurosci*, *7*, 83.

Heiney, S. A., Kim, J., Augustine, G. J., & Medina, J. F. (2014). Precise control of movement kinematics by optogenetic inhibition of Purkinje cell activity. *J Neurosci*, *34*, 2321-2330.

Heuer, A., Smith, G. A., & Dunnett, S. B. (2013). Comparison of 6-hydroxydopamine lesions of the substantia nigra and the medial forebrain bundle on a lateralised choice reaction time task in mice. *Eur J Neurosci*, *37*, 294-302.

Hintzen, A., Pelzer, E. A., & Tittgemeyer, M. (2017). Thalamic interactions of cerebellum and basal ganglia. *Brain Struct Funct*.

Horak, F. B., & Anderson, M. E. (1984). Influence of globus pallidus on arm movements in monkeys. I. Effects of kainic acid-induced lesions. *J Neurophysiol*, *52*, 290-304.

Ilinsky, I. A., Toga, A. W., & Kultas-Ilinsky, K. (1993). Anatomical organisation of internal neuronal circuits in the motor thalamus. In *Thalamic networks for relay and modulation* (pp. 155-164). Elsevier.

Ito, M. (1984). *The cerebellum and neural control*. Raven press.

Jankovic, J., Ben-Arie, L., Schwartz, K., Chen, K., Khan, M., Lai, E. C. et al. (1999). Movement and reaction times and fine coordination tasks following pallidotomy. *Mov Disord*, *14*, 57-62.

Johnson, M. D., Vitek, J. L., & McIntyre, C. C. (2009). Pallidal stimulation that improves parkinsonian motor symptoms also modulates neuronal firing patterns in primary motor cortex in the MPTP-treated monkey. *Exp Neurol*, *219*, 359-362.

Jones, S. R., Pritchett, D. L., Sikora, M. A., Stufflebeam, S. M., Hämäläinen, M., & Moore, C. I. (2009). Quantitative analysis and biophysically realistic neural modeling of the MEG mu rhythm: rhythmogenesis and modulation of sensory-evoked responses. *J Neurophysiol*, *102*, 3554-3572.

Kaufman, M. T., Churchland, M. M., Ryu, S. I., & Shenoy, K. V. (2014). Cortical activity in the null space: permitting preparation without movement. *Nat Neurosci*.

Kim, Y. C., Han, S. W., Alberico, S. L., Ruggiero, R. N., De Corte, B., Chen, K. H. et al. (2017). Optogenetic Stimulation of Frontal D1 Neurons Compensates for Impaired Temporal Control of Action in Dopamine-Depleted Mice. *Curr Biol*, *27*(1), 39-47.

Kravitz, A. V., Freeze, B. S., Parker, P. R. L., Kay, K., Thwin, M. T., Deisseroth, K. et al. (2010). Regulation of parkinsonian motor behaviours by optogenetic control of basal ganglia circuitry. *Nature*, *466*, 622-626.

Kuramoto, E., Fujiyama, F., Nakamura, K. C., Tanaka, Y., Hioki, H., & Kaneko, T. (2011). Complementary distribution of glutamatergic cerebellar and GABAergic basal ganglia afferents to the rat motor thalamic nuclei. *Eur J Neurosci*, *33*, 95-109.

Lee, K. H., Mathews, P. J., Reeves, A. M. B., Choe, K. Y., Jami, S. A., Serrano, R. E. et al. (2015). Circuit mechanisms underlying motor memory formation in the cerebellum. *Neuron*, *86*, 529-540.

Leventhal, D. K., Gage, G. J., Schmidt, R., Pettibone, J. R., Case, A. C., & Berke, J. D. (2012). Basal Ganglia Beta oscillations accompany cue utilization. *Neuron*, *73*, 523-536.

Leventhal, D. K., Stoetzner, C. R., Abraham, R., Pettibone, J., DeMarco, K., & Berke, J. D. (2014). Dissociable effects of dopamine on learning and performance within sensorimotor striatum. *Basal Ganglia*, *4*, 43-54.

Li, C., Chen, L., & Aihara, K. (2006). Transient resetting: A novel mechanism for synchrony and its biological examples. *PLoS computational biology*, *2*(8), e103.

Llinás, R. R., & Steriade, M. (2006). Bursting of thalamic neurons and states of vigilance. *J Neurophysiol*, *95*, 3297-3308.

Llinás, R. R., Ribary, U., Jeanmonod, D., Kronberg, E., & Mitra, P. P. (1999). Thalamocortical dysrhythmia: A neurological and neuropsychiatric syndrome characterized by magnetoencephalography. *Proc Natl Acad Sci U S A*, *96*(26), 15222-15227.

Magnin, M., Morel, A., & Jeanmonod, D. (2000). Single-unit analysis of the pallidum, thalamus and subthalamic nucleus in parkinsonian patients. *Neuroscience*, *96*, 549-564.

Mallet, N., Schmidt, R., Leventhal, D., Chen, F., Amer, N., Boraud, T. et al. (2016). Arkypallidal Cells Send a Stop Signal to Striatum. *Neuron*.

Miller, A. D., & Brooks, V. B. (1982). Parallel pathways for movement initiation of monkeys. *Exp Brain Res*, *45*, 328-332.

Mink, J. W. (2003). The Basal Ganglia and involuntary movements: impaired inhibition of competing motor patterns. *Arch Neurol*, *60*, 1365-1368.

Nakamura, K. C., Sharott, A., & Magill, P. J. (2014). Temporal coupling with cortex distinguishes spontaneous neuronal activities in identified basal ganglia-recipient and cerebellar-recipient zones of the motor thalamus. *Cereb Cortex*, *24*(1), 81-97.

Okun, M. S., & Vitek, J. L. (2004). Lesion therapy for Parkinson's disease and other movement disorders: update and controversies. *Mov Disord*, *19*, 375-389.

Parker, K. L., Chen, K. H., Kingyon, J. R., Cavanagh, J. F., & Narayanan, N. S. (2015). Medial frontal ~4-Hz activity in humans and rodents is attenuated in PD patients and in rodents with cortical dopamine depletion. *J Neurophysiol*, *114*(2), 1310-1320.

Reis, C., Sharott, A., Magill, P. J., van Wijk, B. C. M., Parr, T., Zeidman, P. et al. (2019). Thalamocortical dynamics underlying spontaneous transitions in beta power in Parkinsonism. *Neuroimage*, *193*, 103-114.

Rouiller, E. M., Liang, F., Babalian, A., Moret, V., & Wiesendanger, M. (1994). Cerebellothalamocortical and pallidothalamocortical projections to the primary and supplementary motor cortical areas: a multiple tracing study in macaque monkeys. *J Comp Neurol*, *345*(2), 185-213.

Scharnowski, F., Rees, G., & Walsh, V. (2013). Time and the brain: neurorelativity. *Trends in Cognitive Sciences*, *17*(2), 51-52.

Schmidt, R., Leventhal, D. K., Mallet, N., Chen, F., & Berke, J. D. (2013). Canceling actions involves a race between basal ganglia pathways. *Nat Neurosci*, *16*, 1118-1124.

Schroeder, C. E., & Lakatos, P. (2009). Low-frequency neuronal oscillations as instruments of sensory selection. *Trends Neurosci*, *32*(1), 9-18.

Schubert, T., Volkmann, J., Müller, U., Sturm, V., Voges, J., Freund, H.-J. J. et al. (2002). Effects of pallidal deep brain stimulation and levodopa treatment on reaction-time performance in Parkinson's disease. *Exp Brain Res*, *144*, 8-16.

Serizawa, K., Kamei, S., Morita, A., Hara, M., Mizutani, T., Yoshihashi, H. et al. (2008). Comparison of quantitative EEGs between Parkinson disease and age-adjusted normal controls. *J Clin Neurophysiol*, *25*(6), 361-366.

Sherman, M. A., Lee, S., Law, R., Haegens, S., Thorn, C. A., Hämäläinen, M. S. et al. (2016). Neural mechanisms of transient neocortical beta rhythms: Converging evidence from humans, computational modeling, monkeys, and mice. *Proceedings of the National Academy of Sciences*, *113*(33), E4885-E4894.

Sherman, S. M. (2001). Tonic and burst firing: dual modes of thalamocortical relay. *Trends Neurosci*, *24*, 122-126.

Sherman, S. M. (2016). Thalamus plays a central role in ongoing cortical functioning. *Nat Neurosci*, *19*, 533-541.

Shin, H., Law, R., Tsutsui, S., Moore, C. I., & Jones, S. R. (2017). The rate of transient beta frequency events predicts behavior across tasks and species. *Elife*, *6*.

Stefanics, G., Hangya, B., Hernádi, I., Winkler, I., Lakatos, P., & Ulbert, I. (2010). Phase entrainment of human delta oscillations can mediate the effects of expectation on reaction speed. *J Neurosci*, *30*, 13578-13585.

Tai, C.-H. H., Yang, Y.-C. C., Pan, M.-K. K., Huang, C.-S. S., & Kuo, C.-C. C. (2011). Modulation of subthalamic T-type Ca(2+) channels remedies locomotor deficits in a rat model of Parkinson disease. *J Clin Invest*, *121*, 3289-3305.

Thach, W. T. (1975). Timing of activity in cerebellar dentate nucleus and cerebral motor cortex during prompt volitional movement. *Brain Res*, *88*, 233-241.

Turner, R. S., & Desmurget, M. (2010). Basal ganglia contributions to motor control: a vigorous tutor. *Curr Opin Neurobiol*, *20*, 704-716.

Valls-Solé, J., Rothwell, J. C., Goulart, F., Cossu, G., & Munoz, E. (1999). Patterned ballistic movements triggered by a startle in healthy humans. *The Journal of physiology*, *516*(3), 931-938.

Wong, A. L., Haith, A. M., & Krakauer, J. W. (2015). Motor Planning. *Neuroscientist*, *21*, 385-398.

Wyart, V., de Gardelle, V., Scholl, J., & Summerfield, C. (2012). Rhythmic fluctuations in evidence accumulation during decision making in the human brain. *Neuron*, *76*(4), 847-858.

Yamawaki, N., & Shepherd, G. M. G. (2015). Synaptic circuit organization of motor corticothalamic neurons. *J Neurosci*, *35*, 2293-2307.

Yttri, E. A., & Dudman, J. T. (2016). Opponent and bidirectional control of movement velocity in the basal ganglia. *Nature*.

Zimnik, A. J., Lara, A. H., & Churchland, M. M. (2019). Perturbation of macaque supplementary motor area produces context-independent changes in the probability of movement initiation. *J Neurosci*.

APPENDIX A: VIRUS SEROTYPE NOTES

The following conversation stemmed from a useful post regarding adeno associated virus (AAV) serotypes found on Research Gate. Below, Dr. Caroline Bass generously explains some of the nuances in using different serotypes to target the motor thalamus (Mthal).

MATT: Hi Caroline! Thanks for your wonderful insight into AAV serotypes. We are targeting the basal ganglia recipient thalamus and using a virus under a synapsin promoter. We have available 2/5/6 serotypes for the ChR2 virus. I was told that AAV6 has the potential to not only transfect the terminals, but could hop the synapse and transfect cells themselves. Ideally, we want to hijack either the terminals from the BG in the thalamus OR the cells, but since that circuitry is sign-reversing, BOTH would not be useful! Do you have any experience with AAV6? Or any advice? I hope that was clear enough, thank you in advance,

---

CAROLINE: Hi Matt, I think there is a lot of confusing terminology out there which makes it tough to figure out exactly what is going on. The way I think about it, most AAVs transduce cell bodies, this results in a signal in those cell bodies and their projection terminals. Others have this "anterograde" or cell filling transduction, but additionally have retrograde transduction, meaning that the terminals at the injection site also take up the virus, this results in retrograde transduction of the terminals and their connected cell bodies. There is only one that seems to be primarily retrograde (aav2/retro). Aav6 and 9 seem to have Antero and retrograde properties.

I haven't been convinced of transynaptic properties, i have seen some evidence of this, but it often looks like a highly innervated cell popping out because the terminals surround it. There are some reports of transsynaptic AAVs But I'm not sure this is has been clearly established.

I'm on my phone but if you could state exactly what you want I can give you my best estimation of how to do it.

MATT: Thanks for getting back! We are interested in the pathway-specific contributions of the basal ganglia and cerebellum to the "motor" thalamus. I think one of my friends, Stephanie, may have chatted with you at SfN about this. Off the shelf, we could use ChR2 with hSyn, injecting the virus into the basal ganglia, or cerebellar output/s, and then put our laser over the thalamus, and only turn on the afferent terminals from either location. Specifically, the basal ganglia has GABAergic terminals onto thalamic cells, and if we could isolate expression to those terminals, that would be great. However, if the virus also goes on to transfect thalamic cells, we will have a hard time isolating whether we are modulating terminals, or thalamic cells themselves. I appreciate any thoughts you might have!

CAROLINE: Hey Matt, First, let me say that is a wonderful figure, Really nicely done. I'm glad you are thinking about these issues, as many folks don't delve into the details. First, I would say that you shouldn't overthink these tools. They work but all have limitations, same as transgenic mice. Too often people take a virus

---

or a transgenic mouse as “perfect” when in fact none are. So I prefer to think of these genetic approaches more like pharmacology, where for the most part you can say a drug is a D2 antagonist but it might have some “dirty” or off-target effects, especially at higher doses. The same is true for viruses, for the most part they act fairly consistently, but they do have special considerations, perhaps a better way of thinking about it is what do they do in your hands, in brain regions you’re interested in, with your injection system? You can’t expect a construct to act the same if you inject 3 microliters when I inject 0.3 microliters for example.

In terms of what you are doing, if you can use mice I would definitely just take a GABA specific Cre mouse line and inject a DIO-ChR2 virus. I would not use AAV6 (actually it’s AAV2/6) because you may want to compare cell body and terminal stimulation at some point. AAV2/2 is fairly bad, I don’t know why anyone uses it at this point. It generally doesn’t go far from the needle track. Of course I’m working with rats, so this may be a bigger deal to me. There is no reason why you can’t find another stereotype right now, not with Addgene and other core facilities making them. My preference is AAV2/10, really nice, robust expression that’s easily titrated.

In terms of crossing the synapse, I believe this is possible, but is likely dependent on the brain region and the amounts injected. I do think it’s rare, and difficult to distinguish between crossing a synapse and having a neurons heavily innervated by the presyanptic cell, I have encountered this particularly with some of the retrograde systems.

If you decide to go to a retrograde route, you’re going to find it’s a much different world both in terms of how you approach the manipulation and how you verify expression. This appears to be a major sticking point working with folks who are new to these systems.

Good luck and I’m happy to help if I can.